Development of the Tetrode Recording Apparatus for Simultaneous Recording of Multiple Single Cells in the Superior Colliculus of the Cat

Jeremy C. Murphy

McGill University, Montreal

August, 2001

A thesis submitted to the Faculty of Graduate Studies and Research in partial fulfilment of the requirements of the degree of Masters in Neuroscience

National Library of Canada
Acquisitions and Bibliographic Services
395 Wellington Street
Ottawa ON K1A 0N4
Canada

Bibliothèque nationale du Canada
Acquisitions et services bibliographiques
395, rue Wellington
Ottawa ON K1A 0N4
Canada

Your file Votre référence

Our file Notre référence

0-612-78930-6

Canada

TABLE OF CONTENTS

ABSTRACT

The tetrode is a recording device formed of four recording wires used to improve single unit discrimination in multi-unit recordings. Here, tetrodes were used to record and characterize the activity of multiple different cell types at one locus in the superior colliculus (SC). This project entailed the configuration of the tetrode and data analysis software for recording in the SC. Problems of adequate sampling rates, transfer to disc of large files, identification of spikes in the presence of noise, distortion of spike shapes by simultaneously firing cells and noise, reliable criteria for distinguishing individual cells, time varying changes in spike shapes, and relating individual discharges to motor behavior were addressed. A sampling rate of 35.7 kHz was achieved on each tetrode wire. It was found that peak and valley amplitude parameters are usually sufficient for spike separation but the user must employ various combinations of parameters in order to achieve the most reliable results. Finally, cell analysis indicates that the tetrode is capable of successfully recording from multiple cells of different types in the colliculus, such as buildup and visual.

RESUME

Le collicule superieur (CS) est une structure laminaire située au niveau du tronc cérébral qui est critique dans le contrôle des comportements d'orientation du regard. Plusieurs études chez l'animal éveillé ont décrit les caractéristiques de la décharge des cellules colliculaire en fonction des saccades de l'oeil et du regard. Une importante lacune dans notre connaissance est de savoir comment les cellules du collicule superieur interagissent entre elles et aussi quel peut-être la fonction des circuits locaux formés par ces groupes de cellules. Dans cette étude, des enregistrements multi-cellulaires dans un point spécifique d'un collicule ont été effectués au moyen d'une tétrode; cet instrument étant formé de quatre micro-fils d'enregistrements. Ce projet comprend le développement de la confection des tétrodes et aux techniques informatiques d'analyse des données pour l'enregistrement dans le collicule supérieur. En comparant les caractéristiques des potentiels d'action des cellules à partir de chaque fil d'enregistrement, il a été possible en utilisant un logiciel spécialisé pour ce type de tâche de séparer les signaux provenant de chacune des cellules. Dans cette étude, plusieurs problèmes ont été adressés: la fréquence adéquate d'échantillonage, le transfert de grands dossiers au disque, l'identification appropriée des potentiels d'action en présence de bruits, la distortion de la forme des potentiels d'action due à l'enregistrement simultané de plusieurs cellules et du bruit, les critères adéquats pour pouvoir distinguer chacune des cellules, les changements temporaux de la forme des potentiels d'action (par exemple l'amplitude), et finalement la relation entre les propriétés physiologiques des cellules et les comportements moteurs. La fréquence d'échantillonage pour chacun des fils d'enregistrements a été de 35.7 kHz. Plusieurs critères pour différentier les potentiels d'action ont été necessaires pour séparer les potentiels d'action provenant de chaque cellule. Cependant, l'utilisateur doit employer des combinaisons variées des paramètres afin d'obtenir des résultats adéquats. Finalement, l'analyse cellulaire indique qu'il est possible d'enregistrer plusieurs cellules au moyen d'une tétrode et de pouvoir différientier différents types cellulaires comme des cellules visuelles ou d'orientation.

ACKNOWLEDGEMENTS

It is this brief section that most makes me reflect on the studies accomplished over the past couple of years and brings to light the fact that this epitome would never have been possible without the contributions of many people, both professionally and personally.

Dr. Daniel Guitton was the first person to instill in me a deep interest in neuroscience. As my supervisor, he has provided invaluable suggestions and direction to my work. A very knowledgeable man of many interests, our in depth discussions on the tetrode project and other topics, some related to neuroscience and some not, were informative, insightful, and inspiring.

I thank Dr. Kathy Cullen, Dr. Henrietta Galiana, Dr. Kathy Mullen, and Dr. Angel Alonso for their contributions to my project from their positions as experienced neuroscientists and members of my masters committee. I am greatly appreciative of their gnostic queries, suggestions, and other inputs to my studies.

The three people with whom I endured the best and worst of times during these studies were my labmates Andre Bergeron, Troy Herter, and Woo Young Choi. I am indebted to Andre for educating me on experimental procedures and his patience while doing so. He also provided many helpful suggestions for the tetrode project and the linguistic knowledge for the French translation of the abstract of this thesis. Troy helped solve many crises from equipment failure to computer enigmas. His problem solving efforts and suggestions for the tetrode project were excellent. Woo Young could always be relied upon for theoretical insights pertinent to the tetrode project. It was always interesting to see what he, Andre, Troy, and I would come up with during our informal lab discussions.

Tom Wilson provided me with valuable introduction to the art of recording with tetrodes. Jocelyn Roy deserves many thanks for his efforts in constructing and repairing components of the experimental system as well as his suggestions for improvements to the tetrode design.

I am appreciative of the animal staff of the Montreal Neurological Institute (MNI) for their surgical preparations and caring for the cats involved in these studies. In particular, Mireille Bouchard and Lisa Volume are wonderful people who appreciate a good mixture of serious work and humour as much as I do.

Toula Papadopoulos earns laurels for her help with graduate studies information and organization as well as keeping in step with Dan's hectic schedule.

The last of the MNI staff I would like to applaud are the friends I have made in the neuroscience community. The reciprocative counselling and comradery we have developed is an excellent side effect of my studies here. Notably, Colin Dobson and Tony Ramjuan (the other two Musketeers), Beth Oldford, Natasha Hussein, Penelope Kostopoulos, Tamara Pringsheim, Emmanuelle Hébert, and Maryse St. Georges are great neuroscientists and friends. Other friends I have not mentioned here are far from forgotten; you know who you are and be assured that I know too.

Lastly, I thank my parents and brother who have always provided two of the most important contributions to all of my endeavours - genuine interest and unwavering support. Their involvement is perhaps the most important factor in the successes I have had.

LIST OF FIGURES

CHAPTER 1

INTRODUCTION

The superior colliculus (SC) is a midbrain structure that is an integral component of brain networks controlling eye and gaze (gaze = eye movement + head movement) saccades. Saccade is the term given to the act of quickly relocating the visual axis relative to space; the movement of the eyes in addition to the movement of the head result in a saccadic gaze shift. This action serves to relocate the retinal region of highest acuity, the fovea in humans, area centralis in the cat, from one point of interest to another. The SC plays an active role in controlling saccadic eye movements and gaze movements. It is a very diversified structure and is connected via many projections to the rest of the brain making it a common processing area for multi-modal inputs including somatosensory, auditory, and visual. The SC has the ability to transform the inputs from its many afferents into precise and appropriate motor responses via its array of efferents, allowing fixation of these stimuli. Of particular interest are its direct connection with the brainstem circuits that generate eye and gaze saccades and the collicular afferents from many cortical and subcortical structures that code sensory and cognitive information related to the planning of orientational behaviour. Thus, the SC plays a major role in the processing of sensorimotor integration. Although many diverse studies have attempted to characterize the function of the SC, its role in planning and executing

motor processes resulting in orientating movements is not entirely understood. Even less fully understood is the relation of the individual cells within this structure to one another and the local circuitry they compose forming processing modules that contribute to the generation of orientating behaviour.

It is the central goal of this work to develop the tetrode, the recording apparati, and the various computer hardware and software for the purpose of simultaneously recording the activity of multiple neurons in the SC. This includes: refining the design of the tetrode for optimal recording in the SC; developing computer software data acquisition programs with sufficient capacity to accurately record multiple neuron activity directly to hard disk (via DataWave hardware/software); developing optimal computational methods of action potential characterization and cell differentiation (via AutoCut software); creating programs for data analyses including characterization of individual cell function and cell intercorrelation (via MatLab software). Long term goals of this work are to expand the knowledge of neurons present in the SC and to elucidate the local circuits of the SC.

1.1 The Tetrode: A Multi-Tipped Recording Device

In order to understand the computations that are carried out by the proposed microcircuits in the SC, along with the operational relevance of their afferents and efferents, it may be informative to record from multiple cells simultaneously in alert, behaving animals. Whereas the traditional manner of single cell recording aims to interrelate cells by piecing together single cell activity recordings from different areas of the colliculus, simultaneous multiple cell recording provides the means of interrelating cells that are immediate neighbours. In this manner, local circuits can be studied directly by comparison of multiple cell activity.

It is hoped that a multi-tipped recording device, the tetrode (Figure 1A, p.4), will expedite such a recording process.

A non-traditional style of recording electrode, the tetrode, was implemented in my experimental procedures. Whereas the typical electrode consists of a single, fine tip and can record information from a single cell with satisfactory accuracy, the tetrode consists of four such tips and is much more suitable for simultaneous multi-cell recordings.

1.1.1 Recording Multiple Neurons Simultaneously

The activity of neurons near the recording tip of the tetrode have their activity registered differently on each of the four wires in terms of their spike amplitude and time courses (Figure 1, p.4). These differences allow each cell to be uniquely identified. For instance, an action potential generated by a neuron will be received first by the nearest of the four wires. As this wire is in closer proximity than the other three, the action potential will have a greater amplitude on this wire. The wire furthest away from the neuron will show the smallest amplitude action potential compared to the other three channels. Also, the closest wire would receive the action potential signal slightly sooner than would the other three wires. With these differences occurring on all four wires at once, cell differentiation is possible in areas of multiple cell activity. Thus, were two cells equidistant from the tetrode and exhibiting very similar activity, they would be distinguishable. The same two cells recorded by a single electrode would register the cells' activities simultaneously and superimposed on one another, making it difficult to disambiguate the signals (Figure 1, p.4).

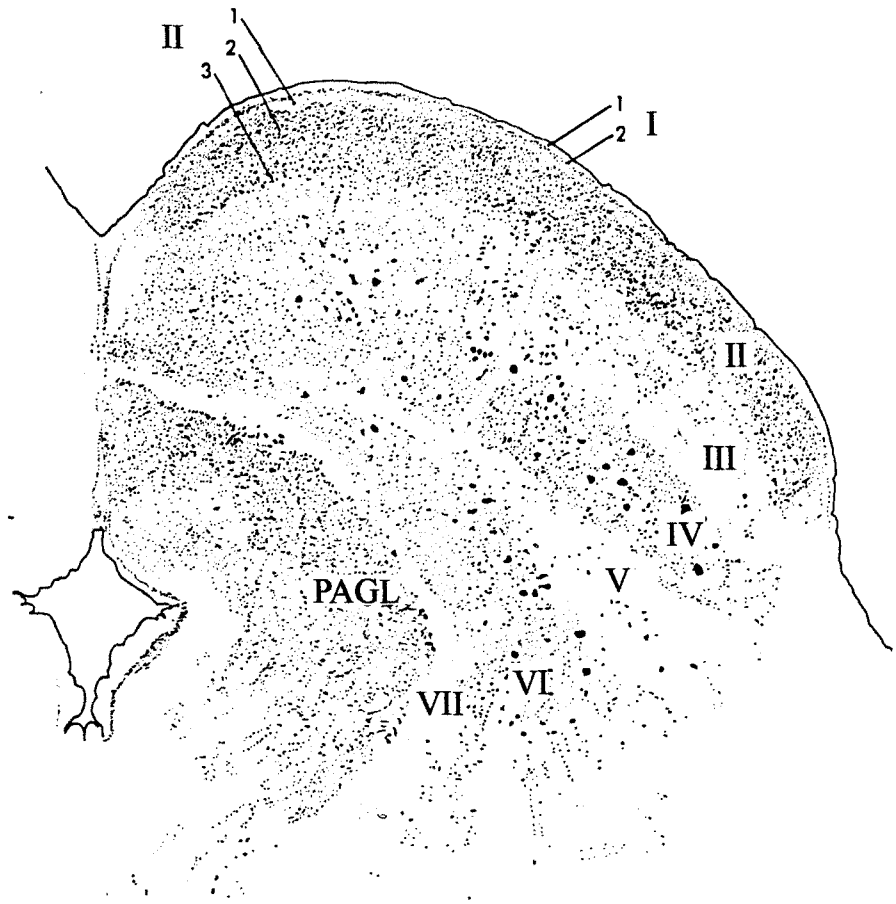

Figure 1 A drawing of the colliculus from a section stained with cresyl violet demonstrating the seven laminae and five sublaminae. $I_{1,2}$, sublaminae of stratum zonale; $I_{1,2,3}$, sublaminae of stratum griseum superficiale (SGS); III, stratum opticum (SO); IV, stratum griseum intermediale (SGI); V, stratum lemnisci; VI, stratum griseum profundum (SGP); VII, stratum album profundum (SAP). PAGL = periaqueductal gray layer. Taken from Kanaseki and Sprague, 1974.

1.1.2 Population Activity

Not only does the tetrode provide increased ability to examine the properties of individual neurons, it also allows the observation of population activity. Since the tetrode can record multiple neurons in a given area simultaneously, the individual activity of groups of neurons and cellular interaction can be observed. This feature is particularly important as in any series of observations or construction of models involving cellular activity, it is the population activity that is of primary interest; how neurons pass signals from one to another and what results are produced.

1.1.3 Decrease in Duration of Experiments

Additional advantages of using tetrodes lie in the reduction of time in performing experiments. The time required to isolate single neurons and record from them over an extensive period so as to properly characterize their activity can be great. To achieve a sufficient sample population requires even more time, especially when a single electrode is employed, recording from only one neuron at a time. This time investment can be greatly reduced with simultaneous cell recording using the tetrode. In fact, the time reduction is in direct proportion to the amount of cells recorded simultaneously. Thus, the number of experiments required to characterize a cell population can be reduced. Not only does this save the researcher time but it also reduces the chances of inconsistencies between trials as there are less trials to compare.

As I have observed, cats can quickly become less alert over the course of an experiment. A decreased state of alertness seems to correspond with a decrease in the firing rate of saccade related neurons. Thus, it is beneficial to have the capacity to acquire as much

data as possible in as little time as possible so as to record from cells while the animal is alert. The tetrode allows the researcher such an advantage.

1.2 Previous Work Using Tetrodes

Although there has been no reported previous work in the SC using tetrodes, they have been successfully implemented in other areas of the brain. Such areas include the rat hippocampus (O'Keefe & Reece, 1993; Wilson & McNaughton, 1993; Henze et al., 2000), cat visual area 17 (Gray & Maldonado, 1995; Hetherington & Swindale, 1999), the cat striate cortex (Gray et al., 1995; Maldonado et al., 1997), and the cat primary visual cortex (Maldonado & Gray, 1996). Also, the accuracy of tetrode recording has been tested by such groups as Harris et al. (Harris et al., 2000).

1.2.1 Tetrode use in the Hippocampus

In the rat hippocampus, multiple tetrodes have been employed simultaneously (Wilson & McNaughton, 1993; McNaughton et al., 1983). In these experiments, 12 tetrodes were controlled via implanted microdrive arrays. Each tetrode was capable of resolving the activity of 5 to 20 neurons and up to 148 neurons were simultaneously recorded in one instance. The tetrodes were made of nickel-chromium alloy (nichrome) and had an overall diameter of 40 μm. When placed in the microdrive array, the maximum spacing between tetrodes was 250 to 300 μm. The data was acquired by seven synchronized computers at 33 kHz per tetrode channel. The identification of cells involved automated inter-spike comparison of spike amplitudes. The successful simultaneous recording of multiple units in the rat hippocampus allowed the researchers to analyze and interpret neuronal ensemble activity in

alert, behaving animals. The tetrode method allowed the possibility of interpretation of neuronal activity in the absence of explicit behaviour, such as during periods of sleep, motor planning, reasoning and memory consolidation.

Other studies in the rat hippocampus area CA1, done by Henze et al., aimed at determining intracellular states of neurons by analyzing extracellularly recorded signals. A secondary goal of the study was to determine a maximum number of cells recordable by a tetrode (Henze et al., 2000). This study used tetrodes of 26 μm overall diameter. The signals were saved to disk at acquisition speeds of up to 50 kHz. The use of tetrodes produced the ability to discriminate multiple single units by taking advantage of the temporal coherence of spikes from closely spaced recording sites. By comparing these extracellular tetrode signals with simultaneously recorded intracellular signals, it was determined that several intracellular parameters can be deduced from extracellular recording. Such parameters include the width and changes in amplitude of the intracellular action potential as well as the speed with which a signal travels throughout the dendritic spine of the neuron. It was also determined that a tetrode placed in the CA1 area of the hippocampus should be able to accurately discriminate 60 to 100 neurons. However, in the study an average of only 6 units were usually recorded by a tetrode, leading to the conclusion that perhaps a large percentage of hippocampal CA1 neurons are silent in any given behavioural condition (Henze et al., 2000).

1.2.2 Tetrode use in Cat Area 17 (the Cat Striate Cortex)

In an effort to characterize neuron arrangement in cat area 17, Hetherington and Swindale employed tetrodes and cluster analysis techniques (Hetherington & Swindale, 1999). It was feared that previous studies of the topographic map of the visual field in area 17 were

marred by the use of subjective plotting methods, sequential recording of single units, and residual eye movements. The use of tetrodes helped to eliminate these biases. Through the ability to record up to 11 neurons simultaneously, 355 units were recorded at 72 sites and it was concluded that cortical maps of orientation and receptive-field position were even more organized than previously thought. The tetrodes used in this study were constructed of 25 μm nichrome wires yielding an overall diameter of 50 μm and a maximum tip spacing of 35 μm. The tetrode signals were digitized at 32 kHz per channel.

The cat striate cortex was one of the first areas besides the hippocampus in which the tetrode was used successfully. Implementation of the tetrode in this area sought to overcome the errors associated with recording form multiple units simultaneously using a single electrode or multiple single electrodes, the ultimate goal being to investigate cortical network function in this area (Gray et al., 1995). Cell discharges in the cat visual cortex decrease in spike amplitude and increase in spike width during the course of a burst, yielding action potentials of different waveforms resulting from the same cell (Gray, 1992). This creates potential problems with cell classification, resulting in the wrongful identification of multiple cells even though only one cell is present.

The tetrodes used by Gray et al. in the cat striate cortex were constructed of 12 μm nichrome wire. The wire tips were plated with gold and subjected to a DC current until the impedance of the tetrode wires was in the range of 0.5-1.0 MΩ. Tetrode signals were digitized at 30 kHz per channel. Gray et al. compared recordings made by single electrodes, stereotrodes and tetrodes. They determined that tetrode methods reduced classification errors of incomplete segregation of adjacent clusters and the lumping of two or more units into a single cluster (Gray et al., 1995). Also, the tetrode produced the best results in the case of

the burst-firing cells in which the amplitude and time course of the action potentials change during the burst. This was due to the constant ratio of the spike amplitude across all channels. In light of these advantages, it was determined that the tetrode was well suited to the study of small groups of neurons within a highly localized region of cortex (Gray et al., 1995; Maldonado, 1997).

1.2.3 Separation Reliability of the Tetrode

The error rates for tetrode recordings are difficult to estimate. Harris et al. attempted to determine whether or not tetrode recordings and spike sorting methods were accurate by simultaneously recording from a cell with both an extracellular tetrode and an intracellular glass pipette (Harris et al., 2000). Harris et al. concluded that manual spike classification errors were usually between 0-30% but could exceed 50% during periods of synchronous population cell discharges and that manual spike sorting errors are mostly due to humans' inability to visualize the full high-dimensional cluster space.

It was found that the synchronous discharge of nearby neurons increases clustering errors in which spikes from different neurons are grouped together. One of the inherent problems in this case is the superimposition of spikes emanating from two different but simultaneously firing neurons. Smaller neurons firing simultaneously could generate spike amplitudes large enough to be mistakenly identified as emanating from a cell displaying larger spike amplitudes. Also, if a cell fires during the spike of another neuron, the waveform amplitude and shape could be altered to the extent that the resulting spike is omitted from all clusters. Harris et al. found that the best currently available solution to the manual clustering errors was to employ a semi-automatic clustering approach in which computer algorithms

made a first attempt to sort cell spike data and then a human operator inspected and made appropriate changes to the clusters (Harris et al., 2000). This approach greatly accelerated the clustering process as well as greatly reduced spike classification errors.

Finally, Harris et al. concluded that spike classification error rates were approximately doubled when using a single wire as compared to using a tetrode. Thus, spike separation is significantly more effective when multiple sites are used for unit recording (Harris et al., 2000).

1.3 Organization of the Superior Colliculus

1.3.1: The Superior Colliculus is a Laminar Structure

The superior colliculus is a laminar structure consisting of seven distinguishable layers when viewed in the dorso-ventral axis (Figure 2, p.11). Kanaseki and Sprague (1974) have labeled seven layers in the SC based on their cyto-architectural studies (Figure 2). They are, from superficial to deep: stratum zonale (SZ), stratum griseum superficiale (SGS), stratum opticum (SO), stratum griseum intermediale (SGI), stratum album intermediale (SAI), stratum griseum profundum (SGP) and stratum album profundum (SAP). It has been generally accepted that these seven layers can be grouped into two distinct regions based on function (Casagrande et al., 1972; Harting et al., 1973). These regions are the superficial layers, consisting of the SZ, SGS, and SO, and the deep layers, consisting of the SGI, SAI, SGP, and SAP.

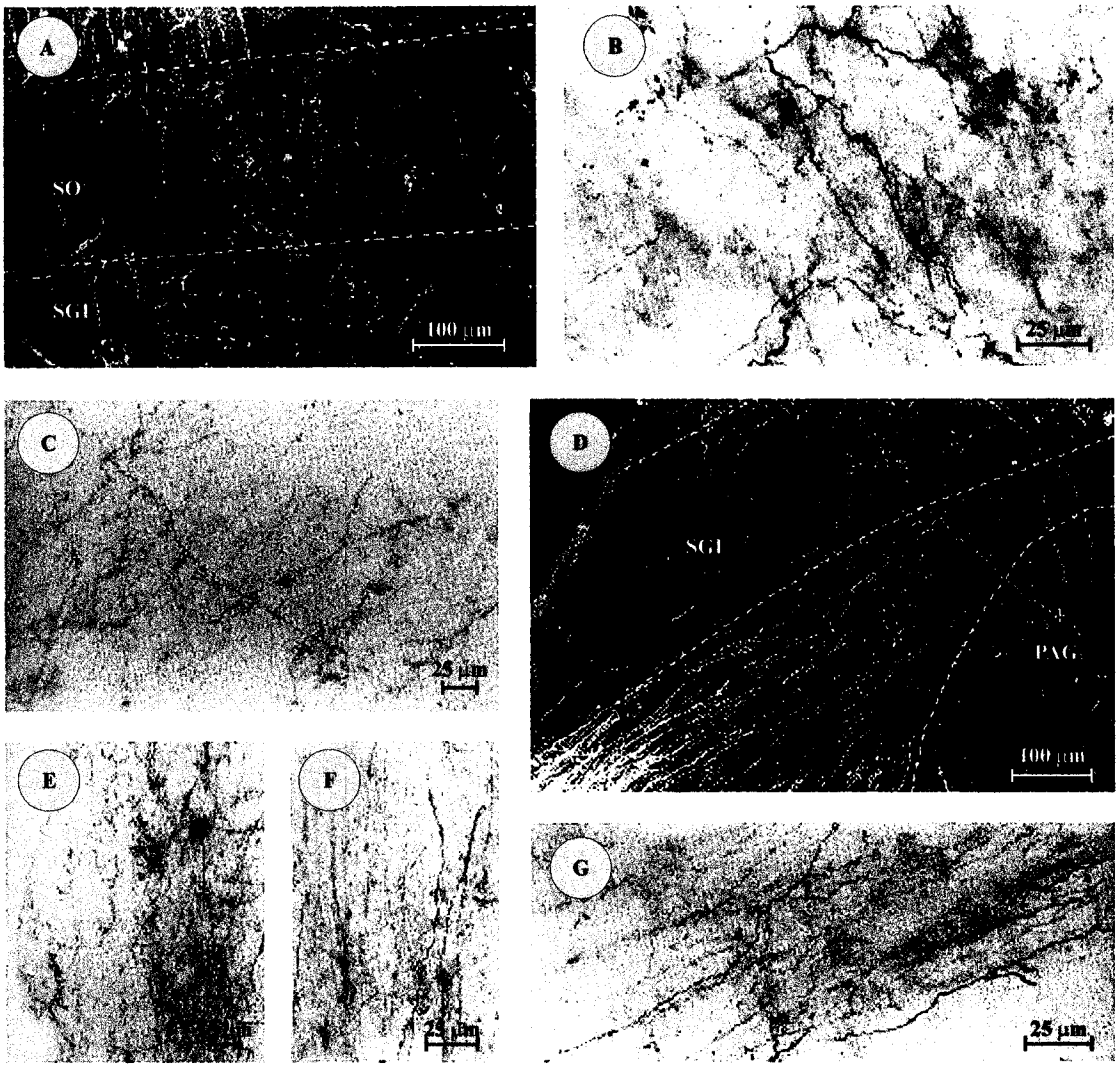

Figure 2 A demonstration of interlaminar connections in the SC using PHA-L as an anterograde tracing agent injected in the SGS. **(A)** Darkfield and **(B)** brightfield photomicrographs of the same section of the SO layer showing PHA-L labelled fibres resultant from an injection in the SGS. Although the fibres passed through the layer without giving rise to extensive terminal arbors, en passant swellings can be seen. **(C)** Once the axons reach this section of the SGI, both en passant and terminal swellings are observed. **(D)** In this darkfield photomicrograph of the SAI, SGP, and SAP, axons course laterally and leave the SC without extensive termination in these layers. The axons shown in **(D)** give rise to terminals in the parabigeminal nucleus, shown in **(E)**, and the dorsolateral pons, shown in **(F)**. **(G)** After descending through the SGI, labelled axons form another dense terminal field in the SGP. Adapted from Rhoades et al., 1989.

The superficial layers are primarily concerned with visual processing as they receive input from components such as the retinae, pulvinar, striate cortex, and extra-striate visual cortex. The cells in these layers are organized retinotopically (Chalupa, 1984) with each colliculus representing the contralateral visual hemifield. This organization has the central visual field located in the rostral SC while the peripheral visual field is located in the caudal SC (Cynader & Berman, 1972; Feldon et al., 1970). It has also been observed that the cat SC includes a representation of the ipsilateral visual hemifield that extends up to 40 degrees. This representation is not present in the SC of humans or monkeys.

The deep layers appear to be largely involved with motor processing of eye and head movements as many of their efferents project to brainstem structures implicated in eye and head motor control. Many electrophysiological studies have shown that microstimulation of the deep layers of the SC in cats and monkeys evoke eye or gaze saccades (Anderson et al., 1998; Freedman et al., 1996; Harris, 1980; Paré et al., 1994b; Robinson, 1972; Roucoux et al., 1980; Schiller and Stryker, 1972; Segraves & Goldberg, 1992). The amplitude and direction of these evoked gaze shifts correspond to the locus of stimulation on the retinotopically organized map of the SC. Thus, a motor map exists in the deep layers that seems to correspond to the retinotopic map of the superficial layers. The similarity of the maps is suggestive of interlaminar connections in the SC between superficial and deep layers. An example of SC interlaminar projections is demonstrated in Figure 3, p.13. Here, an injection of Phaseolus vulgaris leucoagglutinin (PHA-L) has been injected into the most superficial layer of the SC, the SGS, in an axonally rich area. Anterograde transport of this tracer substance by the axons shows that axons originating in the SGS pass through the SO without much sign of termination (Figure 3A), but en passant swellings are present

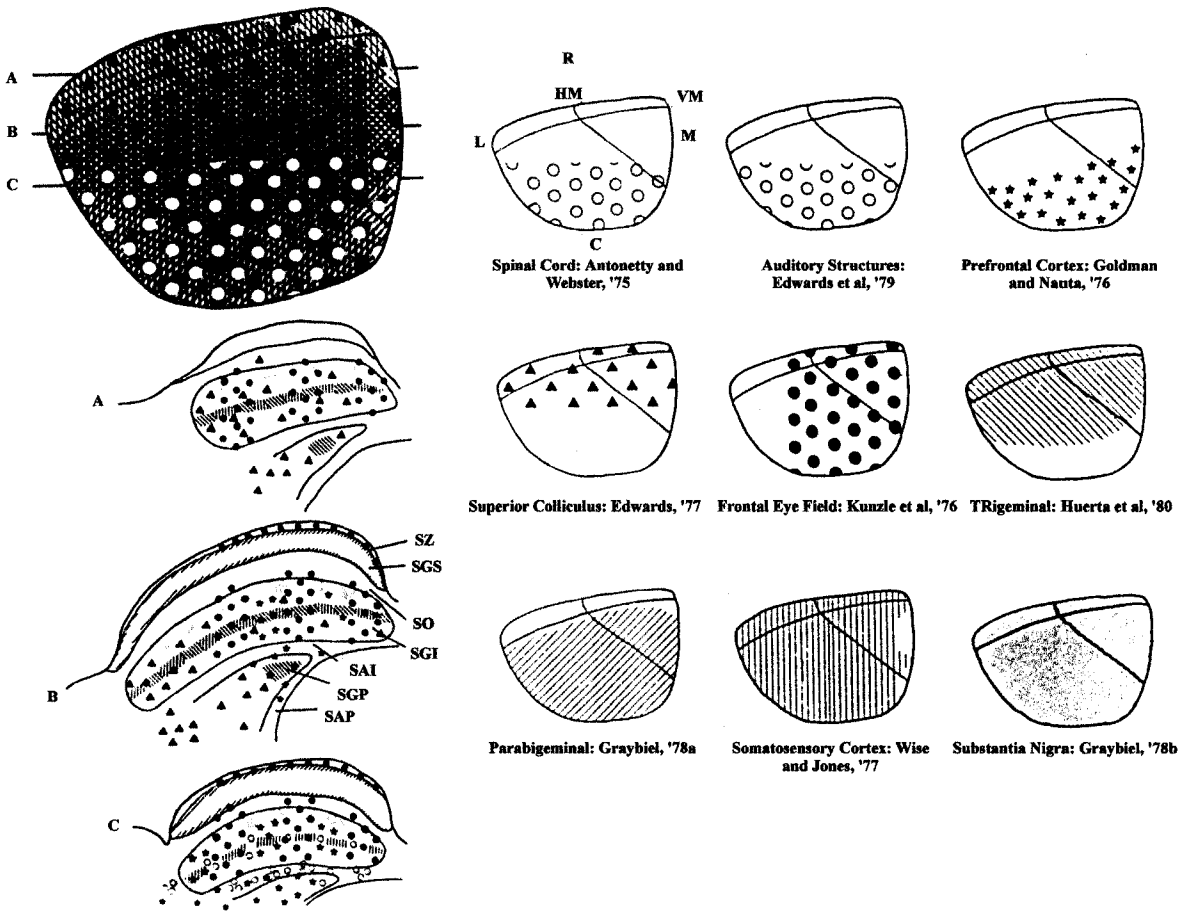

Figure 3 A summary of some of the afferent connections to the SC, mostly in cat. A dorsal view of the locations of the terminal fields of the afferents is shown at top left. The afferents are shown in individual sections at left. Medial is to the right and rostral to the top. Three frontal sections are shown at bottom left taken at levels indicated above. Taken from Huerta and Harting in Vanegas, 1984.

(Figure 3B). In the SGI the axons end in both dense terminal and en passant swellings (Figure 3C). Some labelled axons in the SAI region innervate the colliculus (Figure 3D) and go on to terminate in the parabigeminal nucleus (Figure 3E) and the dorsolateral pons (Figure 3F). The remaining labelled axons continue through the SC and course into the SGP where they end in dense terminal fields (Figure 3G). This axonal trajectory with terminations in various layers is clearly indicative of interlaminar connections in the SC. Although it is generally assumed that the superficial to deep layer connection is important for the visual responsivity of deep-layer neurons, the specific functional relationships between the neurons in the SGS, SAI, and SGP remain unclear.

Like the superficial layers, the deep layers have a topographical map of visual space and the neurons which contribute to this map are in spatial register with those in the superficial layers. In approximate spatial relation to this visual map in the deep layers are topographic maps of auditory and somatosensory space as well as a motor map (Drager & Hubel, 1976; Stein et al., 1976; Stein, 1981). The similarity in spatial organization of these maps as compared to those of the superficial layers may indicate that the level of connectional organization present in the deep layers is at least as high as that present in the superficial layers.

1.3.2 Collicular Connectivity

A) Collicular Afferents

Most afferent axons to the superficial layers are organized as a continuous sheet extending both medio-laterally and rostro-caudally. These afferents originate predominantly from the ventral lateral geniculate nucleus (Edwards et al., 1974), the parabigeminal nucleus (Figure 4, p.16: Graybiel, 1978a), the contralateral retina (Harting and Guillery, 1976), and the striate cortex (Updyke, 1977; Tigges and Tigges, 1981). Unlike the horizontal distribution in the horizontal plane, afferents to the SGS are very restricted in the dorso-ventral plane. This has lead to further division of the superficial layers into sublaminae. The organization of the efferents from the superficial layers have a similar horizontal organization which reinforces the idea of sublaminar divisions, as discussed below.

It has been observed that many neurons in these sublaminae have dendrites that can extend into adjacent sublaminae in the SGS. Also, there is some overlap of the afferent projections to the SGS sublaminae. This may indicate that the independence of the information channels flowing through the SGS is compromised by 'cross-talk' between otherwise separate information channels. This is to say that efferent collicular neurons are primarily influenced by a single input channel, but their efferent signals could be modified by a secondary input signal in the SC.

Unfortunately, the connections of the intermediate and deep layers of the superior colliculus are less clear than those of the superficial layers. The bulk of the afferents to these layers come from cortical and subcortical structures (Figure 4, p.16). It is suspected that the deep layers are also subdivided into sublaminae based on afferent and efferent connections and are restricted in the dorso-ventral plane. This is true in the case of the projection of the

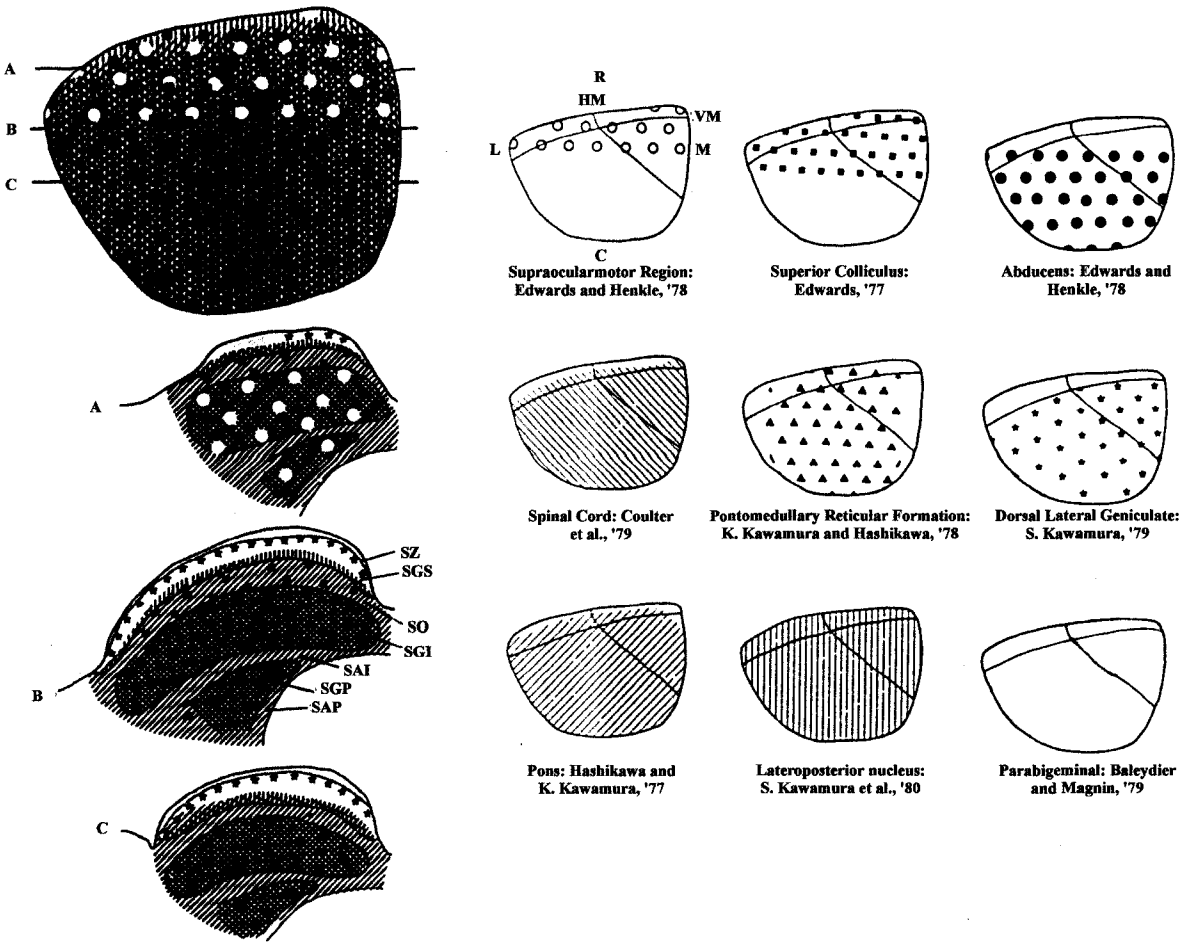

Figure 4 A summary of some of the efferent connections from the SC based on HRP retrograde transport studies, mostly in cat. Tectofugal neurons are shown at top left in a dorsal view; this view is shown in individual efferent sections to the right. Medial is to the right, rostral is at the top. Three frontal sections of the levels indicated above are shown at bottom left. This data is based largely on information gathered from the cat. Taken from Huerta and Harting in Vanegas, 1984.

substantia nigra whose axons enervate only the dorsal border of the SGI. Also, afferents from the nucleus of the posterior commissure terminate in a region below the substantia nigra projection while the spinal trigeminal nucleus terminates in an even more ventral region (Graybiel, 1978a; Huerta et al., 1981b; Huerta and Harting, 1982b). Another example of this spatial distribution are the afferents from the hypothalamus which terminate in regions specifically along the ventral, dorsal, and lateral borders of the SGI.

Interestingly, the inputs to the deep layers of the SC do not form continuous sheets that extend medial-laterally, like those of the superficial layers. Instead, the incoming fibres have a discontinuous distribution in this dimension, organized in patches when viewed in horizontal sections. These patches are also limited to a particular zone of the dorso-ventral extent of a given layer. This is to say that many structures project to the deep layers of the SC in both a stratified and discontinuous manner. Examples of such structures include the prefrontal cortex (Goldman & Nauta, 1976; Beckstead, 1979), the frontal eye fields (Kunzle et al., 1976; Leichnetz et al., 1981), somatosensory cortex (Wise and Jones, 1977; Stein et al., 1983), the hypothalamus (Harting et al., 1979), the nucleus of the posterior commissure (Huerta & Harting, 1982b), the spinal trigeminal nucleus (Tashiro et al., 1980; Huerta et al., 1981a,b, 1983), the deep nuclei of the cerebellum (Kawamura et al., 1982; Sugimoto et al., 1982; Uchida et al., 1983), and the spinal cord gray (Antonetty & Webster, 1975). Other notable intermediate and deep layer afferents include the substantia nigra (Ficalora and Mize, 1989), the zona incerta (Ficalora and Mize, 1989), and the contralateral colliculus (Appel and Behan, 1990).

There are several notable differences between the medial and lateral areas of the deep layers in terms of afferents. Patchy afferents located in the medial regions of the SGI are

generally smaller and more dense than are those situated more laterally. Also, there is a greater number of efferent projecting neurons in the lateral regions. It has been suggested that these medial-lateral variances may mediate different behavioural modes (Kilpatrick et al., 1982).

Some afferents to the deeper layers may also form patches in the form of bands stretching in the rostral-caudal direction. Structures whose projections may form such bands include the substantia nigra (Graybiel, 1978b), somatosensory cortical neurons (Flindt-Egeback, 1979), the spinal trigeminal nucleus (Huerta et al., 1982a, b, 1983), and the nucleus of the posterior commissure (Huerta &Harting, 1982b). Meanwhile, some inputs, like commissural (Edwards, 1977), are observed to terminate in patches exclusively in the rostral portion of the deeper layers while other inputs, like those of the inferior colliculus, seem to terminate exclusively in caudal areas.

The organization of the deep layers of the SC is not easily divided into sublaminae, as are the superficial layers. Instead, the afferent regions of the deeper layers are patchy and stratified in the dorsal-ventral extent. This may indicate that the deep layers are constructed of afferent modules, a term used to describe the separation of afferents into subdivisions of sublaminae. Thus, if the afferent and efferent systems of the deep layers of the SC are to be closely located, as they are in the superficial layers, the cells of efferent channels must be organized in clusters corresponding to patches of afferents, or longitudinal bands, corresponding to inputs arranged in bands. Of course, as is the case in the superficial layers, several afferents from different regions may be responsible for the output of given cells with efferent projections. If this is the case, the cells of origin of an efferent projection would be scattered throughout the deeper layers.

B) Collicular Efferents

The organization of efferent projections contribute to the division of the SC into distinct layers (Figure 2, p.11; Figure 5, p.20). In correlation with the afferent connections described above, the efferents from the superficial layers project foremost to nuclei related to vision while intermediate and deep layers project to assorted areas, including motor areas related to eye and head movements.

Some important examples of collicular efferent projections include those to the thalamic nuclei, such as to the latero-posterior pulvinar complex, the dorso-lateral geniculate nucleus, and the ventral-lateral geniculate nucleus (Harting et al., 1973 a,b,c). These projections stem largely from the superficial layers of the colliculus. Once passed to the various thalamic nuclei, information emanating from the colliculus can reach many different cortical zones.

Similar to the afferent connectivity of the SC, the efferent connectivity is organized in an even distribution in the SGS along the rostro-caudal and medial-lateral directions. Another similarity lies in the observation that the efferents are restricted to distinct levels in the dorso-ventral plane. Prime examples of this restriction in the cat are the tecto-geniculate neurons that lie in the dorsal SGS while tecto-pulvinar neurons lie in the ventral SGS (Figure 5, p.20: Kawamura & Kobayashi, 1975; Kawamura et al., 1980; Spreafico et al., 1980; Caldwell & Mize, 1981; Rodrigo-Angulo &Reinoso-Suarez, 1982; Mize, 1983a). Also found in the superficial layers is a projection to the parabigeminal nucleus (Harting et al., 1973a). These tecto-parabigeminal efferents originate in the SGS and SO layers. Interestingly, the lateral tegmentum just adjacent to the parabigeminal nucleus is innervated by connections originating from the deeper collicular layers (Graybiel, 1978).

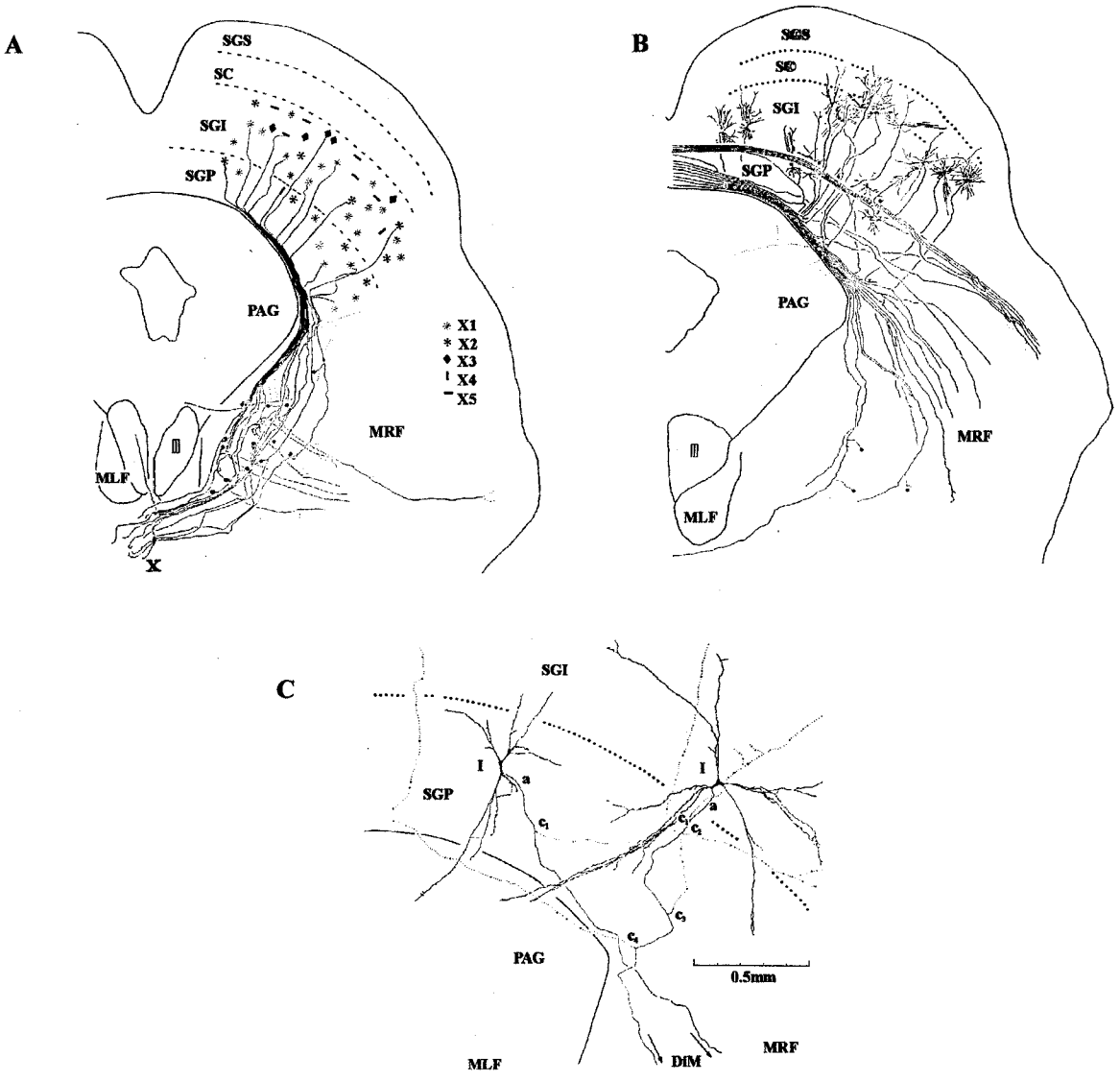

Figure 5 Examples of X, T, and I neurons and their laminar distribution and axonal trajectories throughout the SC of the cat. (**A**) X neuron axons follow the edge of the PAG and branch into ipsilateral collaterals before their decussation. Solid circles indicate points where ventral ascending collaterals of X axons assume rostral trajectory. Solid circles outside the MRF and PAG regions indicate points where the axons bifurcate into other tracts. (**B**) Solid circles in the MRF indicate points where collaterals of crossed descending T axons assume rostral trajectory. (**C**) I axons (*a*) contribute to the descending (DiM) ipsilateral tectofugal bundle. Recurrent collaterals emanate from both I neurons (c_1-c_4). Adapted from Moschovakis and Karabelas, 1985.

The intermediate and deep layers are the source of a larger variety of efferents than the superficial layers. The two major efferent pathways are the ipsilateral tecto-pontine and the contralateral tecto-reticulo-spinal (predorsal bundle) descending tracts. These tracts relay to various regions including nuclei in the pons, the abducens nucleus, the brainstem reticular formation and nuclei (Hashikawa and Kawamura, 1977), and regions in the cerebellum (Weber et al., 1978). These descending tectofugal pathways are involved in various functions including head, neck, and limb movements, eye movements, and pinna movements (Vanegas, 1984).

Another division of the intermediate and deep layer SC efferents is that of the ascending pathways. These tracts project to both motor and sensory nuclei. Destinations include the pretectum, the Edinger-Westphal nucleus, and the rostral interstitial nucleus of the medial longitudinal fasciculus (all discussed by Harting et al., 1980). These tectofugal projections are known to be involved in movements of the eyes, movements of the pinnae, movements of the head, and relaying information to cortical regions such as visual areas.

Moschovakis and Karabelas have created a system of classification for several types of efferent neurons residing in the deeper layers of the SC of squirrel monkey (Moschovakis & Karabelas 1985). The term 'X neuron' has been given to those neurons whose perikarya are large, shape is multipolar, and whose axons join the predorsal bundle. They reside in the SGI and SGP. X neurons are further divided into five subgroups, X_1 through X_5, based on cell size, dendritic organization, location in the SC, and relative abundance. All X neuron axons follow a common trajectory, projecting to the predorsal bundle (Figure 6A, p.23).

A second cell classification of Moschovakis and Karabelas is the T neuron. These are smaller neurons whose axons contribute to commissural projections of the SC (tecto-tectal

projections) as well as at least one other projection of the SC. Such projections include medial descending ipsilateral, lateral descending ipsilateral, medial dorsal ascending, and the predorsal bundle (Moschovakis & Karabelas, 1985) (Figure 6B). T neurons are divided into two subgroups based on somatic variation; T_1 and T_2.

A third group of neurons whose axons course caudally through the ipsilateral dorsal MRF and join the medial descending ipsilateral bundle are called I neurons (Figure 6C). These neurons reside in the SGI and SGP and their dendritic trees extend into adjacent layers of the SC as well as beyond the boundary of the SC in certain cases.

These neurons are either directly or indirectly related to the ascending or descending pathways involved in saccade generation. Although they are now readily identifiable and their tectofugal projections known, the knowledge of their functions and the extent of their interconnections is speculative at best. With continually improving models and experimental techniques, it should be possible to further characterize these cells.

C) Local Circuitry and Tecto-Tectal Connections

Even given these specific examples and elaborate descriptions of the relative location of cells and their afferent and efferent projections, it remains largely unknown how collicular cells form the local circuits in which these types of signals are transferred from input to output. It seems that most input channels bear consistent spatial relationships to cells of origin of specific output channels. An example of these tightly coupled afferent and efferent patches is that of the spinal trigeminal nucleus to SGI of the SC and vise-versa. The contralateral projecting colliculo-trigeminal cells in the SGI are located within the patches of

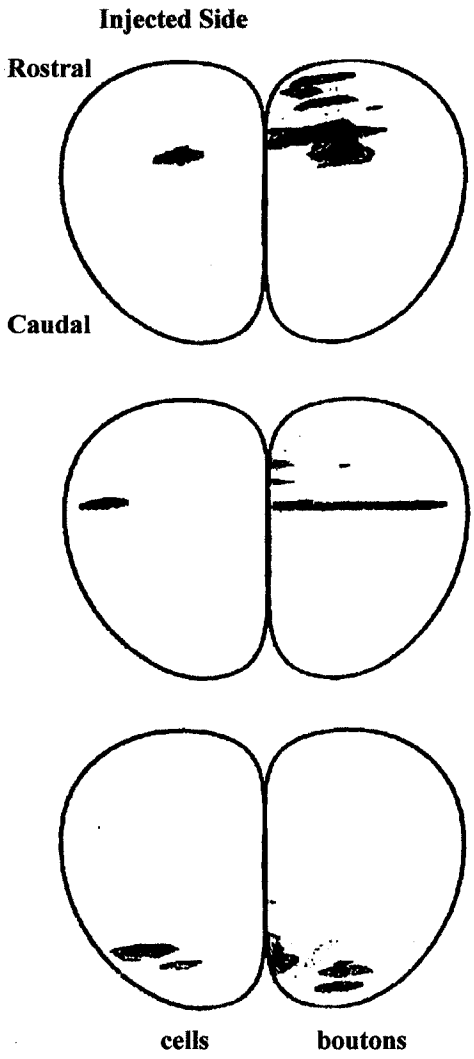

Figure 6 Three cases of biocytin tracer labelling of tectotectal connections in the SC of the cat. The SC is seen from a dorsal perspective with the rostral pole at the top while the caudal pole is at the bottom of the diagram. The left colliculus shows the injection site of the biocytin. The right colliculus shows the labelled cells and boutons. Top: injection in the intermediate layers labels cells in the intermediate layers in the same rostro-caudal extent of the opposite colliculus as well as cells in the rostral pole. Middle: injection in the deep layers labels cells in the deep layers in the same rostro-caudal extent of the opposite colliculus. Bottom: injection in the deep layers labels cells in the deep layers of the opposite colliculus in the same rotro-caudal extent. This labelling is indicative of the presence of tectotectal circuits. Taken from Behan and Kime, 1996.

the contralateral trigeminal input; a presentation of tightly coupled modules of afferents and efferents.

However, these observations have been identified largely by light microscopy, slice preparations, and retrograde or anterograde transport labeling. These methods are effective for identifying relative cell type, size, and position, but they are insufficient for identifying cellular inter-connection. A non-traditional approach has recently been undertaken that hopes to clarify the local circuitry of the SC. Using photostimulation and whole cell patch-clamp methods, some local excitatory circuits in the intermediate gray layer of the SC have been deciphered in the tree shrew (Pettit et al., 1999). It has been found that local circuits in the intermediate gray are excitatory and contribute to pre-saccadic motor commands. In particular, it is thought that these circuits provide the substrate for positive feedback that sustains and intensifies the low-frequency activity that precedes the command burst for a saccade. Also, these neurons may contribute to the prolonged bursts of excitatory post synaptic currents observed in intermediate layer neurons in response to electrical stimulation of sensory inputs from the superficial layers (Lee et al., 1997).

Recently, it has been discovered that as well as having interlaminar connections within a single colliculus, the SC also has intercollicular connections, referred to as tectotectal connections (Behan & Kime, 1996). Again, through use of anterograde tracers, this time Biocytin, it was found that there exist tectotectal neurons in the rostral two thirds of the deep layers (Figure 7, p.25). In fact, the two SC have mirror-like symmetry across the midline as there is frequent point-to-point correlation between them, especially in the fixation zone, an area in the intermediate to deep layers of the rostral colliculus that houses cells whose activity contribute to fixation of the eyes. Biocytin injections in the various locations of the SGS of

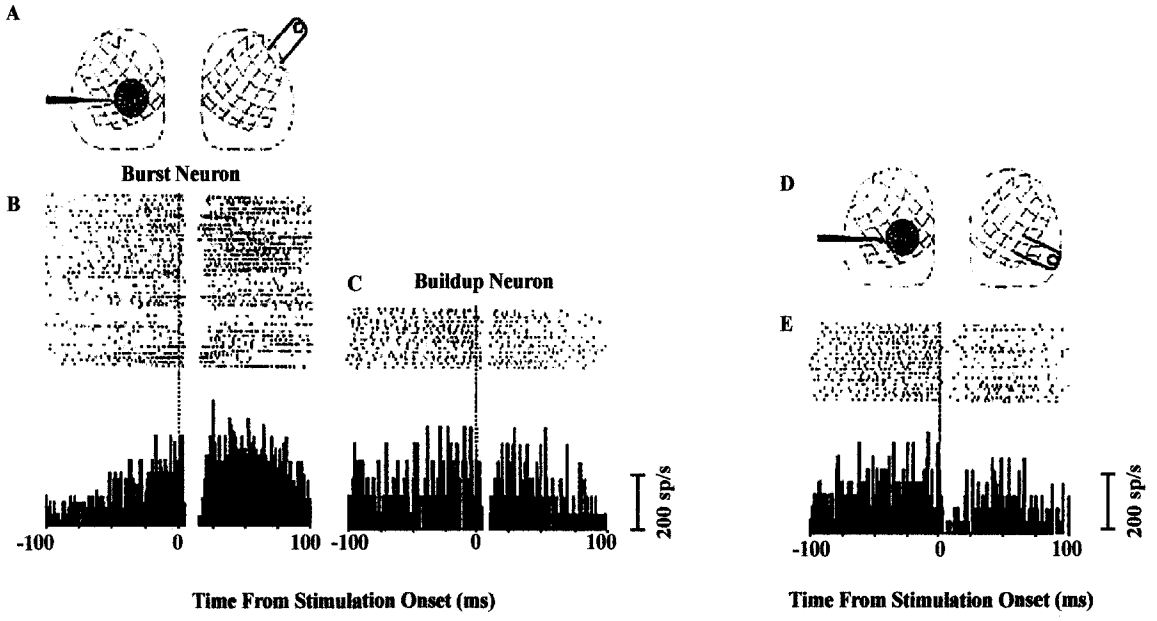

Figure 7 A demonstration of possible tecto-tectal connections in the SC of the monkey taken from Munoz and Istvan, 1998. (**A**) Placement of a recording electrode in the saccade region in the left colliculus while a stimulating electrode is placed in the fixation zone of the right colliculus. (**B**) Recording from a burst neuron and (**C**) recording from a buildup neuron during stimulation while the monkey executed saccades of direction and amplitude that matched each cell's optimal saccade vector. (**D**) Placement of electrodes while recording from a saccade neuron during stimulation of the contralateral saccade zone. (**E**) The activity of a saccade neuron is interrupted by stimulation of the contralateral saccade zone.

one colliculus often labeled between 3 and 150 neurons in other layers (SO, SGI, SAI, SGP, and SAP) in the opposite colliculus. This is indicative of collicular neurons whose axons are probably wholly confined to routes between the colliculi, thus forming microcircuits. It is thought that many of the axons and boutons labeled using this method are probably recurrent collaterals of the T and I type cells described by Moschovakis and Karabelas. Since the colliculi serve to orient animals to the opposite hemifield, tectotectal connections might serve to inhibit neurons in the contralateral colliculus during eye movements; ie: an increase in activity of neurons in one colliculus would be associated with a decrease in activity of neurons in the other colliculus.

Douglas Munoz has investigated this hypothesis and has also determined that tecto-tectal connections exist, this time via electrophysiological methods (Munoz and Istvan, 1998). For example, during a saccade, stimulation of the contralateral fixation zone induced inhibition of saccadic neurons (burst and buildup) in the ipsilateral colliculus (Figure 8B, C, p.27). Similarly, stimulation of the contralateral saccade zone led to inhibition of saccade neurons in the ipsilateral saccade zone (Figure 8E, p.27). Also, fixation neurons in the ipsilateral colliculus were exited when the contralateral fixation zone was stimulated.

A large population of GABAergic neurons have been observed in the SC (for review see Mize, 1992; Okada, 1992). The size of these cells are almost always small and they are particularly present in the superficial layers, especially in the SGL. Mize has hypothesized that GABAergic cells situated horizontally in the superficial layers may be candidates for mediating long distance lateral inhibition across the collicular surface (Mize, 1992), given their extensive dendritic spread. Meanwhile, GABAergic pyriform and stellate type cells give rise to short, local axons and could be mediators of localized forms of inhibition. Okada also

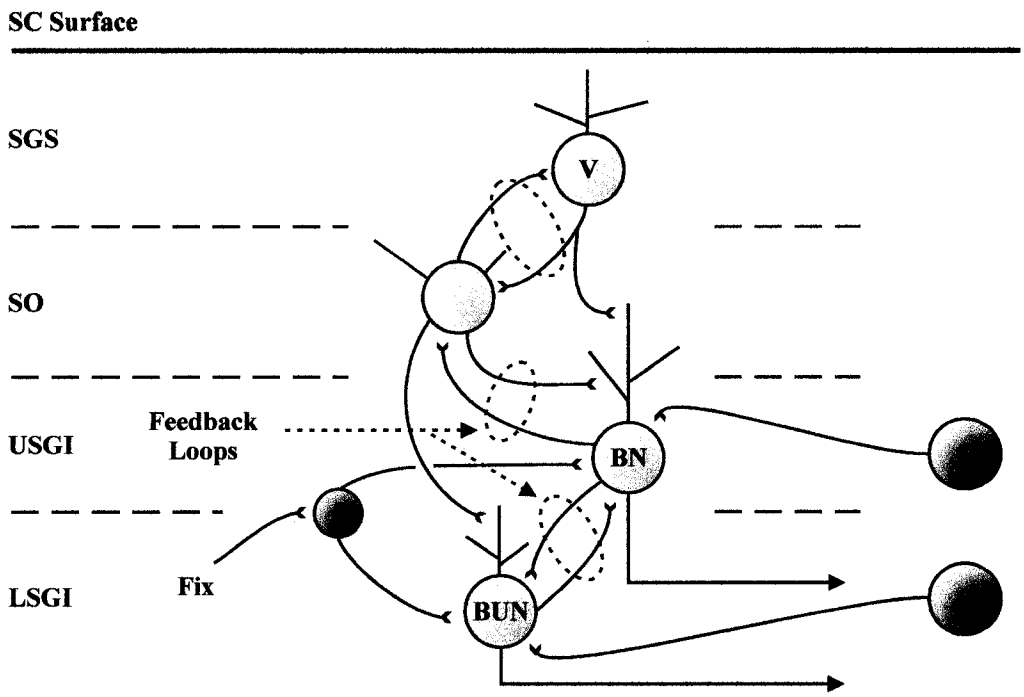

Figure 8 Example of possible local circuits in the SC (adapted from Lee et al. 1997, Grossberg et al. 1997,Munoz & Istvan, 1998, and Behan & Kime, 1996). Visual cells (V) in the SGS form connections with cells in the SO and with burst neurons (BN) in the upper SGI (USGI). The burst neurons form connections with buildup neurons (BUN) in the lower SGI (LSGI). Feedback loops may exist between the buildup neurons and the burst neurons as well as between burst neurons and neurons in the SO. It is also possible that feedback loops between neurons in the SO and visual cells in the SGS exist. Input from the rostral fixation zone (Fix) may modulate the activity of the burst and buildup neurons, perhaps via inhibitory interneurons (I). Commissural inputs (C) from the fixation and saccadic regions of the opposite colliculus may also modulate the activity of the saccadic cells.

supports the hypothesis that these GABAergic cells, especially in the SGL, are inhibitory interneurons responsible for mediating signals from certain collicular afferents (eg: the ispsilateral corticotectal pathway) (Okada, 1992). Further studies indicate the existence of horizontally oriented local circuits that may mediate a reciprocal relationship between fixation and saccade related neurons (Meredith and Ramoa, 1998). While stimulating certain neurons in the rostral or caudal regions of the SGI *in vitro*, the activity of various neighbouring neurons within the same layer was recorded. It was observed that many recorded neurons responded with a suppression of ongoing activity. The presence of GABAergic (inhibitory) interneurons was determined by the application of a GABA agonist. This was done in light of studies indicating that such neurons are capable of inducing inhibitory postsynaptic effects (Mize, 1992; Okada, 1992). Blocking the activity of the identified interneurons affected the responses of the neighbouring recorded cells upon stimulation. The previous responses of activity suppression were absent when these cells were blocked. Furthermore, the studied neurons were separated from the superficial layers by the severance of the SO from the SGI to ensure a lack of transmission via the well established circuits between the deep and superficial layers. This assured that the circuit was indeed local in the SGI. These studies are highly indicative that there are local circuits in the SC that are connected via inhibitory interneurons.

A depiction of possible local circuits in the SC is shown in Figure 9, p.33, providing a brief summary of the tectal interconnections described above. Adapted from Lee et al., 1997, Grossberg et al., 1997, Behan & Kime, 1996, and Munoz & Istvan, 1998, this diagram demonstrates possible connections and feedback loops between various types of neurons present in different layers of the colliculus as well as local same-layer circuits and circuits

formed with commissural inputs. Visual information received by neurons in the SGS could be fed down to intermediate layers of the colliculus where the input would be processed by burst (in monkey) and buildup neurons. These neurons could respond to the input by generating saccades. Also, inhibitory input from the rostral fixation zone could modulate the activity of the saccadic neurons, perhaps via inhibitory interneurons. These neurons could also be modulated be commissural inputs from the fixation and saccadic zones of the opposite colliculus. In addition to these saccade related inputs to the collicular circuitry, various other cortical inputs could also be present as the colliculus is a structure of multi-sensory input and output. Evidently, the processes by which saccades are generated are not elementary and much study is required to decipher the networks involved in such a task.

1.3.3: Cell Activity in the SC of the Alert Animal

There are a variety of different cell types in the colliculus that, based on recordings in alert animals, appear to contribute to saccade generation. A few predominant cell types are described below along with their characteristic activity.

A) Fixation Neurons

In the rostral region of the SC in the intermediate to deep layers can be found the fixation zone. When the eyes fix on a target, fixation neurons maintain a tonic activity. When a saccade is generated this tonic activity ceases slightly before saccade onset and resumes just before the acquisition of a new target. It has been observed that the duration of the pause of fixation cell tonic activity is correlated with the duration of the saccade. This is less evident in small amplitude saccades as some cells do not seem to decrease their firing rate in this case

(Munoz & Wurtz, 1993a). As described above, the saccade-related pause in fixation cell activity usually begins slightly before saccade onset. In monkeys, this pause precedes contraversive saccades by 36.2 ms and ipsiversive saccades by 33.0 ms (Munoz & Wurtz, 1993a). These cells also reactivate slightly before the termination of the saccade; 2.6 ms for contraversive saccades and 9.9 ms for ipsiversive saccades. Upon reactivation, fixation cells are often observed to increase their rate of discharge as compared to activity before saccade onset. This increased activity, that is not related to the presence of a visual target, lasts several hundred milliseconds. Given these characteristics, fixation cells are thought to suppress saccade generation by inhibiting, via inhibitory interneurons, saccade-related cells in the SC (Munoz & Wurtz, 1993a,b). Since fixation cells appear to pause no matter what the direction of the saccade, ipsilateral or contralateral, it is speculated that fixation cells are related to the generation of all saccades, be they generated by either side of the SC. This observation may support findings that indicate the presence of the tectotectal circuitry described above.

B) Buildup Neurons

Several hundred milliseconds before the onset of a saccade, buildup neurons commence their activity, indicating that they are involved in saccade preparation. Often the activity of these neurons will increase with saccade anticipation in the monkey (Munoz and Wurtz, 1995). Thus, actual generation of a saccade is not necessarily required for these cells to be active, only the anticipation that a saccade is to be made. These cells can usually be identified as those that have activities between the apparition of a visual target and the onset of a saccade to the target.

Many buildup neurons also display a burst of activity at the time of a saccade. This is to say that between the onset of a visual target and the onset of a saccade to the target, the buildup neurons discharge at a low frequency (>30 spikes per second) and the discharge frequency increases with the onset of saccade (≤94 spikes per second). For each location on the motor map, buildup neurons burst for a preferred saccade (gaze shift) vector. Other key features of buildup neurons are the aforementioned long-lead preparatory activity, attainment of peak low level (non-burst) discharge for a specific value of gaze motor error (the difference between current and desired gaze position), and the cells' peak burst discharge which occurs later in the movement for larger amplitude saccades (Munoz and Guitton, 1991). Buildup neurons tend to share the lower intermediate to deep layers of the SC with the fixation neurons, although their position is usually caudal to that of the fixation neurons.

C) Burst Neurons

The main characteristics of these cells are their inactivity during fixation and activity as a high frequency discharge immediately before the onset of saccades having a specific range of amplitudes and directions. Each cell has its 'preferred' saccade vector. These cells usually have discharge frequencies of about 100 spikes per second in monkey (Munoz & Wurtz, 1995). They too reside in the intermediate layers of the SC with the buildup neurons, although it is thought that they may form a more or less distinct layer, lying just dorsal to the layer of buildup neurons. It is uncertain as to whether or not burst neurons are present in cat.

D) Other Neuron Types

Besides the main types of SC neurons noted above that have been characterised in depth by various researchers, there are probably many more types of neurons present in the SC that have not been well characterised. Golgi studies such as those described above indicate that there are many different types of neurons present in the SC with great variance in size and shape and dendritic field characteristics (for examples: Norita, 1980 in cat; Langer & Lund, 1974 in rat). Some of these neurons may be GABAergic inhibitory interneurons, as described above (Mize, 1992; Okada, 1992). The activity of these types of neurons is unknown and, like their physical characteristics, could be very different from one another.

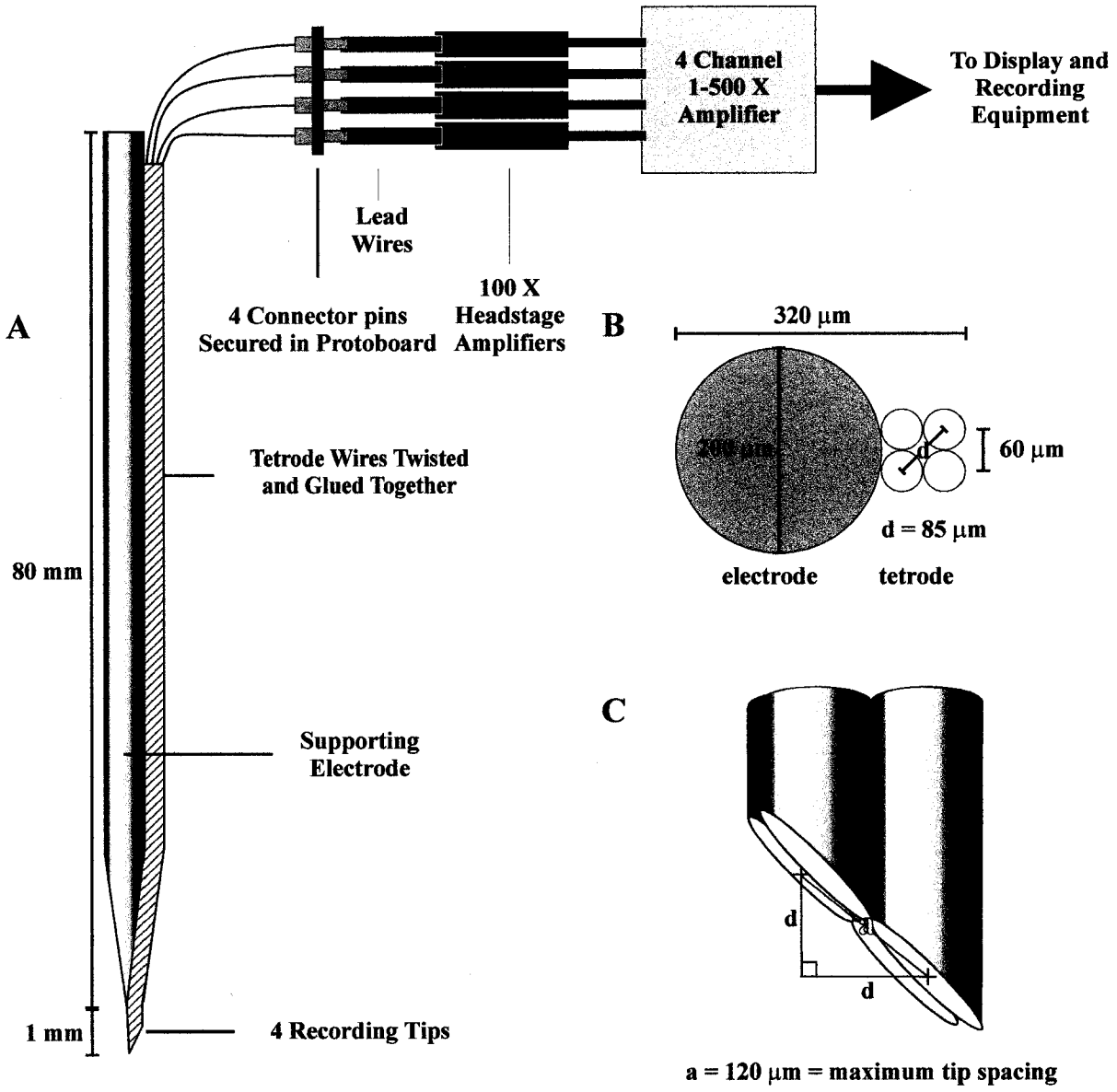

Figure 9 Schematic of a typical tetrode. (**A**) Four 25 micron wires are twisted and glued together forming the tetrode. The tetrode is affixed to a typical 200 micron tungsten electrode for support. The tetrode wires form leads to connector pins that are secured in a small protoboard providing increased security when handling the fine wires. The pins are connected to a 1-500x variable amplifier which relays signals to display and recording equipment. (**B**) A cross section of the tetrode shows the total diameter of the apparatus and the maximum distance between two recording wire tips in two dimensions. (**C**) In three dimensional space, the maximum tip spacing of the tetrode is 120 microns.

CHAPTER 2

METHODS

The data acquired for this work was obtained from four alert, trained cats that were trained and prepared for chronic recording in the superior colliculus.

2.1 Animal Training

The cats used as subjects in these experiments were first trained for the experimental procedure and subsequently surgically manipulated. Any program involving the animals was first approved by the McGill University Animal Care Committee and complied with the Canadian Council on Animal Care policy on use of laboratory animals.

The training of the cats involved very basic procedures and usually lasted about 14 days. First, the cat had to become accustomed to maintaining calm for periods of an hour while it was enclosed in a loosely fitting cloth bag, its head protruding. After the cat was familiarized with this arrangement, it was placed in a gently restrictive plastic box while in the bag. The box restricted body movements but allowed free movement of the head. The cat was fed while in the box so as to encourage calmness and patience. It was fed in such a manner as to encourage the generation of saccadic orienting movements (see below). When the appropriate response was elicited from the cat a reward of food was granted. Once the

cat could patiently endure this procedure over the course of two to three hours it was accepted for use in the experiment and submitted to the surgical preparations.

2.2 Animal Preparation

A detailed description of the surgical procedures is presented in Guitton et al., 1984, 1990 and Guitton and Munoz, 1991. First, the cat was appropriately anesthetized and its body temperature and breathing regulated. The head was secured in stereotaxic head holding equipment. The skull bone was exposed in the area where the recording implant was to be positioned. On the eye of the surgeon's choice, an eye coil was implanted using the standard technique described by Fuchs and Robinson, 1966. The eye coil consisted of a fine Teflon-insulated wire with three turns forming a ring with a long lead of two twisted wires. The coil was inserted by cutting and retracting the conjunctiva of the eye and suturing the wire coil to the globe of the eye. The lead from the eye coil was threaded through a surgical needle and pushed subcutaneously upwards close to the skull along the orbital bone so that it protruded through the opening made for the recording well. The ends of the two wires were soldered to female amphenol micro-miniature relia-tac connectors and inserted in a small, insulated housing.

With the stereotaxic reference of the head holder it was possible to estimate the coordinates of the SC to allow for recording cellular activity. A hole was drilled in the skull at a location permitting access by the tetrode to the SC. A hollow stainless steel cylinder 15 mm in diameter and appropriate for holding a micropositioning system was positioned on the cranial surface and mounted over this opening. This formed the 'well' through which the superior colliculus could be accessed. The well was affixed to the skull using dental cement.

A U-shaped crown was then imbedded in the posterior area of the well formation. This provided a point of contact with which an attachment could be made to a braking system in order to restrict the movement of the cat's head. Also, in certain subjects, a stimulating electrode was placed near the predorsal bundle. This allowed antidromic stimulation of SC output cells, the tecto-reticular neurons. Finally, the eye coil leads were cemented into the implant and their electrical resistance verified. The cat was administered antibiotics and was allowed a full two weeks of recovery before participating in the experiment.

2.3 Tetrode Construction

The tetrode consists of an array of four electrodes that are spaced closely together. These wires are not electrodes in the traditional sense of the term as they are not four rigid, thin, metal rods. Instead, they are four very fine wires with the insulation removed at the tips. The wire used in my experiments was 25 μm in diameter. A length of about half a metre of the wire was taken and folded in half twice. At one end of the folded wire there were two loops, while at the other there was one loop and two wire ends. The two loops at one end were placed over a metal rod which was held in a vice and projected off the edge of a counter. The loop and wire ends that hung over the edge of the counter from the rod were then clamped together using a hemostat. The hemostat was then turned repeatedly so that the four wires were twisted together. Once the wires were twisted together, leaving about 40mm untwisted at the end of the assembly nearest the rod, super glue was applied to the twisted wires, fusing them together. Once the glue had set, the wire assembly was cut at an angle near the hemostat using a pair of sharp surgical scissors. The loops over the metal rod were then cut leaving four lead wires. The insulation was removed from these wires via exposure

to a flame. To provide rigidity, the assembly of twisted wires was then glued to a traditional electrode that was 80-90mm in length and 200 microns in diameter. The four wire assembly extended about 1 mm past the tip of the support electrode at the recording end. At the non-recording end, the wires protruded by about 40 mm and were left separated from one another. Each wire lead was soldered into a male amphenol micro-miniature relia-tac connector (pin) so as to connect the tetrode to the rest of the recording apparatus. The pins were secured in a small, plain bare PC prototype board of 3.96 mm hole spacing (Vector Electronic Company) to make the tetrode easier to handle and more resilient. The pins protruded through the prototype board where they could be connected to relay wires and amplifiers. Super glue was used to hold the pins in place. A depiction of a tetrode assembly is shown in Figure 10A, p.38.

Before the tetrode could be used in an experiment it was tested for functionality and impedance. For this, a BL-1000 microelectrode tester from Winston Electronics Co. was used. Each tetrode wire was tested individually. Ideally, the impedance for each wire should lie between 1 and 3 MegaOhms. If a wire yielded very high impedance (>6 MegOhms) it was a sign that the construction was imperfect. Glue on the tip of the wire, improper soldering of the wire into the connector pin or improper removal of the insulation on the wire lead are the three most likely problems. If, after all necessary rectifications were made, any of the tetrode wires were still faulty the tetrode was not used for recording.

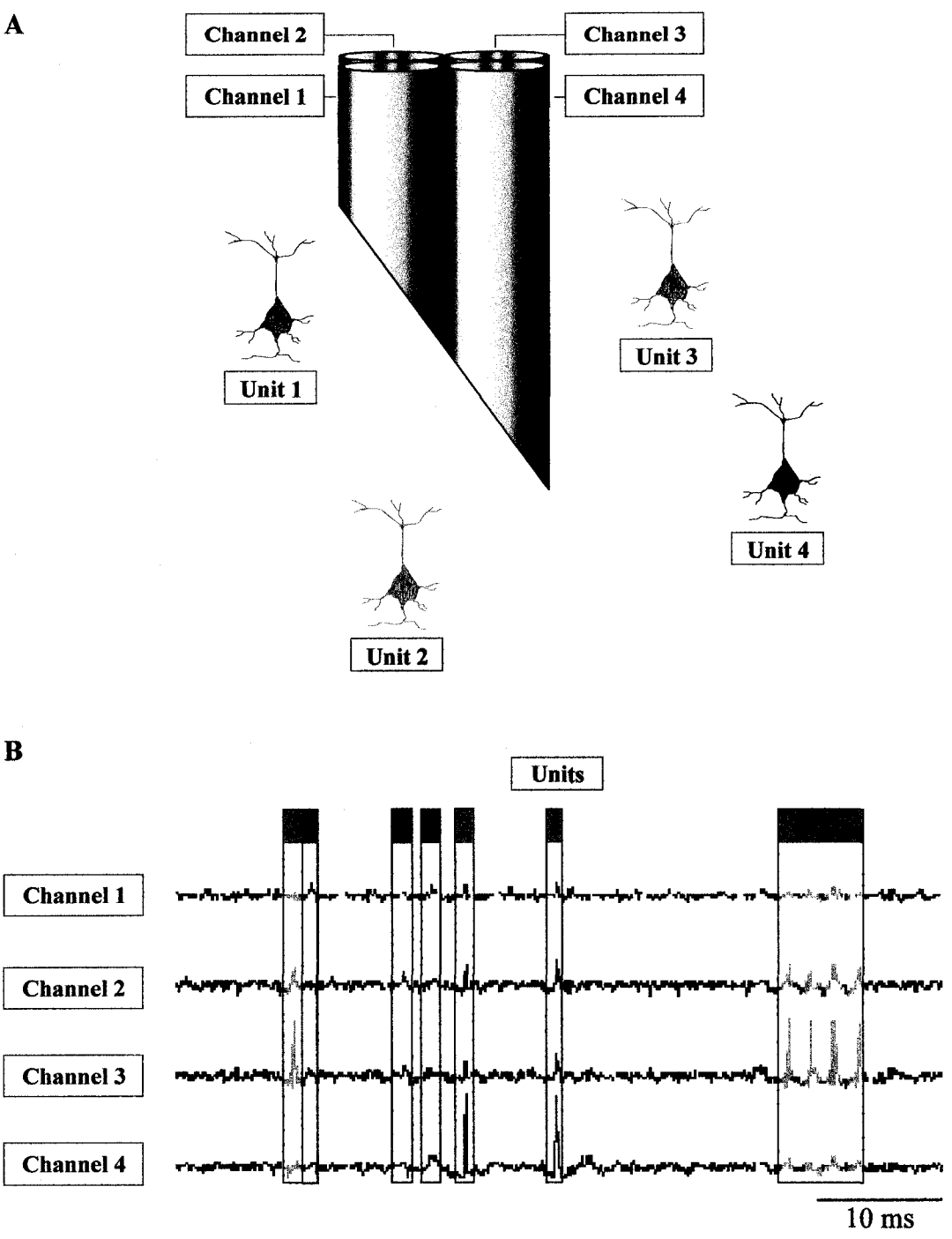

Figure 10 Depiction of a tetrode recording signals from four individual neurons. **(A)** The signal from each neuron is received with slight variance between the four different channels due to the differing spatial relationship between the neuron and the four wires. **(B)**With spike separation analysis, the four units **(1, 2, 3, 4)** are identified in the data. Each unit is present to some degree on all four channels.

2.4 Experimental Techniques

The search coil in magnetic field technique (Robinson, 1963) was used to measure the positions of gaze, head, and target relative to space. Details of the technique and the system used as well as calibration procedures have been summarized in Guitton et al., 1984. Briefly, calibration of the gaze and head coil signals was done by placing the coils in a calibration apparatus with three dimensional rotational ability. This apparatus was placed within the magnetic field and the coils were rotated horizontally and vertically. The coil signals were relayed to a computer monitor via an amplifier whose gain could be adjusted via a potentiometer. The spatial head and gaze signals were displayed on an image of a dartboard-like target on the computer monitor, showing the location of the head and gaze from the centre position (cat looking straight ahead). The signal amplifier was adjusted until the head and gaze signals on the target corresponded to the spatial positioning of the head and eye coils in the magnetic field. The target spoon used in the experiment was similarly calibrated.

2.5 Behavioural Paradigm

A simple behavioural paradigm was designed to elicit a large number of coordinated eye-head displacements of various amplitudes from the alert cats. The cat was put in the restrictive bag and box and which was secured on a platform in the centre of the magnetic field system. The cat's head was left unrestricted. An opaque barrier was placed 40 cm in front of the cat and the target spoon, laden with pureed cat food, was hidden behind it. By making the spoon appear to either side of the vertical barrier, the hungry cat made gaze displacements to the food target. When the behaviour of the cat matched the desired response, the cat was rewarded with the food on the target spoon. Slight variances of this

paradigm were employed so as to fully study the responses of recorded cells. Various amplitude gaze shifts were elicited by using barriers of varying widths. Often, the ambient light status was varied from light to dark 120 ms after the appearance of the food target so that gaze shifts were performed in complete darkness (memory guided gaze shifts). The ambient light was extinguished for 1 s. The light source used was a fluorescent bulb with a rapid decay time (~100 ms).

During the trials, it was useful to use antidromic stimulation or stimulation via the recording electrode in an attempt to locate collicular output cells next to the recording electrode within the colliculus. This was done using a train of electrical pulses whose duration varied between 10 and 500 ms. The pulse width was 0.3 ms, the pulse rate was 300 spikes per second, and the current amplitude was varied between 20 and 80 μA. The pulse trains were applied via a stimulating electrode in the predorsal bundle, if the cat was so implanted. Evoked gaze shift direction and amplitude were compared to a collicular motor map schema (Figure 13D, p.58, Figure 16D, p.61) in order to get a general idea of the placement of the recording electrode in the SC.

2.6 Data Acquisition

Neuron activity was detected with the tetrode which relayed signals to headstage amplifiers (100x) and then to a main amplifier (1-500x). From here the signals were transferred to a 32 channel data acquisition panel (DataWave Technologies) which supplied the signals to a 12 bit resolution DT2839 analog to digital (A/D) acquisition board. This board was configured through DataWave software, Experimenter's Workbench, which is an object oriented programmable software interface that operates through DOS. The signals

were sampled at 35.7 kHz per tetrode channel (Figure 11, p.42). The accompanying horizontal head, horizontal gaze, target, target appearance indicator, and light status signals (low frequency or 'slow wave' signals) were sampled at 1 kHz per channel. In all, nine data channels were registered and were displayed via Experimenter's Workbench on a computer monitor.

Only spike data, not all raw neuron activity data, is needed for cell characterization. Thus, on-line thresholds were set at appropriate amplitudes to trigger data recording (Appendix A.1). The thresholds were based on the level of background activity and were set on all four tetrode channels independently. A variety of threshold options were available. Several options were available for types of thresholds including positive peak time (the time at which the maximum peak amplitude of the spike occurs), negative peak time (the time at which the minimum valley amplitude of the spike occurs), positive slope crossing time (the time at which an event crosses the threshold while having a rising slope and then re-crosses the threshold before a user defined time limit), negative slope crossing time (the time at which an event crosses the threshold while having a negative slope and then re-crosses the threshold within a user define time limit), positive threshold crossing (any event crossing a positive threshold), negative threshold crossing (any event crossing a negative threshold), and positive or negative threshold crossing. The parameters used for these experiments were either positive or negative threshold crossing. The thresholds could be changed by the user on-line during an experiment. Each time a threshold was crossed, data was recorded for user defined periods before and after the event. With each threshold crossing, the recorded data (i.e.: the spike) was marked with a time-stamp accurate to the nearest tenth of a millisecond.

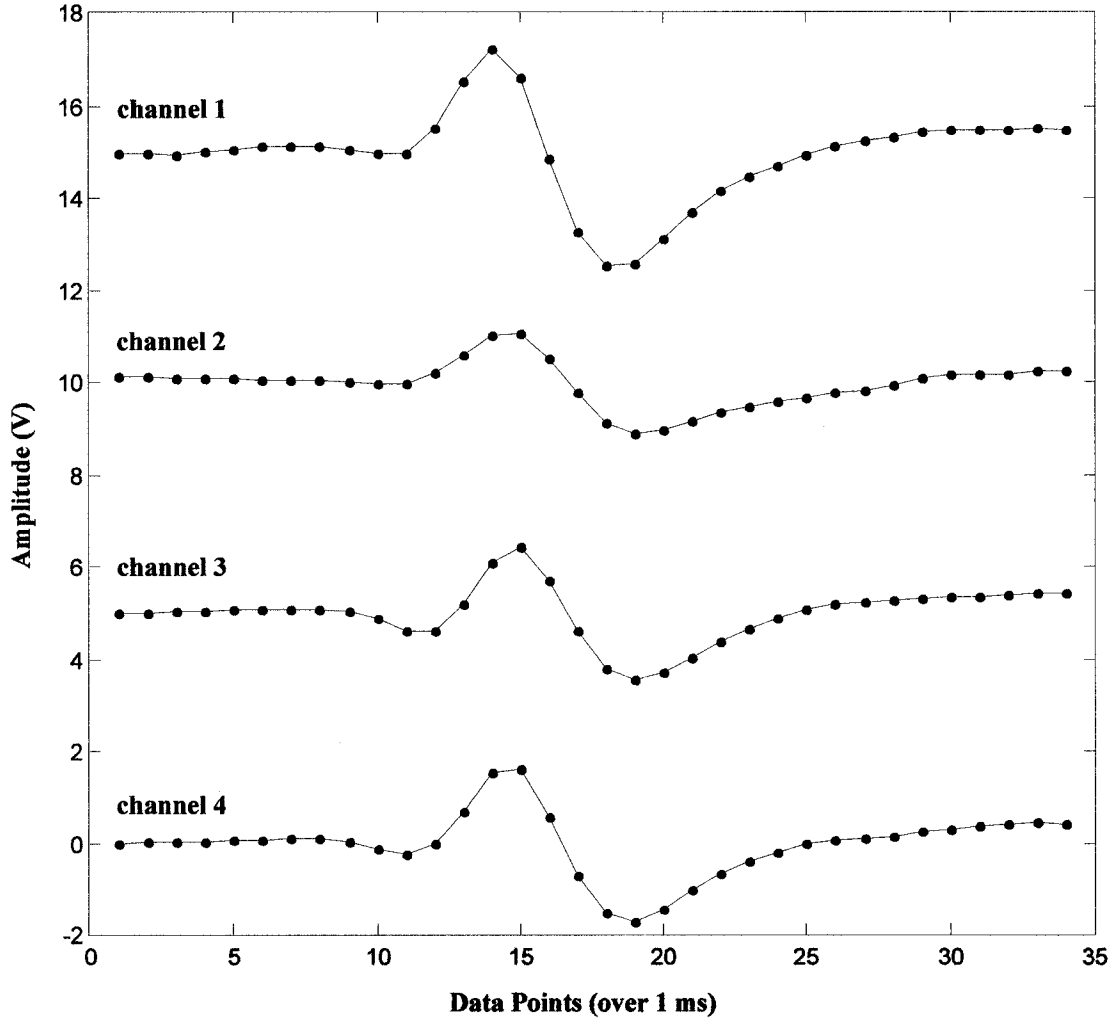

Figure 11 Example of a single spike recorded on all four tetrode wires. The sampling frequency is 34 kHz, yielding 34 sampled points of data over a single millisecond. The spike waveform is slightly different on each channel due mostly to the difference in spatial relationship between each wire and the neuron. The wire of channel 1 is the closest to the neuron while the wire of channel 2 is the furthest from the neuron. Were the tetrode to record from two active neurons with similar spike amplitudes, the difference in spatial relationship between the two neurons and the tetrode wires would allow spike analysis software to segregate the cells' activity.

Time stamps were relative to the beginning of the data file so that 0 ms marked the beginning of the data acquisition. The 'lockout' feature of the software avoided triggering the same spike data more than once, since the same spike could trigger all four channels. An event on one wire locked out triggering on any wire for a user defined period of time. Thus, if the same event occurred on more than one channel the data from the four channels was collected only once, not four times. A lockout period of 0.2 ms was used in my experiments.

Unlike the tetrode channels, the remaining non-spike signals were recorded continuously to disk (Appendix A.2). An experiment data file consisted of ten variables including four tetrode channels, five slowwave channels, and a timestamp record for each data point. This data was stored in a Universal File Format (UFF) file. Files consist of ten minutes worth of data, thus multiple files were usually required for a single experiment.

2.7 Data Analysis

A preliminary overview of the data was performed in the data editor portion of the DataWave software in order to get a "feel" for the data. This consisted of scrolling through the spike data from the beginning of the file and observing general characteristics of the spike data. The data file of recorded spikes was then imported into a DataWave accessory package, Autocut (version 3.0) which is designed for cluster analysis (Appendix A.3). By comparing and categorizing the data according to user selected parameters, the spikes were separated into clusters that represented the cellular activity as recorded by all four wires of the tetrode. 34 parameters were available and were divided into four groups: Amplitude (maximum amplitude of spike waveform peak and valley), Time (time of occurrence of spike), Latency Difference (difference between spike occurrence between two wires), and Phase

Angle (peak or valley). In order to understand the peak phase angle parameter, consider the Cartesian coordinate system with peak amplitude of channel 1 on the horizontal axis, channel 2 on the vertical axis. Plot a waveform's peak maximum amplitude as a point in that plane (Peak 1, Peak 2). Draw a line from that point to the origin. The angle between the line from the origin to Peak 1, 2 and the horizontal axis is the peak phase angle. Phase angle is a useful parameter to choose when the peaks of spikes from the same cell are varying. Because the phase angle is a measurement of the ratio of the a spike's peak on two channels, when the spike peak changes in amplitude the phase angle ratio will remain constant.

In order to assign spikes to clusters, AutoCut employs algorithms that search the space defined by the parameters chosen by the user. Waveforms are assigned to clusters based on the multidimensional distances between the parameter values. The most distant points are chosen as cluster centres and all points that fall within a critical distance of that centre are assigned to that cluster. After the addition of each new spike, the cluster centre is recalculated. Values must be within 2.5 standard deviations of the centre of a cluster to be included in the cluster and this must be true for all dimensions used to define clusters. The value of cluster boundaries can be changed by the user in order to create tighter or broader clusters. The spike assignments continue until each spike in the data file, or up to 16 383 spikes maximum, have been assigned to a cluster. Spikes falling outside the boundaries of any cluster are assigned to the '0' cluster. A maximum of 20 clusters can be assigned in AutoCut, excluding the 0 cluster (Appendix A.4). Ideally, the amount of clusters formed was equal to the amount of cells present. The clusters were calculated automatically, but it was best to refine the categorization manually (see Discussion) as there were some spikes that represented discrepancies in the recorded data.

Clusters are displayed as scatter plots in a maximum of 28 different views on the AutoCut screen (Appendix A.3) from eight user selected parameters. In these views, the four tetrode channels are labelled X, Y, Z, and W, corresponding to channels 1, 2, 3, and 4. When viewing the two dimensional cluster plots (for examples see Figures 12, p.57, and 15, p.60), a value on one channel is plotted against another value on a second channel (eg: Peak X vs. Time Y). Once the clusters were assigned, the individual cell activity was compared to the eye and head movement data using DataManager software (Appendix A.7). Time stamping the data channels allowed re-alignment of the tetrode and eye and head channels. The cells' activities were then ready to be correlated to eye, head, and gaze movement parameters. By examining the activity of the cells along with gaze shift behaviour it was possible to determine the type of cells present in the recording. For further analyses, including valid saccade detection, firing frequency calculations, and plotting, the cell clusters and non-spike data channels were transferred from DataManager to MatLab as ASCII format files (Appendix A.8). Once in MatLab the ASCII files were reformatted to m-files, a format that was more rapid and efficient for MatLab use. Further details of these methods are presented in following sections.

CHAPTER 3

RESULTS

3.1 Improvements on tetrode design

The tetrode is a fragile instrument and any modifications that improve its structural strength are very beneficial. As it takes on average 20 to 30 minutes to construct a single tetrode, broken tetrodes cost the experimenter time and wears on patience. While the four wires and supporting rod assembly are relatively sturdy, the wire terminals attached to connector pins are not. The weight of the pins is enough to break the 25 micron wire if the tetrode is not handled with care. Glueing the pins in a piece of protoboard had the effects of keeping the wires separated and distributing the weight of the four pins and prototype board evenly among the four wires, thus making the wire assembly less fragile (Figure 10A, p. 38). If a wire did break, it was a relatively simple matter to resolder it back into the pin in the prototype board. The board also provided a large surface area to manipulate and thus the pins were easier to attach to relay wires leading to the headstage preamps. Often the tetrode could be placed in the cannula and the pins attached to the relay wires without having to fix the cat's head.

3.2 Improvements on Recording Techniques

Recording tetrode signals at high sampling frequencies directly to computer hard disk avoided some of the technical complications and sampling frequency limitations associated with other forms of data recording, such as on digital audio cassette tapes. The sampling frequency achieved with direct to disk recording had a 35.7 kHz per spike channel maximum (Figure 11, p. 42). This was the upper limit achieved by maximizing the software configurations. The DT2839 A/D board used was capable of dividing a maximum of 416 kHz sampling frequency evenly among multiple channels. This was a considerable improvement on the previous system that used a DT2821 A/D board. The maximum sampling frequency of the old acquisition system was 250 kHz divided across 9 channels. Since nine analog inputs were present, the maximum possible sampling frequency with the new system was 46.2 kHz per channel. However, other software requirements such as online data display and analysis diminished this rate to a maximum of 35.7 kHz per channel. Using the option of point reduction, in which for every recorded point a user defined number of points are not recorded, the non-spike channels were further reduced to sampling rates of 1 kHz. Timestamp data was recorded in addition to the nine analog channels with resolution to the nearest tenth of a millisecond.

File sizes were kept to a duration of ten minutes and thus contained 20 megabytes of data on average. This size allowed satisfactory file manipulation times in all programs used in offline data analysis. Larger files tended to take too much time to load and made analysis sluggish. If the experimenter neglected to keep files to this length, one could always break a large file up into smaller files using the DataWave software option File Cutting.

3.3 Software Configurations for Data Acquisition

Many software manipulations had to be considered in order to achieve the maximum sampling frequency of 35.7 kHz. This constituted a major part of this project. The DataWave software settings found to be the best for the requirements of this experiment are listed here.

The first consideration was the acquisition object parameters. The sampling frequency was set by selecting 7200 data points sampled over a 21 ms sweep, yielding approximately 35.7 kHz per channel ($7200 / 20.16ms * 1000ms / s$). All channel gains (voltage resolutions) were set to 1. This allowed acquisition of voltages between ±10 V at a resolution of 4.88 mV. Four data buffers were used to temporarily store sampled data.

Secondly, the software oscilloscope displays were refined (Appendices A.1 and A.2). Multiple software oscilloscope windows could be displayed on a single screen but the sampling frequency capacity of the system was inversely proportional to the amount of data displayed in these windows. Also, multiple screens could be created; the user could switch between screens during the experiment. The configuration that allowed both acceptable sampling frequency and data display used a screen displaying the continuous acquisition of the raw data for the four tetrode channels, including thresholds, along with a separate window for each tetrode channel displaying events crossing the threshold all on one screen (Appendix A.1). The continuous tetrode data acquisition window plotted amplitude (±2 Volts) versus time (4 seconds) and was automatically reset every four seconds. A skip factor of 8 was used for this display, showing one data point for every 8 skipped in order to save memory for other applications. Although spike resolution was low using this value as the skip factor, the presence of all spikes could still be detected. The four event windows,

positioned in a column to the right of the large tetrode data window, also plotted amplitude (±2 Volts) versus time (1.4 ms) and were automatically reset with each new event. These windows used a skip factor of 2, thus displaying every second data point for an event, and were set on speed scope format so that resetting was more rapid. A second screen was created with a single software oscilloscope window displaying the non-spike data (Appendix A.2). This window plotted amplitude (±8 Volts) versus time (4 seconds) and was reset every four seconds. It had a skip factor of 0 as the 1 kHz sampling frequency did not require display reduction.

One analysis object was required for event detection on each of the four tetrode wires. The most important feature of these objects was the maximum expected events per data sweep. This set aside memory for event storage and transfer to disk and had an enormous effect on the amount of memory available for other applications. The value of this parameter was set to 40 (40 possible events across four wires over a 20.16 ms sweep). The lockout time was included in this object as well and was set to 0.2 ms. The thresholds were set at preliminary limits of -300 mV to -2500 mV for negative slope crossing detection and at +300 mV and +2500 mV for positive slope crossing detection. These values were typically altered on each wire once the experiment began and as the experiment progressed to rest just above the background noise.

Four analysis objects were required for event extraction, one for each tetrode wire. They were set to record data 0.5 ms before and 0.9 ms on each wire after a threshold crossing event occurred on any wire. This data was recorded from the data buffers.

The slow wave channels were point reduced as their resolution did not require the sampling rate of 34 kHz allocated to each of these channels. Instead, a sampling frequency

of 1 kHz was sufficient. To reduce from 34 kHz to 1 kHz, the point reduction object was set to record one point for every 34 acquired. This worked out to 136 unrecorded points per second over all four channels.

Finally, any unnecessary screen elements, such as the experiment status information for acquisition parameters and experiment loop counters, were turned off as they require memory allocation to run.

All of these objects were placed in a subroutine which was set to loop one million times so as to approximate an infinitely long experiment. The routine could be terminated by the user at any time.

3.4 Autoclustering

AutoCut was capable of analysing a maximum of 16 383 spikes out of an entire file of spike data. If a data file consisted of more than 16 383 spikes, the remaining spikes in the file were clustered based on the analysis of the first 16 383 spikes, even though the remaining spikes were not displayed. Of the 34 available spike analysis parameters, peak and valley waveform amplitude voltages were the most useful for classifying spike data and assigning spikes to clusters. Each wire had peak and valley parameters, thereby giving 8 parameters for the four wires. These 8 parameters were converted into standard scores (z-scores) and displayed in various [$N(N - 1)/2 = 28$ possible] two-dimensional projections (e.g. peak on channel 1 vs. valley on channel 4) as points on a computer screen. Individual cells were usually readily identifiable as clusters in all such plots (Figure 12, p.57, Figure 15, p.60). Since spike variability occurs due to noise and changing firing frequency, the parameter values are not independent and the clusters tend to be elliptical. Thus, elliptical boundaries were

used to define the cell clusters. Usually, the program would perform the initial cluster analysis and boundary determination. After close inspection of the various two dimensional plots, the user could alter the boundaries according to his judgement. If there was still some uncertainty in the validity of some clusters or their boundaries spike waveforms (Appendix A.5), both individual and average, and spike raster plots (Appendix A.6) could be viewed. This approach was very useful in determining if cluster were accurate and if certain spikes were noise or improperly recorded spikes. These clusters or spikes would be 'freed', not to be used in further analysis. The final cluster boundaries determined from the sample (maximum 16 383 spikes) were used to classify the rest of the data file.

3.5 File Transfer

After the completion of cluster analysis MatLab was used for any further data manipulations. Transferring data from the UFF format to ASCII format proved a long and tedious process (Appendix A.9). The procedure required the use of the DataManager software. The file to be transferred was opened in DataManager and each of its clusters and slow wave data were transferred to ASCII format individually. For example, if the file contained three clusters the data for each cluster was saved as an individual ASCII file, i.e: cluster1.asc, cluster2.asc, cluster3.asc. Each file consisted of five columns: four columns of tetrode spike data and one column of timestamp data. The slow wave data was also saved as an individual file and consisted of six columns: timestamp, horizontal head position, horizontal gaze position, light status, barrier status (triggered pulse), and target position, i.e: slowwave.asc. Thus, four separate files would be required to transfer data from UFF to ASCII.

Since MatLab processes ASCII files relatively slowly, it was more efficient to transfer the files into m-file format. This required loading all cluster and slow wave data files into MatLab and saving each file as an individual m-file, ie: cluster1.m, cluster2.m, cluster3.m, and slowwave.m.

3.6 Programs Compiled for Data Analysis in MatLab

Various programs were compiled in MatLab for cell and saccade analysis (Appendix A.9). First, a digital filtering program (smoothy.m) was made to eliminate noise in the slow wave data. A search program was then created to find trials (findevents.m). This algorithm searched the slow wave data file locating triggered pulses that were recorded when the target spoon broke the optical barrier. Five new variables were created to store trial data, one for each slow wave variable. Each time a pulse was found, data from each slow wave signal (head position, gaze position, light status, barrier status, and target position) was placed in a column of its respectful new variable. Thus, each new variable contained data for one signal over multiple trials. An amount of new variables equal to the amount of clusters found in the experiment were then created to store spike data occurring in correspondence to the slow wave data already separated into trials.

A saccade detection program (saccade_detect.m) was compiled to analyse the data in the trials and determine whether or not the trial contained a valid saccade. Two new variables were created, one for valid saccades and one for invalid saccades. These variables contained four pieces of data characterizing each saccade: time of saccade onset, time of saccade stop, saccade direction, and saccade amplitude. In cases of multiple step saccades these variables contained four pieces of data for each step.

Since the actual waveform shape of the spike data was no longer required, a program was written that replaced all spike data with binary data (binarybaby.m). The spike data was not continuous in time, as was the slow wave data, so spike data was aligned with the slow wave data by replacing waveforms with a value of one while zeros filled in the space between spikes. Another program (gaussmeout.m) then replaced the ones with Gaussian waveforms, of width determined by the user, for use in spike frequency density calculations.

Finally, programs were designed to plot the trials (lookingood.m, lookinbad.m, plot_onset.m, plot_end.m, plot_target.m). These programs displayed slow wave data, cell activity data, and spike frequency density data for either one trial at a time or multiple trials simultaneously.

3.7 Preliminary Results of Tetrode Recording

The protocol used in these experiments required the cat to fixate an opaque barrier on which there was no significant target. The cat would make saccades to either side of the barrier to fixate a food target when it was presented. While recording in the superior colliculus, cells exhibiting activity related to these movements were recorded. These included visual and motor related cells: cells that were active when a target was presented in the cats visual field (visual cells), cells that were active when the cat was fixating (fixation cells), and cells that were active several hundred milliseconds before a saccade, during a period of saccade anticipation (buildup cells). Fifteen experiments were performed in which two or three units were recorded simultaneously. Two of the typical examples of these successful tetrode recordings are summarized in Figures 12 through 16 and are discussed below.

3.7.1 Experiment 12 (Cells M30051 and M30052)

Figure 12, p. 57, shows cluster analysis of the spike data for experiment 12. The data was analysed several times using different parameters each time. The most accurate results were obtained using peak and valley amplitudes as well as peak phase angle for a total amount of 14 parameters. Out of 14 063 spikes analysed in this cluster analysis, 4 251 of them were assigned to unit 1 and 8 144 of them to unit 2. 1 668 spikes were classified as noise. These 14 063 spikes represented the first five minutes of a 55 minute record. After reviewing the 91 2D cluster plots (some shown in Figure 12) and the waveforms (Figure 14A, p. 59) for each of the identified units and the noise, it was determined that the cluster analysis was accurate. Not many cluster alterations were needed for this data; the two cells' waveforms were quite different from one another and thus their clusters were distinct. The cells were labelled M30051 (cell 1) and M30052 (cell 2).

The sorted spike data was exported for further analysis in MatLab. Here, trials that the cat performed successfully were grouped and displayed according to similar gaze amplitude (Figure 13, p.58). The activity of the two cells was compared to the gaze and head movements of the cat. Both cells were maximally active during leftward gaze shifts of 30°. When the gaze traces were aligned on saccade onset, cell 1 was seen to be tonically active until about 200 ms before saccade onset during which time there was a slight increase in activity (Figure 13A). Approximately 100 ms after saccade onset, the firing frequency of cell 1 was greatly diminished. At the end of the saccade and while the cat fixated the target the cell was completely inactive. Cell 2 was seen to have an increase in activity about 90 ms before saccade onset. Aligning the gaze traces on saccade offset, it was seen that both cells had minimal firing frequency after the saccade had stopped (Figure 13B). Aligning the gaze

traces on target onset revealed that the peak firing frequency for both cells occurred about 100 ms after the target appeared (Figure 13C). Before and after its peak the activity of cell 2 was fairly tonic. These findings indicate that both cells were probably types of buildup neurons. They could be responsive to visual input, although at long latencies.

3.7.2 Experiment 11 (Cells M290501, M290502, and M290503)

Figure 15, p.60, shows cluster analysis of the spike data for experiment 11. Using cluster parameters of peak and valley amplitudes yielded the best results in this case, making a total of 8 parameters. Out of 2 000 spikes analysed in the cluster analysis, 53 of them were assigned to unit 1 431 were assigned to unit 2, and 1 459 of them were assigned to unit 3. These 2 000 spikes represented the first two minutes of a 9 minute record. Unfortunately the record was not longer as experimental complications terminated the experiment. After reviewing the 28 2D cluster plots (some shown in Figure 15) and the waveforms (Figure 14B, p.59), it was a little uncertain whether or not the first and second units were truly distinct cells. Repeating the cluster analysis using different variables resulted in the identification of three units each time. Viewing the average of the waveforms for the two units in question (Figure 14 C) showed that the units were similar in shape and amplitude on the same channels. These cells were labelled M29051 (cell 1), M29052 (cell 2), and M29053 (cell 3).

The three cells were maximally active during leftward gaze shifts of 20°. Figure 16, p.61 shows the activity of the three cells when gaze traces of 20° are aligned at saccade onset, saccade offset, and target onset. The firing frequency of cell 3 peaked immediately after saccade onset and was infrequently tonic afterwards (Figure 16A). The

peak firing frequencies of cells 1 and 2 were seen when the traces were aligned on saccade offset, although the activity of cell 1 was never very frequent (Figure 16B). These findings indicate that cell 1 was probably a fixation neuron, although it could have been an inhibitory interneuron, given its activity at the end of the saccade and the infrequency of its activity. That is, if cell 1 is truly a distinct neuron at all (see discussion in Section 4.2.2). Given its tonic activity and increase in firing frequency at the end of the saccade, cell 2 was probably a fixation neuron. Although cell 3 displays a distinctive peak in firing frequency when the gaze traces are aligned on target onset, indicating that it may be a cell that responds to visual input, the peak occurs about 220 ms after the appearance of the target in the cat's visual field. Typical visual cells in cat usually respond in less than 100 ms (Guitton & Munoz, 1991). Thus, this cell type is probably more motor related than visually related, although it is clear that it is not a typical buildup neuron.

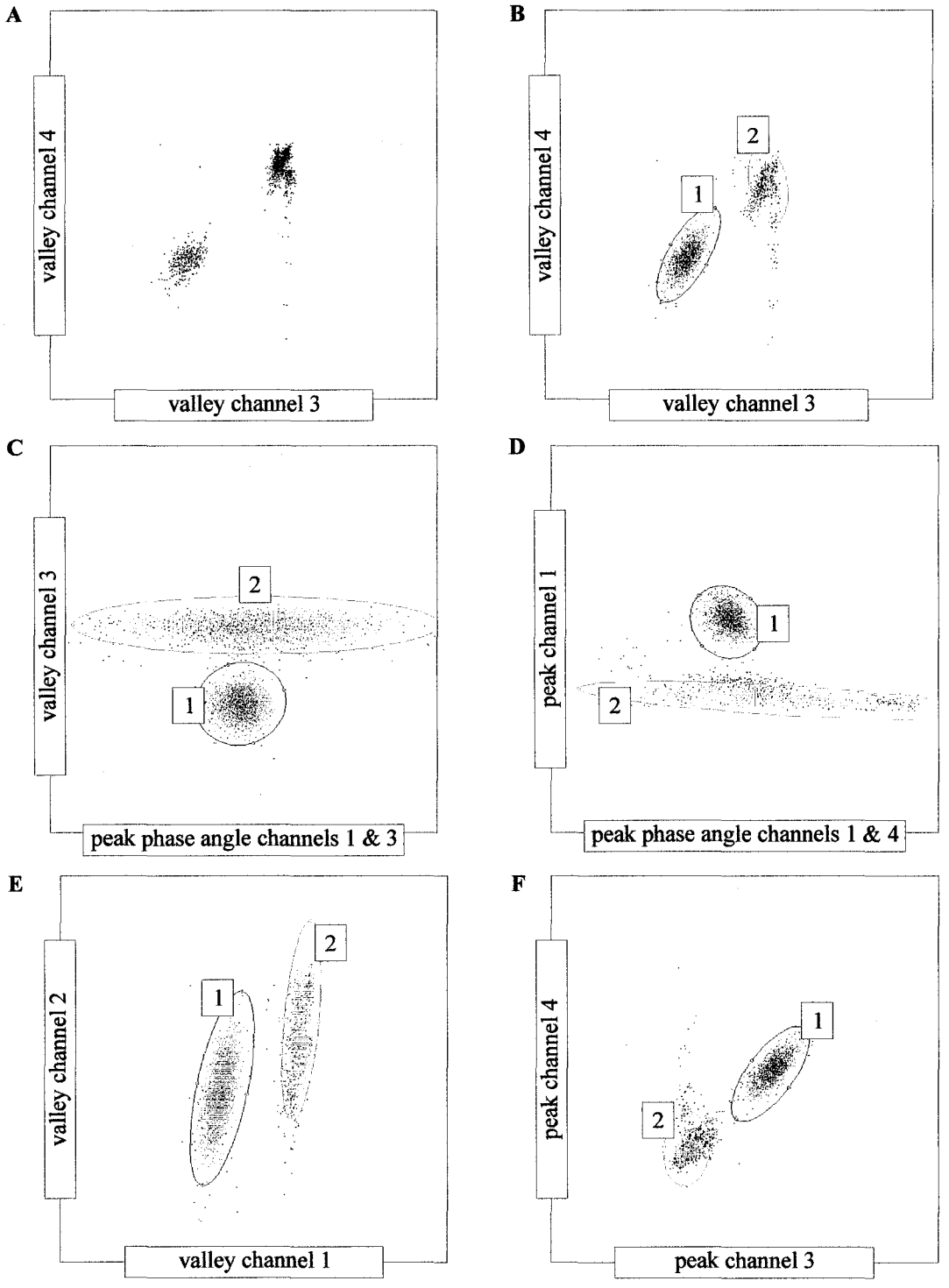

Figure 12 Examples of cluster analysis plots for experiment 11. Panel A shows unclustered data consisting of 14 063 spikes in a space comparing the spike valley amplitudes on channel 3 versus the spike valley amplitudes on channel 4. The cluster analysis performed on this data used 14 parameters: the peak and valley spike amplitudes on each of the four tetrode wires and the peak phase angle between each wire. These parameters yielded two distinct clusters indicating the presence of two individual cells. Cell M30051 spike data is indicated as 1 while cell M30052 spike data is indicated as 2. Black dots are representative of noise that has been excluded from both clusters.

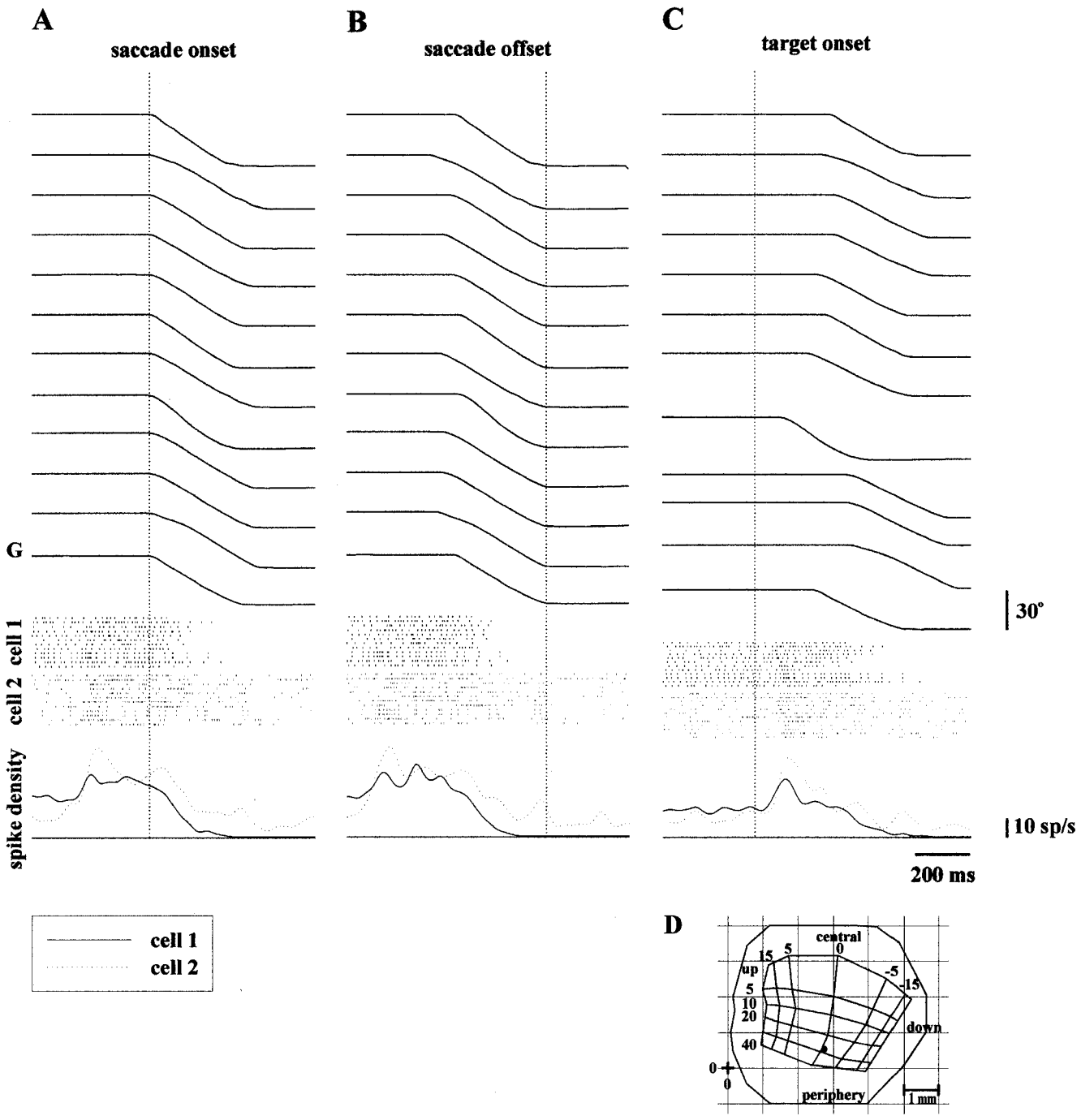

Figure 13 Discharges of two simultaneously recorded cells during leftward, contralateral 30 degree gaze shifts. In each panel (**A, B, C**) the same trials are shown aligned on different features of the gaze trajectory (G). (**A**) Traces aligned on onset of saccade (vertical dotted line) show that cell 1 has a peak firing frequency just before saccade onset and is probably a buildup neuron. (**B**) Traces aligned on saccade offset. (**C**) Traces aligned on target onset show that cell 2 has a peak in firing frequency approximately 100 ms after the appearance of the target in the visual field of the cat, indicating that the cell is probably visually related. (**D**) A motor map of the right superior colliculus shows the approximate gaze amplitude associated with cells in certain areas of the SC. The dot represents the approximate placement of the tetrode during this experiment, based on stereotaxic coordinates. The legend to the bottom left identifies the spike frequency density traces associated with cell 1 and cell 2.

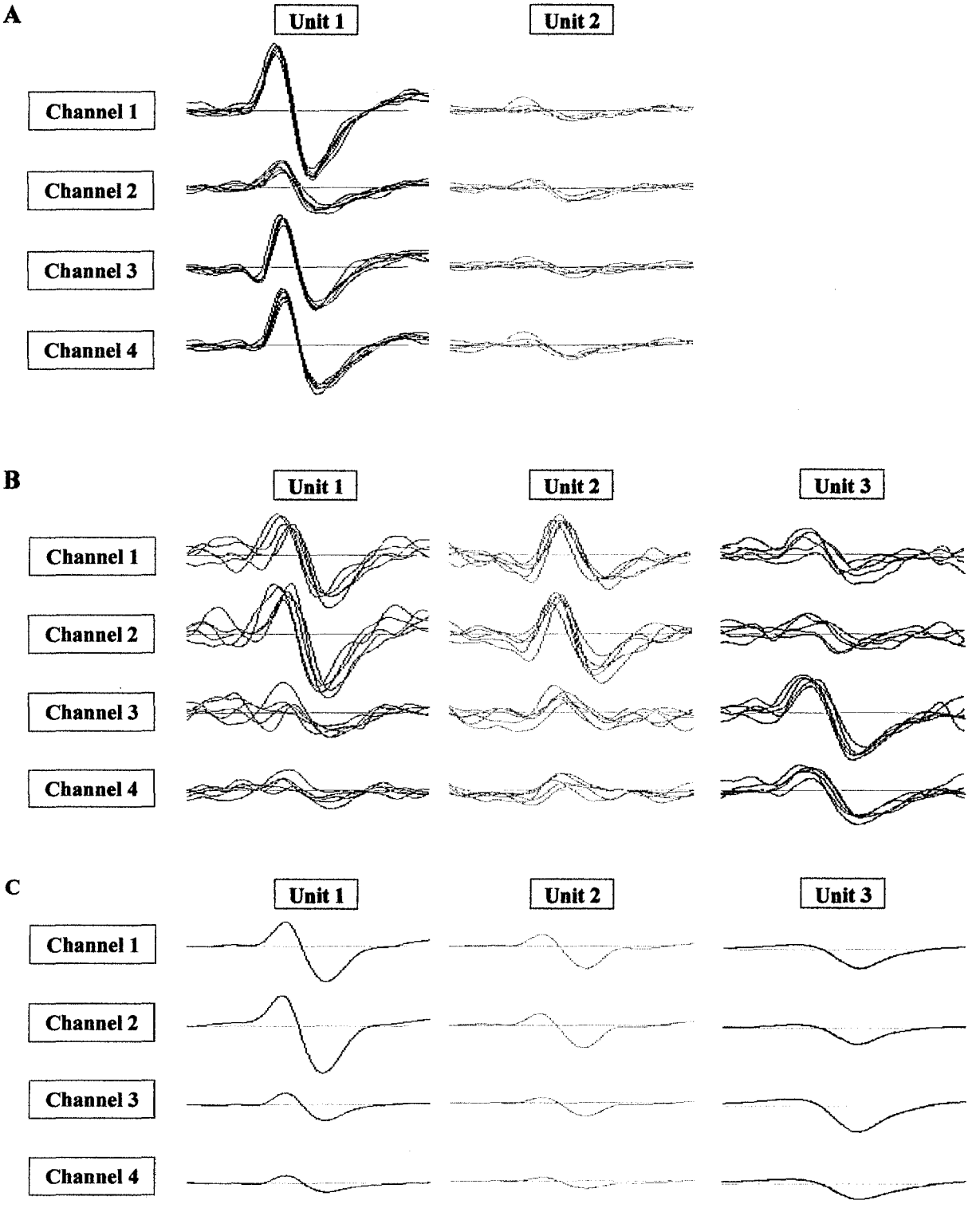

Figure 14 Example of waveform analysis in AutoCut. **(A)** Typical waveforms for each of the two cells identified by cluster analysis in Figure 12. **(B)** Typical waveforms for each of the three cells identified by cluster analysis in Figure 13. **(C)** The waveform averages of the three units on each wire in **(B)**. By scrutinizing groups of waveforms their averages for each cell, the accuracy of the cell identification performed by cluster analysis can be assessed and corrected, if necessary.

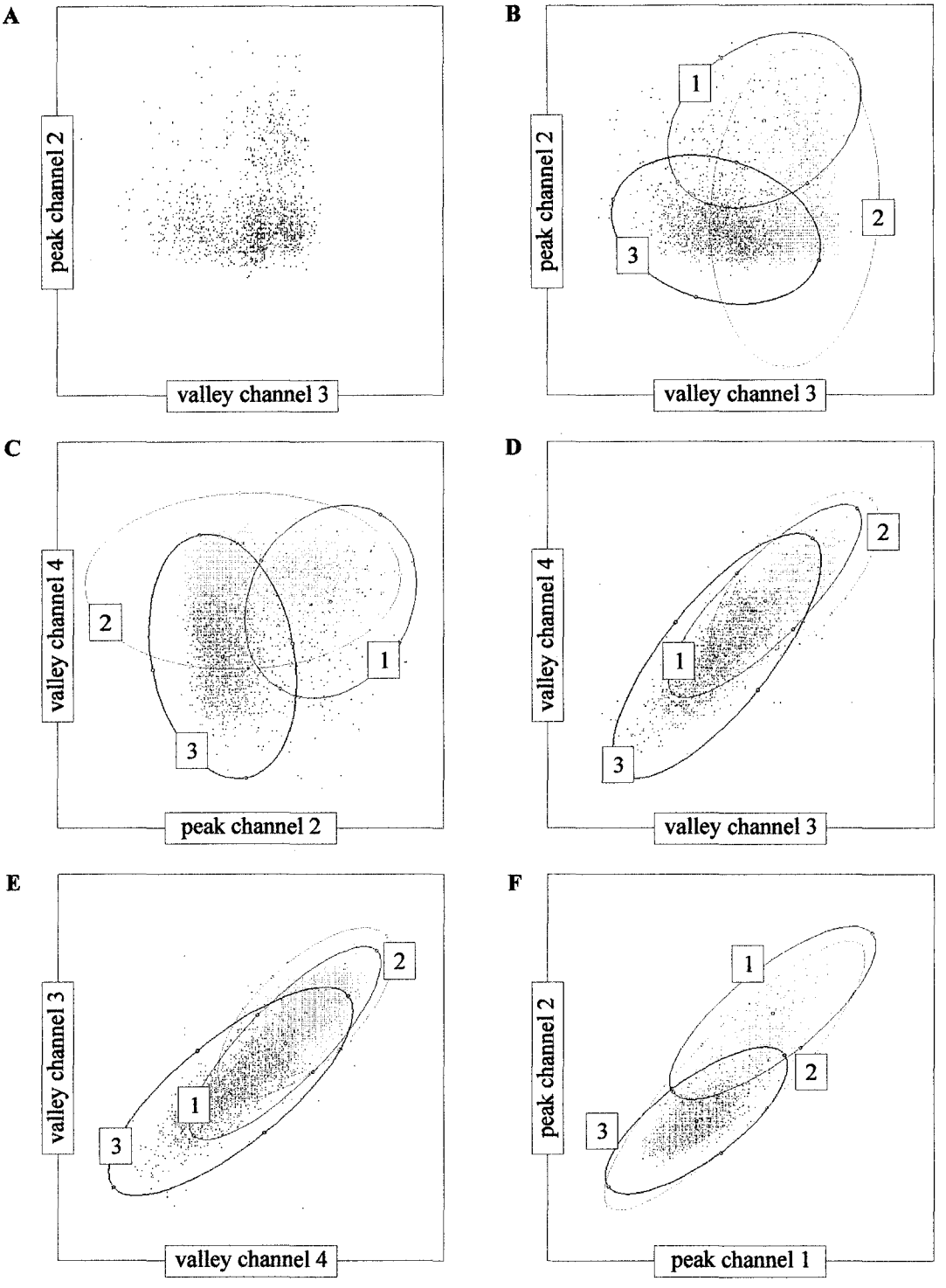

Figure 15 Examples of cluster analysis plots for experiment 10. Panel A shows unclustered data consisting of 2 000 spikes in a space comparing the spike peak amplitudes on channel 2 versus the spike valley amplitudes on channel 3. The cluster analysis performed on this data used 8 parameters: the peak and valley spike amplitudes on each of the four tetrode wires. These parameters yielded three distinct clusters indicating the presence of three individual cells. Cell M29051, M29052, and M29053 spike data are indicated as 1, 2, and 3, respectively. Black dots are representative of noise that has been excluded from all clusters.

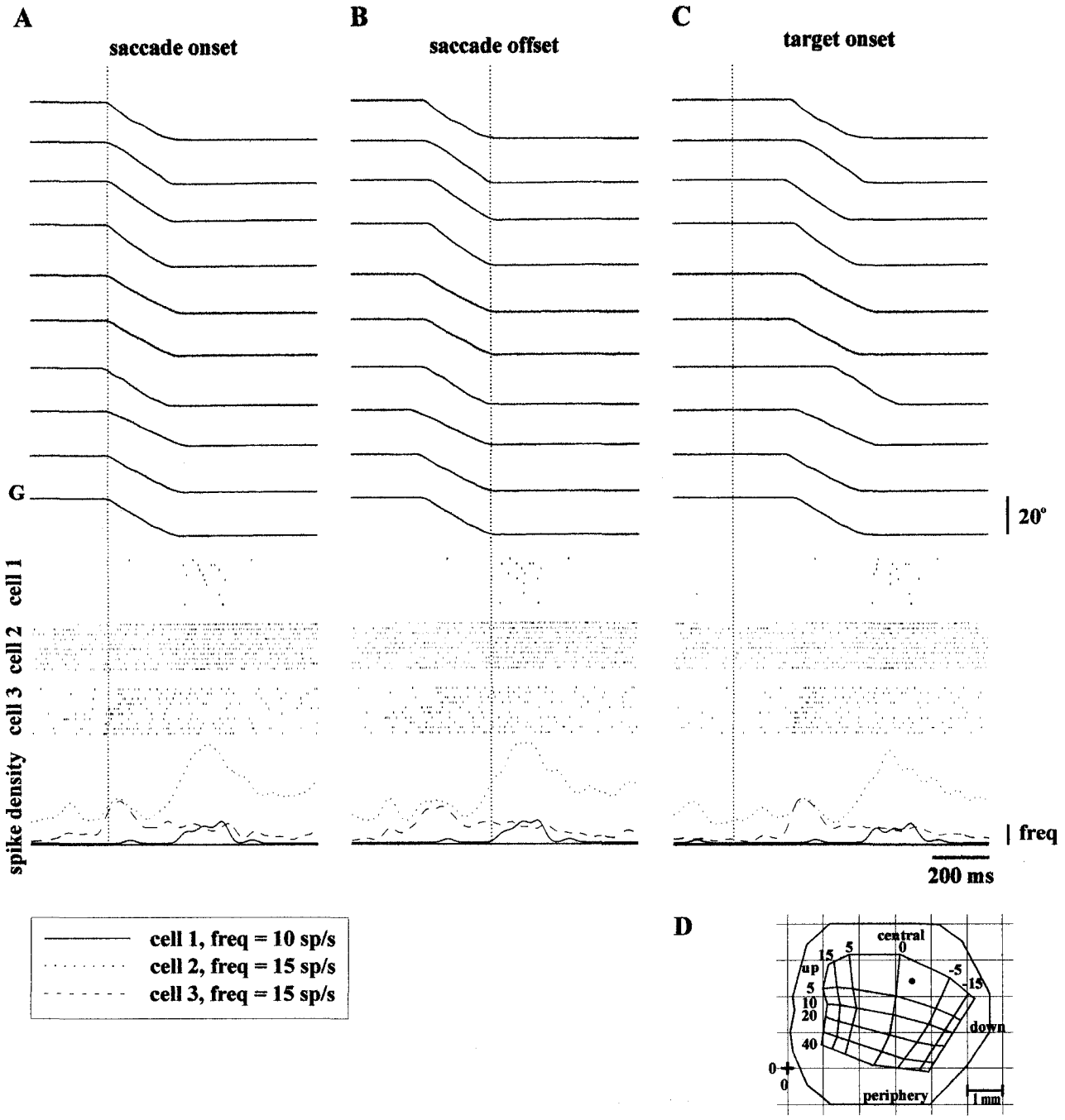

Figure 16 Discharges of three simultaneously recorded cells during leftward, contralateral 20 degree gaze shifts. In each panel (**A, B, C**) the same trials are shown aligned on different features of the gaze trajectory (G). (**A**) Traces aligned on onset of saccade (vertical dotted line) show that cell 3 has a peak firing frequency just after saccade onset and is probably related to motor control. (**B**) Traces aligned on saccade offset show that cell 2 and cell 3 have peak firing frequencies at saccade termination indicating that they are probably related to fixation. (**C**) Traces aligned on target onset show that the peak firing frequency of cell 3 occurs more than 200 ms after target appearance in the cat's visual field, a latency too great for the cell to be visually related. (**D**) A motor map of the right superior colliculus shows the approximate gaze amplitude associated with cells in certain areas of the SC. The dot represents the approximate placement of the tetrode during this experiment, based on stereotaxic coordinates. The legend to the bottom left identifies the spike frequency density traces associated with each of the three cells. The firing frequency measurement bar (freq) values are indicated for each cell.

CHAPTER 4

DISCUSSION

4.1 Tetrode Design Considerations

4.1.1 Wire Thickness

The first consideration on tetrode use in the superior colliculus was the thickness of the wires used. The thickness of the wires needed to be such that their spacing was sufficient for simultaneous multiple cell recording in the SC. The first construction attempts were made with 12 micron stainless steel Teflon insulated wire. It was hoped that this wire would be sufficient for multiple unit recording while producing minimal tissue damage. However, in addition to being extremely difficult to work with and immensely fragile, the results acquired with these wires were unsatisfactory. Although the quality of the signals was good, there were no instances of multiple cell recording; only single units were detected with the 12 micron wire tetrodes. This was probably due to the tiny spacing of the wires which was only approximately 60 microns maximum. In comparison with the spacing of active neurons in the SC, the 60 micron maximum spacing of the 12 micron wire tetrode was insufficient to simultaneously record from multiple neurons.

The second attempt used 25 micron stainless steel insulated wires. In addition to being considerably easier to work with and less fragile, many instances of multiple cell recording were encountered. The maximum tip separation of tetrodes made with these thicker wires was approximately 120 microns, twice that of the 12 micron wires (Figure 10A, 10B, p.38). Almost unfailingly, two cells were encountered and could be simultaneously recorded. In some cases, three cells were encountered. The 120 micron spacing seemed more appropriate for the anatomical organization of cells in the SC. Cells in the SC have been explored via Golgi and electron microscope observations and grouped into three categories based on size. Large SC cells measure between 35 and 60 microns, medium sized SC cells measure between 20 and 30 microns, and small SC cells between 8 and 15 microns (Norita, 1980; Moschovakis & Karabelas, 1985). The maximum distance between any two neighbouring collicular cells is approximately 250 to 350 microns (Norita, 1980). These sizes and spacings would explain the unsatisfactory results produced by the 12 micron wire tetrode. Its maximum tip spacing of 60 microns would probably be capable of recording from multiple cells only in very specific circumstances in which the active cell density was greater than is typical. The tip spacing of 120 microns achieved with the 25 micron wire was more suitable.

4.1.2 Tissue Damage

A major concern in performing these experiments was the extent to which the tissue in the superior colliculus was being damaged by the tetrode assembly. The width of the tetrode (120 microns) plus the width of the electrode tip (200 microns) gave the assembly a width of 320 microns at its thickest point. Given that the cat SC is only about 4 mm wide laterally and 4 mm long, the passage of a 320 micron recording assembly produces

considerable damage. The observation that less and less successful recordings were made over time was in part attributed to this damage. In an effort to reduce this damage, support electrodes of 100 micron tip diameter were used, reducing the overall width of the apparatus to 220 microns.

It was speculated that a second factor contributing to tissue damage could be present, that of the cyanoacrylate glue (super glue) used to fix the tetrode wires and electrode together. It was possible that the toxic nature of the glue could damage the tissue. Although alternatives were researched, a suitably biocompatible glue could not be found. Vet Bond glue (3M) was used in the hopes that this version of cyanoacrylate glue, used in veterinary applications, was less toxic. When consulted on this issue, two veterinarians were of the belief that once dry the cyanoacrylate glue would pose minimal threat to the tissue.

4.1.3 Wire Preparation

Meticulous care had to be taken in the preparation of the tetrode as the wires were so fragile. One concern in the assembly was the method used in stripping the insulation from the wire ends that were to be soldered into the connector pins. This method consisted of approaching each of the four wires close enough to a flame to burn the insulation off, leaving the wires bare. Due to the instability of the flame, the wires often came too close and were damaged. When this occurred, the wire had to be recut and another attempt to remove the insulation was made. It was also a concern in the instances where the insulation was successfully removed that exposure to the heat was enough to alter the properties of the wire. The supplier of the microwire, California Fine Wire Company, assured that such treatment should have no effects on the wire performance.

Several wires of same diameter and material but different resistance were tested to determine which values were the best for the tetrode applications. A test stimulus was applied in saline solution. This signal was relayed to an oscilloscope by various tetrodes made of different resistance wires. Assuming that all other variables between the different tetrodes were constant, it was determined that the 100 Ohm/foot and 150 Ohm/foot wires gave superior performance to the 250 Ohm/foot and 500 Ohm/foot wires. The signals relayed by these wires were greater in amplitude and contained less noise, in general.

Another property of the wires that was difficult to assess was that of impedance. In general, it was observed that impedances of less than 1 MΩ and greater than 4 MΩ yielded poor signal results. Unfortunately, it was not possible to tailor the impedance of the wires to the desired value; it was a more or less random variable. However, the impedance value was usually between 1MΩ and 3 MΩ , which was suitable. If the impedance was higher than 4 MΩ, it could be reduced by passing an electric current through the wires. This was achieved by placing a wire lead from the positive terminal of a 9 V battery into saline solution and running the current through the solution, through the tetrode wires, back to the negative terminal of the battery. The degree to which the impedance was reduced was proportional to the amount of current passed through the wires.

The last preparation made to the tetrode wires was the supportive protoboard in which the connector pins were secured. Various protoboard configurations were attempted including affixing the board directly to the supporting electrode. The most successful configuration was to leave approximately 5 cm of tetrode wire running off the end of the supporting electrode, soldering them into individual connector pins and securing these pins into a small piece (2.5 cm x 0.5 cm) of protoboard. The pins projecting through the back of

the protoboard were then connected to the lead wires for the headstage preamplifiers. The tetrode wires running off the end of the supporting electrode were short enough and the protoboard provided enough rigidity so that movement of the cat's head would not affect the position of the wires and thus the signal. The protoboard also made it easier to handle the tetrode lead wires; they could be manipulated as a group instead of individually, decreasing chances of damage.

4.2 Data Acquisition Considerations

The advent of recording experiment data directly to computer hard disk at high sampling rates has made handling and analysing electrophysiologically recorded data more versatile and rapid than ever. Although many benefits are present in the methods used in these experiments, there are several inherent imperfections and drawbacks, as discussed below.

4.2.1 The Benefits and Detriments of Increased Sampling Rates

One of the most difficult aspects of electrophysiological recording is getting a sufficient sampling rate. Using the DT2839 A/D board with all of the software settings described in section 3.3, a maximum sampling rate of 35.7 kHz per tetrode channel was achieved. This was well above the previously available maximum rates of 10 kHz per channel, using a digital acquisition tape (DAT), and 25 kHz per channel, using a DT2821 A/D board. Usually, the duration of an SC cell spike was slightly less than 1 ms. Thus, approximately 35 data points could be collected along the spike waveform (Figure 11, p.42). There were usually 15-20 data points defining the main profile of the waveform with 14-24

points defining the beginning and ending profiles (the profiles before and after any significant amplitude change occurred). For the tetrode data, it was desirable to attain the highest sampling rate possible. The more data points used in defining the waveform of a spike, the more accurate the shape of the spike and the easier it would be for AutoCut to cluster like waveforms. Since the automatic clustering analysis must almost always be refined manually, having precisely defined waveforms would make cluster analysis more accurate, thus saving time.

The maximum sampling rate was determined by several software factors, in addition to the maximum rate capacity of the A/D board. Since the maximum sampling rate of the board was 416 kHz, the combination of number of data points collected and duration of data sweep for the acquisition object had to be less than 416 kHz. Also, the number of acquired points had to be equally divisible between the nine channels. Thus, the parameter settings in the software acquisition object found to be most suitable for the experiment were 7200 points over 21 ms. The acquisition object rounded the data sweep of 21 ms to the nearest possible value of which the board was capable, 20.16 ms. 7200 points over 20.16 ms gave a sampling rate of 357 142.844 Hz It would seem that there is still room for improvement here, as the overall sampling frequency is somewhat removed from the maximum rate capability of the board (416 kHz). However, since the acquisition object must share memory with other software elements, the rate of 35.7 kHz was the maximum attainable. Thus, there is a trade off between various software settings.

The first objects that must be refined to use the least amount of memory possible are those used for display. These are the software oscilloscopes that display continuously acquired and event (spike) data. The four tetrode channels are displayed in a multi-buffer

oscilloscope window of four second duration. The four event windows show individual recorded spikes for each tetrode channel. The ideal settings for these windows would be to display every acquired point. However, in one millisecond, up to 285 points would have to be displayed, if an event occurred: 4 channels x 35.7 data points for the display of the continuous tetrode data, plus 4 channels x 35.7 data points for the display of the recorded event on all four wires in the event windows. This is a very large demand on the software over more than a few milliseconds. Compromises had to be made. Less points were displayed for both the continuously acquired tetrode data window and the event data windows. By displaying only one point for every sixteenth point acquired, the tetrode data was satisfactorily represented on screen, enough for the user to set thresholds and observe spike and background activity. The event windows displayed every second acquired point. This was enough to show the user the overall shape of the waveform of a spike. Reducing the amount of points displayed in the software oscilloscope windows greatly increased the amount of memory available for use in increasing the sampling frequency. Setting the event windows to the 'speed scope' setting, instead of a regular software oscilloscope, freed some memory for use as well. Speed scope enabled the windows to simply overwrite the window display with a black panel and then display the new event data every time an event was detected instead of having to reset the window for each event. The window used to display the continuous slow wave data was assigned to a second screen to which the user could switch whenever desired, although it was rarely necessary to refer to this screen after calibration of these movement channels. The data displayed in this window was not reduced from the sampling frequency of 1 kHz as displaying these five channels at this rate did not require an amount of memory that significantly competed with other software elements.

Another software element that competed for memory was the analysis object used for detecting events on the four wires. It was necessary to estimate the maximum number of events that might occur during a single sweep, whose duration was 20.16 ms, as set in the acquisition object. This setting reserved space in memory buffers for event transfer to disk. Ideally, one would want to set this value as high as possible, in the event that a great deal of spikes occurred rapidly. However, a maximum value of 40 expected events had to be used. This was the highest setting that still allowed acquisition and display of the data to occur at decent rates. This seemed to be satisfactory for all data that was acquired. If more than 40 events occurred in the 20.16 ms sweep, any events over 40 would not be recorded. The user had to be very attentive to ensure that this never happened.

The last software element that competed significantly for memory were the analysis objects used for extracting events. One object was required for each tetrode channel. With these objects one had to specify the recording window around an event. Naturally, one would want to set this window to large proportions, ensuring that the entire spike was captured each time without fail and even allowing for a little leeway on either side of the main spike. A large window would allow the user to be less specific and not to have to tailor the settings to a precise waveform duration. This approach would ensure that long duration waveforms would be captured in their entirety, even if they were rare in occurrence amongst shorter waveforms. This setting also had to be compromised. The longer the recording window, the more memory required to store the data. Thus, during data acquisition, capturing several rapid events could quickly use up all of the transfer buffers leaving none free for more events. I chose 0.5 ms before and 0.9 ms after the threshold crossing. Since the duration of the spikes encountered in the experiments were about 1 ms, this window was adequate to capture the

main spike as well as a little extra before and after the spike. Also, this window duration was the maximum allowable before memory allocation errors occurred during data acquisition, all other settings being at the values described above.

Given all of these software components competing for memory allocation, it was very challenging to finally arrive at all of the settings described above. Many trials had to be performed with various settings for each of the major memory consuming elements before the best configuration was determined. Unfortunately, no matter what the settings, the acquisition system will always have a maximum acquisition and data transfer rate. Using these settings, it is estimated that a single cell firing at frequencies greater than 200 Hz would be enough to overload the acquisition system and cause recording errors. As long as cells encountered had less frequent activity than this, the 35.7 kHz sampling rate remained successful.

4.2.2 Threshold Considerations

At the outset of an experiment, thresholds were chosen and set to arbitrary values. The settings were changed once the initial signals were observed and the level of background noise examined. The thresholds could be set during online data acquisition so that it was not necessary to stop recording during an experiment. The user had to be attentive to the on-screen signals and change the thresholds when necessary throughout the experiment. Several threshold changes had to be made during a typical experiment.

The amplitude thresholds were the most useful types of thresholds; the type employed depended on the nature of the signals present. In general, the negative threshold crossing type was used but by times the positive threshold type was preferred. These types of thresholds

had a lower and upper limit. The lower limit was set as close to the level of the background noise as possible and the upper limit was set to what was estimated to be a realistic maximum amplitude for the signals present. Any signals that did not attain the lower limit or that surpassed the upper limit were not recorded. This filtering out of large amplitude signals, which were usually due to noise from tetrode or lead wire collision on top of the cat's head, made the negative only and positive only thresholds preferable to the negative/positive threshold type.

Due to the nature of the tetrode, signals from different cells could have different amplitudes on different channels. When this occurred, it was useful to explore setting different types of thresholds on different channels to take advantage of the best available signal. For example, one could set a negative threshold crossing on two channels to record activity from a cell with pronounced negative amplitude while a positive threshold could be set on the other two channels to record activity from a second cell with pronounced positive amplitude. Although this was rarely necessary, in certain circumstances setting different thresholds on different channels could make the difference between recording successfully from multiple cells and only being able to record one cell.

4.2.3 Loss of Spike Data Using Tetrode Recording Methods

Although tetrode recording is very useful in recording multiple units simultaneously and avoids certain errors associated with single electrode recording, it is far from a perfected method. There are several points along the data acquisition path at which information from the cell can be lost or misrepresented.

A) Losing Spikes Through Lockout

The use of the 'lockout' feature when acquiring data was essential in keeping data files to a manageable size. By triggering recording from a spike on one channel instead of all four, the data from the four channels was recorded only once, not four times (ie: data is not recorded by triggering off the same spike on each of the four channels). In order to perform this operation, a 'lockout time' had to be specified so that the same spike detected on more than one channel but at a slightly different time did not trigger recording more than once. Lockout blocked any recording for a user specified time duration. For my experiments, this value was set to 0.2 ms. Thus, for 0.2 ms after a spike crossed a threshold on one channel, no recording could be triggered by events on any of the other three tetrode channels. This could cause a problem in the presence of multiple units. For example, if an event occurred on channel 1, channels 2, 3,and 4 would be locked out for the next 0.2 ms. If a second cell were firing on channel 2 and/or channel 3 and/or channel 4 during this period of lockout but was not registering on channel 1, it's activity would not be recorded for those 0.2 ms. Although during the course of my experiments this situation rarely occurred, it is an existing concern, particularly if the tetrode used has a significantly larger tip spacing, thus increasing the possibility that cells are not recorded on all four channels. This possibility is exceeding difficult to circumvent, given the nature of the recording hardware and software. At present it would seem that the researcher will simply have to put up with the possibility of losing spikes in this manner.

B) Losing Spikes Through Data Acquisition Error

Although the user could go to great lengths to refine and perfect the data acquisition system, occasional acquisition errors are almost inevitable. The major acquisition error resulting in the loss of spikes was associated with event thresholding. The thresholds had to be set very closely above the background noise in order to record small amplitude cell activity. In some cases, noise crossing the threshold would trigger recording. Usually, this would just result in the noise being assigned to the noise cluster when analysed in AutoCut. However, if the noise triggered recording a few milliseconds before a true spike occurred, the recording window would capture first the noise, then the true spike at the end of the window, instead of in the centre. In this case, the entire spike would not be captured. Such recordings would usually result in the formation of a cluster. However, since the cluster contained incomplete waveforms, the information was of no value. Furthermore, the information was not rectifiable. Such spikes usually seemed to belong to other cells. These spikes could not simply be reassigned to other clusters, however, due to their incompleteness. Thus, this data was discarded. Luckily, such occurrences did not result in the loss of spikes. The true spikes would still trigger the correct recording window and be properly recorded. The noise triggered data simply introduced a data analysis complication for the user.

C) Losing Spikes Through Simultaneous Cell Firing

Another unavoidable circumstance resulting in the loss of spikes is that of simultaneous cell firing. It is very probable that if two or more cells fire simultaneously in the vicinity of the tetrode, the tetrode will record spikes that are a combination of waveforms from the simultaneously firing cells. When analysed by the auto-clustering software, such

spike superpositions would be classified in three ways: 1) as noise, 2) as separate clusters or 3) the inclusion of the spike in the cluster of another cell.

If a separate cluster were created, it could be very difficult for the user to determine whether or not the cluster contained spikes representative of the activity of one cell or the activity of multiple cells. Certainly, if the superposition of waveforms resulted in waveforms that were odd in shape, one could surmise that the cluster did not represent the activity of a regular cell and this data could be disregarded. However, if the superimposition of waveforms resulted in waveforms that appeared standard in shape, this data could easily be mistaken for a signal emanating from a single cell. It is up to the user to use all of the tools available to scrutinize the data as closely as possible so that such misclassifications do not occur. Viewing the individual and average spike waveforms for each cluster as well as the spike train plots is quite essential in the verification of cluster authenticity.

In the case of spike waveform superimposition resulting in the inclusion of the spike in the cluster of another cell, it is again very difficult for the user to deal with such an error. By definition, since the spike was included in a cluster, it is similar to the other spikes in the cluster and the user cannot possibly identify it as misplaced. This inclusion error could occur as a result of a couple of different circumstances. One possibility is that of multiple smaller cells firing simultaneously. Their activity could be superimposed in such a manner as to appear similar to the activity of another cell of larger amplitude activity.

Another case of false classification is that of cells that are usually silent firing sporadically. The activity of these cells could be included in the cluster of another cell as their spike count would not be sufficient to form recognizable clusters. In either case the user would be hard pressed to identify these errors as being present. If these errors were somehow

identified, the user would have great difficulty rectifying them as adding and subtracting individual waveforms from a cluster is a difficult matter in AutoCut. In any case, this would be an extremely tedious task.

4.3 Data Analysis Considerations in AutoCut

Performing analyses on the spike data was a complicated task and one that necessitated caution and objectivity. If data inspection was too careless, the data could be biased and spike data, if not the data for an entire cell, could be lost or misrepresented. Data analysis had to be accurate and thorough so as to correctly identify the presence of cells in the tetrode recordings. The most crucial step of the data manipulation was cluster analysis as this was where the most errors could occur in examining and classifying spike data. If care wasn't taken, too many or too few cells could be erroneously identified or spikes could be misclassified and assigned to improper cells. The user had to employ all of the software tools available in order to avoid these errors and achieve the correct analyses.

4.3.1 Initial Cluster Analysis

The first concern in the analysis of the spike data arose in AutoCut. The program is designed to assign spikes in a data file to clusters to identify cells and characterise their activity. However, the program cannot analyse all of the spikes in a file containing more than 16 383 spikes. Instead, it classifies and allows the user to manipulate up to 16 383 spikes on screen. When the file is saved in AutoCut format, the program classifies the extra spikes according to the final boundaries decided upon by the user. Thus, the user had two options for this part of the analysis: analyse large files and rely on the classification of up to 16 383

spikes to determine the classification of the remaining spikes without user verification or convert the large files into multiple files containing less than 16 383 spikes each and analysing each file separately. The later option greatly increased the time required for analysis. In general, analysing a single, large file (>16 383 spikes) yielded satisfactory results.

A second concern in AutoCut was the choice of parameters used to assign spikes to clusters. Generally, some choices of parameters were always better than others. For certain files, choosing different parameters yielded better clustering results. The Peak and Valley Amplitude parameters were usually the most reliable and accurate. When these parameters produced ambiguous or questionable clusters, the Time parameters were usually the second choice. The Time parameters would be used in conjunction with the Amplitude parameters for the second clustering attempt. If results remained unsatisfactory, different parameter combinations would be tried until the best results were found. These combinations were made from the subgroups of the major parameter groupings of Amplitude and Time: Peak, Valley, Peak Time, and Valley Time. Once the best clusters were found, they were manually scrutinized and refined by the user by freeing the spikes from clusters that were incorrectly created and/or merging clusters that contained data from the same cell. Such manual refinement was almost always required. The Phase Angle and Latency Difference parameters were rarely useful as they had a tendency to produce a great number of clusters. Also, the clusters that they did produce were at times difficult to interpret.

AutoCut also featured 'Weighting' for each parameter. Weighting produced clusters that relied more heavily on certain parameters, allowing the user to focus on specific differences between spikes. For example, if upon perusing the spike data it was noticed that spikes appearing to be from different cells had very different valley amplitudes but their peak

amplitudes were almost the same, one could assign the valley amplitude parameter a greater weight. The default value was 1. A value of 2 weighted the parameter 100% more, a value of 3 weighted it 200% more, etc.. Unfortunately, this feature was not always useful. Although the use of various weight values was investigated, the default value of 1 was almost always used as it usually produced satisfactory clusters.

The last features offered for parameter modification in cluster analysis were 'Lower Limit' and 'Upper Limit'. These specifications allowed the user to set maximum and minimum values on the parameters. This could be useful for filtering out spikes due to noise, if they were above a reasonable maximum. Although, such spikes should not be present in the first place as they would not have met the thresholding criteria set in the data acquisition program. The limits for Peak and Valley parameters were presented in digital, A/D units so that they would be consistent between files, no matter what the actual units of the data in the file (eg: μV, mV, ms, s). The total amount of A/D points is set to 2248. With the gain in the acquisition software set to 1 the amplitude range is ±10 V. Thus 2248 points is equal to ±10 V. Since the spike amplitude was usually less than 2 V after acquisition, the upper and lower limits were set to ±2 V or 450 A/D points. The time limits could be adjusted to filter out any spikes shorter or longer than a certain duration. The limits for time were also complicated as they were presented in terms of sampling frequency units. The user had to open the data file in Replay Manager in the DataWave software program and count the number of points in a spike. Since a certain amount of time was recorded before and after a triggered event, every spike in the file would consist of the same number of data points. This number could then be used as a limit. For example, if a spike on one channel consisted of 34 points, the time limits could be set to 0 and 34. Spikes falling outside this range would be ignored and

assigned to the noise cluster. This system of limits, although perhaps practical from the point of view of maintaining consistency between files, was inconvenient for the user.

The user could also specify the range of spikes to be analysed in a file. Up to 16 383 spikes could be analysed, starting at any spike in the file. Usually the first 16 383 spikes were used as this constituted a large enough sample for analysis of the entire file. However, if the user noticed significant changes in cell activity that occurred later on while performing the experiment, he could choose to compare the analysis of the first 16 383 spikes and another set of spikes later on in the data file to ensure proper analysis of the entire file. Although useful, it was rarely necessary to use this feature.

4.3.2 Cluster Analysis Verification

Often, the use of supporting features of AutoCut was necessary to verify the legitimacy of certain clusters. This was done by viewing the spikes in Waveform Display (Appendix A.5) and Raster Display (Appendix A.6). Waveform Display allowed the user to see each cluster's spikes as individual waveforms, as groups of waveforms (Figure 14A, B, p.59), or as the waveform average of all spikes in the cluster (Figure 14C). One could view the waveforms of a single cluster or of those of multiple clusters simultaneously. This tool was extremely useful in determining which clusters were accurate and which were either repetitive noise or should have been a part of a neighbouring cluster.

Raster Display allowed the user to see when spikes occurred. It consisted of a time axis for each of the four channels. Starting at 0 ms the spikes for user selected clusters would be displayed over sweeps of 2 seconds up until the end of the analysed spikes. Using this tool, the user could establish whether or not spikes from one cluster were occurring at similar

times as spikes from another cluster. If so, perhaps the two clusters contained data from the same cell. This would have to be further verified using the Waveform Display.

These two tools were used in the analysis of data from every experiment. They were both very useful and reliable and helped minimize the errors present in cluster analysis. Without them, it would have been at times impossible to be certain that the cluster data was entirely accurate.

4.4 Two Examples of Preliminary Tetrode Recordings

After the lengthy process of cluster analysis, cell activity analysis became a matter of computer programming in MatLab. Although the programs demanded large time investments to create, they were invaluable as time saving analysis tools.

One main question was that of the duration of the Gaussian window to use in the spike frequency density calculations. After experimenting with several values, it was decided that a duration of 20 ms was sufficient. A value much less than this resulted in densities that were too precise; a value much greater than this resulted in densities that were too general. A Gaussian window replaced each spike in a data file, centred about the spike's peak. The spike frequency density helped show cells' activity during saccades as well as revealing if any correspondence existed between two or more cells.

The results of two typical examples of successful tetrode recording in the SC were discussed in Section 3.7. Below, these two examples (A and B) are discussed in more detail.

4.4.1 Example of a Simple Analysis Cell Analysis

As discussed in Section 3.7, the cluster data shown in Figure 12, p.57, is representative of two individual cells recorded simultaneously (cells M30051, cell 1, and M30052, cell 2). During recording and from an initial overview of the raw data in DataWave it was evident that there was a large amplitude burst-type or visual-type cell present. More speculatively, it seemed that a tonic cell whose amplitude was just above the level of the background noise was also present. In viewing the raw data, the second cell was difficult to discern from the noise. Viewing the data recorded from threshold crossings, there was certainly some noise that was recorded in addition to the low amplitude cell spikes. Via cluster analysis the spikes from both the first and second cells were accurately separated from the noise (Figure 12). The combination of parameters which yielded the best spike sorting results in this case were peak, valley, and peak phase angle. Thus, 14 parameters were used to classify the spike data for this experiment: 4 peak, 4 valley, and 6 peak phase angle.

In panel C of Figure 12, the cluster for cell M30051 (cluster 1) is small. This is indicative of little variance in the relationship between the peak phase angle of channels 1 and 3 and the amplitude of the spike valley on channel 3 for this cell. The relationship is similarly consistent between the peak phase angle of channels 1 and 4 and the amplitude of the spike peak on channel 1 for this cell, as shown in panel D. The spike data for cell M30052 (cluster 2), however, shows that the relationship between the peak phase angle of channels 1 and 3 and the amplitude of the spike valley on channel 3 is quite variable (panel C). Similarly, a variable relationship is seen between the amplitude of the spike peak on channel 1 and the peak phase angle of channels 1 and 4 for cell M30052 (panel D). The relationship between the amplitude of the spike valley on channels 2 and 1 (panel E) is quite variable for

both cells. The relationships between the amplitude of the spike valley on channels 4 and 3 (panel B) and between the amplitude of the spike peak on channels 4 and 3 (panel F), however, are quite consistent. Interestingly, when only the peak and valley amplitude parameters were used the cluster analysis results (not shown) were not as good as when the peak phase parameters were also used, despite the successful cluster formations shown in panels B and F. Also, when only the peak phase angle parameters were used the cluster analysis results (not shown) were not as good. This demonstrates that the accuracy of cluster analysis is parameter inter-dependent in that AutoCut assigns spikes to clusters based on the inter-comparison of all selected parameters simultaneously. This approach is somewhat confusing for a user who is trying to determine the best parameters to use for analysis. It seems that the best approach is to try a few different combinations for each set of data in order to see which parameters yield the best results.

The success of cluster analysis results is judged manually. Through examination of the waveforms of spikes assigned to each cluster, verification of the validity of each cluster is assessed. Figure 14A, p.59, shows a group of typical spikes for each of the cells identified by the cluster analysis in Figure 12. This shows that the two units have been adequately separated from any noise. The waveforms for both cells are consistent in amplitude and duration. Waveform characteristics were particularly important to verify in the case of the second unit whose activity was often intermixed with noise, as can be seen in Figure 12 where the black dots representing noise are situated predominantly in the vicinity of the second cluster. The consistency of the waveforms shown in Figure 14A for Unit 2 demonstrates that the cell activity has been adequately separated from the noise.

Signal Strength on the Tetrode Wires

The varying amplitudes of a unit's spikes between channels demonstrates the effective nature of the tetrode. Examining the waveforms of Unit 1 over the four channels in Figure 14A one can see that the amplitude of the signal varies from channel to channel. The signal is best recorded on the first channel, then the fourth, then the third, and finally the second. One might surmise that the difference in signal strength between the four wires is due to differences in the wires themselves, perhaps a difference in impedance or integrity. If the waveforms of the Unit 2 are examined, however, it can be seen that this cell's signal is recorded best on the fourth channel, then the first channel, then the second channel, then the third. If the signal strength were due solely to the properties of the four wires, the signals of the two units would be best recorded on the same wires. This not being the case, it is evident that the varying signal strength is more likely due to the spatial relationship between the two units and the four tetrode wires. This is solid evidence that if two units displaying similar spike amplitude were being recorded, the tetrode, along with spike sorting software, could accurately separate the activity of the two cells, as long as the two cells were not firing in synchrony or had similar spike amplitudes while being situated at equal distances from the tetrode wires.

Cell Classifications

Figure 13, p.58, shows the discharge characteristics of the two cells in relation to gaze movement, as was presented in section 3.7.1. Cells M30051 and M30052 were identified as buildup and visual cells, respectively. These cell types are usually defined as being present in the SGI and SGS, respectively. Although it is difficult to specify exactly where the tetrode

is placed in the colliculus when recording, in this case one could estimate that it was placed in the upper collicular layers at approximately the coordinates displayed in Figure 13D.

Although the tetrode is not the best type of recording electrode to use for recording cells from different layers of the colliculus simultaneously, it does have approximately 85 microns of vertical tip separation and thus could be situated in two layers at once. Also, various cells in the colliculus are not necessarily strictly confined to a layer, nor are the layers strictly separated from one another. Thus, recording from buildup and visual cells simultaneously, even though they usually described as being in separate layers (see section 1), is possible.

4.4.2 Example of a Difficult Analysis Cell Analysis

The cluster data shown in Figure 15, p.60, is representative of three individual cells recorded simultaneously (cells M29051, M29052, and M29053). The parameters yielding the best results in this case were peak and valley amplitudes (8 parameters). In every representation shown in Figure 15 the clusters have the typical oblong geometry. Although 3 clusters have been identified, they are large and overlapping and the data points of the first unit are almost entirely within the boundaries of the second unit. Thus, it is again important to verify the legitimacy of the clusters.

Figure 14B, p.58, shows groups of waveforms for each of the three units on the four tetrode channels. The waveforms belonging to the third unit are obviously distinct from those of the first and second units, both in amplitude and shape. The waveforms belonging to units 1 and 2, however, are not so distinct from one another. Also, the signals for both unit 1 and 2 are best recorded on the same channels: channel 2, then channel 1, then channel 3, then

channel 4. Along with the fact that the unit 1 cluster comprises only 53 spikes as compared to the 1 431 and 1 459 spikes in unit 2 and unit 3 clusters, respectively, a convincing argument has been made against unit 1 being an individual cell.

However, when using different parameters for analysis, three clusters were almost always calculated. Thus, statistically speaking, three cells were present. Also, when the average waveforms are examined (Figure 14C) it can be seen that although the averages are similar, the amplitudes of the second unit averages are less than those of the first unit averages. For further exploration into whether this unit was legitimate, the gaze movement data was compared to the unit's discharge characteristics. In Figure 16, p.61, the gaze movement is shown with the spike discharges for the three identified units. Ten trials are displayed. It is obvious that units 2 and 3 are fixation-type and buildup-type neurons, respectively, by viewing their firing frequencies in panels A and B. The first unit has very little activity at all which may indicate that the spikes of the first unit actually belong to one of the other units but fall outside their cluster boundaries due to waveform eccentricities. Even after several attempts at verifying the validity of unit 1, it is sceptical whether or not it is truly an individual cell.

The arguments considered above effectively demonstrate the difficulties involved in verifying the legitimacy of clusters identified by AutoCut. It is important that the user employ all of the software analysis tools and methods available while trying to maintain objectivity and patience in his evaluation.

Signal Strength on the Tetrode Wires

There are still some useful results to be considered from the data of cell 3. The signal for the third cell is best recorded on the third channel, then the fourth channel, then the first channel, then the second. The signal is not strongest on the same wire as the signals from the other two units, indicating that here, as in the first example, the spatial relationship between the cells and the tetrode can be relied upon to produce accurate spike sorting and cell identification.

Cell Classifications

Cell 2 was probably related to fixation as it was most active at the end of the saccade (Figure 16A). This is not a surprising find given that the tetrode was probably in the intermediate to deep layers of the colliculus in or near the rostral fixation zone at approximately the coordinates indicated in Figure 16D. Cell 3 was probably related to generating saccades (Figure 16B). Cell 3 was difficult to classify as its firing frequency was very low before saccade onset, peaked at the beginning of a saccade, and was tonic after the saccade had terminated. It could have been a type of burst neuron but not a classic example of one. It is possible that the cluster determined for unit 1 is truly representative of a third cell that was recorded, perhaps a very infrequent interneuron that is active at the end of saccades. Since various types of neurons are present in the colliculus besides the major types presented in the Introduction, many of which have not been studied in depth, it is always possible that the tetrode could record from cells exhibiting unfamiliar activity. This issue is both interesting and frustrating for the user as he must consider all cells identified by analysis as individual cells until proven otherwise. This is a potentially lengthy process and one without total

resolve until other recordings are made in which cells of similar unfamiliar activity are registered and analysed as confirmation. Assuming that the cells in the colliculus are quite diverse, as indicated by the studies presented above, such confirmation may never arrive.

4.5 Determining Local Circuits Using the Tetrode

4.5.1 Tetrode Limitations in Determining Local Circuits

As already stated, the tetrode's ability to record from multiple cells simultaneously makes it an excellent candidate for determining local circuitry in the SC. The extent to which the tetrode can fulfill this potential will always be limited, however. The tip spacing of the tetrode is a limiting factor. The tips can only be so far apart before activity from a cell ceases to register on all four wires. This restricts recording in both the vertical and horizontal planes. Particularly, recording of interlaminar circuitry, such as that presented in Figure 8, is unlikely with the tetrode as the vertical spacing of the tetrode wires is 85 microns compared to the approximately 3 mm dorso-ventral extent of the colliculus in cat. In an ideal experiment, it might be possible to perform multiple recordings at increasing depths in the colliculus while generating the same behaviour from the cat for each recording. The data from all of the recordings along the descent could then be compared with the aim of correlating cell data to see if any cells along the descent are related. Similarly, multiple recordings along medio-lateral and rostro-caudal extents of the colliculus could be made to determine local circuitry in the horizontal plane. Recordings in both the horizontal and vertical planes could be made using multiple tetrodes simultaneously.

4.5.2 Determining if Cells are Related to one Another

Even once successful multi-cell recordings have been made with the tetrode, it is difficult to determine if the cells are related to one another via local circuitry. Examining cell discharge in relation to the gaze and head trajectories of the animal is helpful in determining when multiple cells are active during saccadic eye movements. However, similar temporal cell discharge is not sufficient evidence for cells being related via direct connections. To be sure that cells are involved in common circuits, it is necessary, as often is in many domains of neuroscience, to perform various types of experiments on the same animal and then combine their outcomes, providing a comprehensive study. Combining experimental procedures such as those used here with the tetrode and those used in cell labelling (eg: using horseradish peroxidase such as experiments done by Moschovakis & Karabellas, 1985) would allow both recording of cellular activity and cell identification upon histological study of the SC. By knowing the activity of the cells along with the cell's connections, one could start to get an accurate analysis of the local circuits involved in generating saccades. Obviously, the more approaches employed in studying the same cells, the more accurate will be the analysis and characterisation of the cells.

CHAPTER 5

CONCLUSIONS

The studies presented in this thesis explore the feasibility of using tetrodes to record from multiple single cells simultaneously in the superior colliculus. The preliminary results of this long term project indicate that recording in the superior colliculus using tetrodes is indeed possible and represent the first description of such an endeavour.

5.1 Summary of Major Results

Successful use of the tetrode in the superior colliculus demonstrates that whereas tetrodes are traditionally used in areas of the brain with high active cell density, such as the hippocampus, they can also be employed with positive results in other parts of the brain that have less dense cell activity. Although it is evident that it is difficult to achieve in the SC the same amount of simultaneously recorded neurons seen in hippocampus tetrode studies (Henze et al., 2000; Csicsvari, 1998; O'Keefe and Reece, 1993; Wilson and McNaughton, 1993), even the recording of a few cells simultaneously is beneficial to our knowledge of local circuitry in the SC.

The only major modification to the tetrode apparatus was the addition of the supporting protoboard in which the tetrode lead wire pins were secured. Although a small

modification, it was of great benefit to the experiment giving weight distribution to the four fine tetrode wires and allowing easy manipulation and repair.

Perhaps the greatest achievement of this project was attaining a method of data acquisition that allowed a sampling rate of 35.7 kHz per tetrode wire. This allowed greatly improved spike resolution as compared to older techniques employed, as discussed earlier. Also, recording the data directly to computer hard disk was of great advantage as the intermediate step of transferring data from a recording device to disk was eliminated.

Exploration of the software data analysis tools proved to be very beneficial. Determining which parameters were often best for accurate spike separation gives the user a good starting point for data analysis. Developing methods on how to manipulate clusters and use various AutoCut tools in order to produce the most accurate results made data analysis in subsequent analysis programs more reliable (Appendix A.6). Also, developing a system of file transfer from Universal File Format used by DataWave to ASCII and then to mat format was essential as the final cell and saccade data analyses were most easily performed in MatLab. Once programs were constructed to manipulate and analyse the spike and non-spike data, MatLab gave the user great versatility in data analysis and display. The creation of these programs made much of the data analysis and display automated, thus reducing the amount of time the user had to spend on such tasks.

The successful recording of multiple single collicular cells by the tetrode was very encouraging. These preliminary recordings give hope that the continuation of this project will contribute useful knowledge of local circuitry in the SC and thus the saccadic system will be better understood.

5.2 Future Considerations

In any experimental procedure there is always room for improvement. As technology advances and ideas come to light tetrode recording in the SC may undergo many improvements in years to come. Several immediate possibilities for improvement are suggested below.

5.2.1 Improvements to the Tetrode Design

The tetrode apparatus could be ameliorated by eliminating the lead wires that connect the tetrode lead pins to the headstage amplifiers. Designing an arrangement that secures the headstage amplifiers solidly to the cat's implant is tricky but possible. If the tetrode lead pins could be plugged directly into the amplifiers and the amplifiers were well secured the possibility of noise due to wire movement appearing on the tetrode channels would be greatly reduced.

The diameter of the electrode used to support the four tetrode wires could be reduced. Electrodes or even simple metal rods of 100 micron diameter could be used instead of the 200 micron electrodes currently used without greatly reducing the rigidity of the apparatus. This would lessen the amount of tissue damage caused by the penetration of the tetrode. Simultaneously, the diameter of the tetrode wires could be increased in order to increase the tip spacing. The overall diameter of the tetrode apparatus would remain the same (320 microns) but more surface area would be devoted to recording.

It would be ideal if the tetrode were a premade recording instrument. The experimenter would save a great deal of time were he able to order tetrodes as easily he can electrodes instead of having to build them himself. Thomas Recording (Germany) makes

tetrodes intended for use in areas of the brain that have a high density of active cells. The outer diameter of these tetrodes is 96 microns and the maximum tip spacing is 38.4 microns. The tetrode consists of a core recording wire surrounded by three other recording wires, all of which is encased in the insulator quartzglas. Unfortunately, tetrodes with other tip spacing are not available. Perhaps in time, however, as tetrode recording becomes more widely used, tetrodes of various tip spacings will be produced.

5.2.2 Improvements to the Data Acquisition System

There are several advantages to changing the data acquisition system from the DataWave package used in these studies to another package, such as that offered by Neuralynx (Tucson, Arizona, USA). The Neuralynx Cheetah Data Acquisition system offers the experimenter more versatility. Spike channels and non-spike channels can be recorded at different sampling rates instead of recording all channels at the same rate and then reducing the number of points recorded to disk for the non-spike channels. This allows for greater sampling frequencies on the spike data channels. Another advantage to the Neuralynx system is the file format in which the data is saved. The output data file can be directly converted to mat file format for use in MatLab. Neuralynx allows the recording of entire experiments to disk, not just thresholded spike data. This way experimental data can be perused again and again and optimal thresholds can be set for capturing spike data. Thresholding the data can be done either on or offline. Neuralynx also offers online spike sorting so the experimenter can assess how many cells are present while recording. The last advantage offered by the Neuralynx package is that its software is Windows based. This is a more convenient operating environment than DOS, on which DataWave operates, and allows the user more

versatility between different programs. A disadvantage to the Neuralynx system is that its spike sorting program "Spike Sort" employs only peak and valley amplitude parameters to define clusters. Although these parameters are usually sufficient to isolate cells, a few other parameters involving time or phase would be useful. Naturally, the other disadvantage of replacing the recording system is the cost involved.

These studies have provided positive results from using tetrodes in the superior colliculus while investigating the limits of the tetrode recording technique. With further refinements and continued experiments tetrodes should help reveal a great deal about the configurations and functions of the cells and the local circuits involved in generating saccadic eye movements.

APPENDIX A

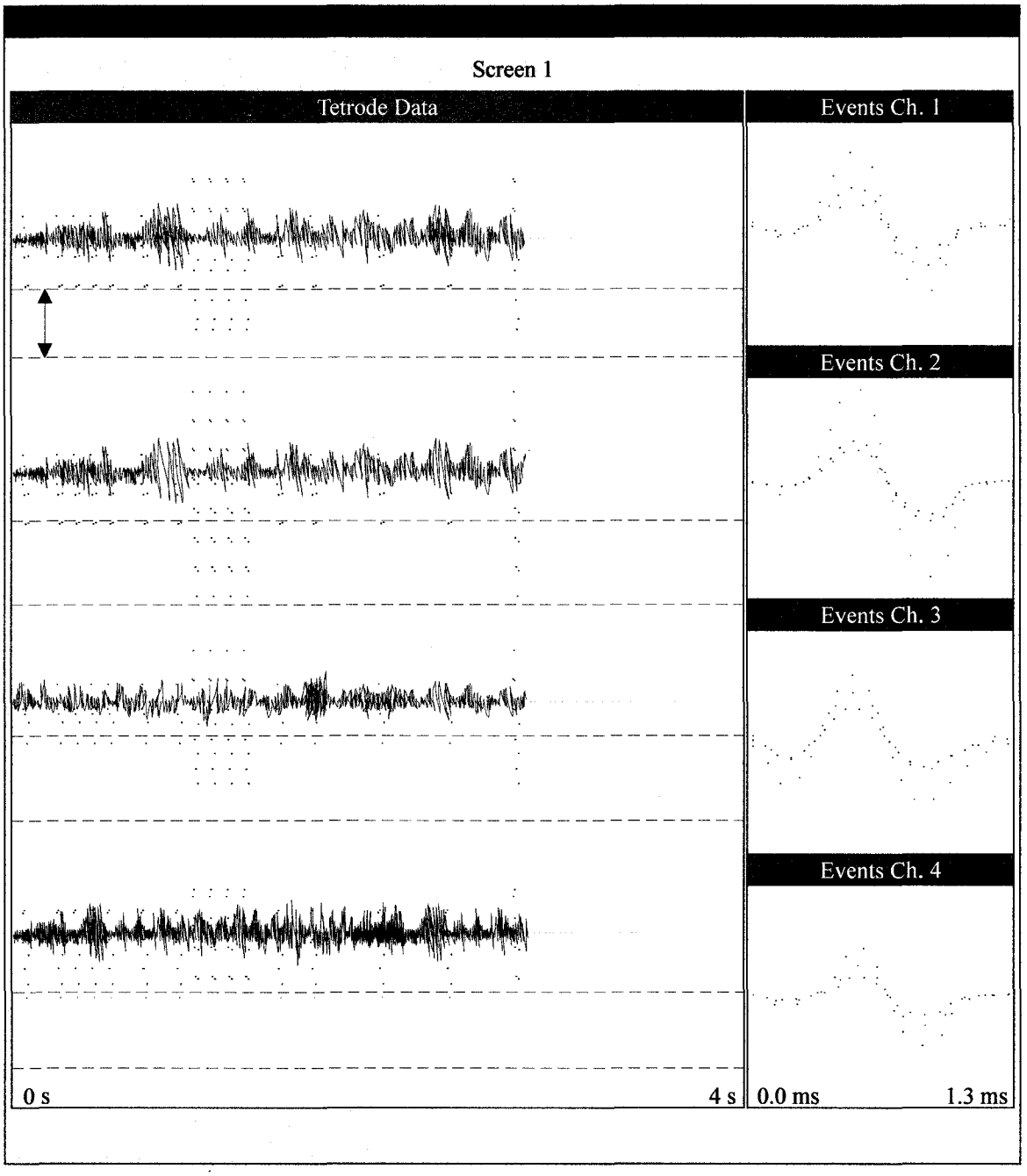

Appendix A.1 Layout of Runtime Screen 1 in DataWave data acquisition software program. In this user defined display, 5 windows are shown. The large window displays the continuously acquired tetrode data (background noise and spikes) over a sweep 4 seconds in duration. Threshold levels are indicated for each channel as horizontal dotted lines. An event must fall within the specified range (indicated by arrow) in order to be recorded. The four windows to the right display events that have crossed a threshold on each channel. Whenever an event triggers on any channel, the event window of the channel that was first triggered will display the data present on each channel at the time of the event. The duration of the event window in this example has been set to 1.3 ms.

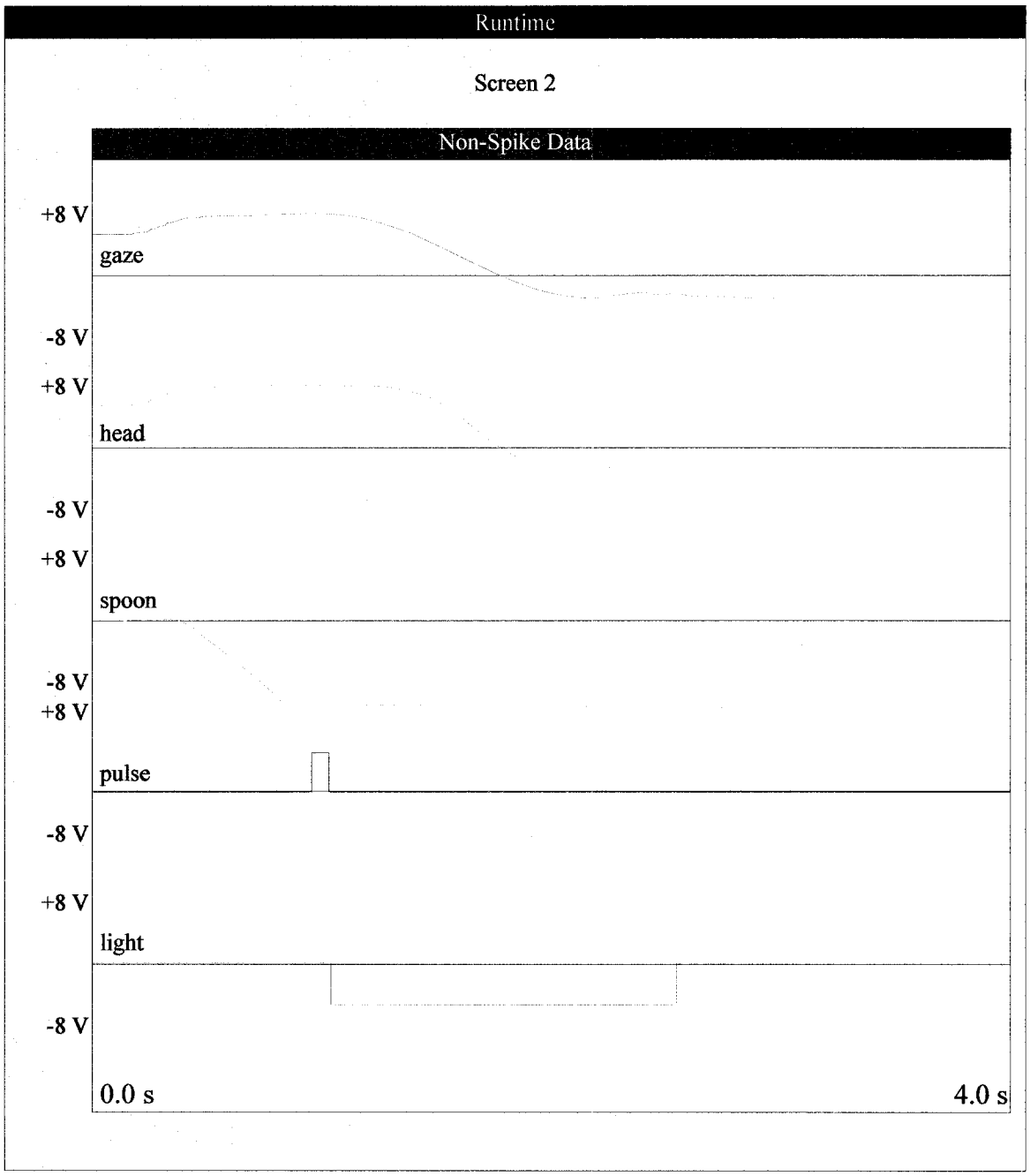

Appendix A.2 Layout of Runtime Screen 2 in DataWave data acquisition software program. Five non-spike channels are displayed: gaze position, head position, spoon position, pulse occurrence, and light status. The sweep duration in this example has been set to 4 seconds; the amplitude for each channel is +/- 8 Volts. The data displayed in this window is sampled at 1000 Hz.

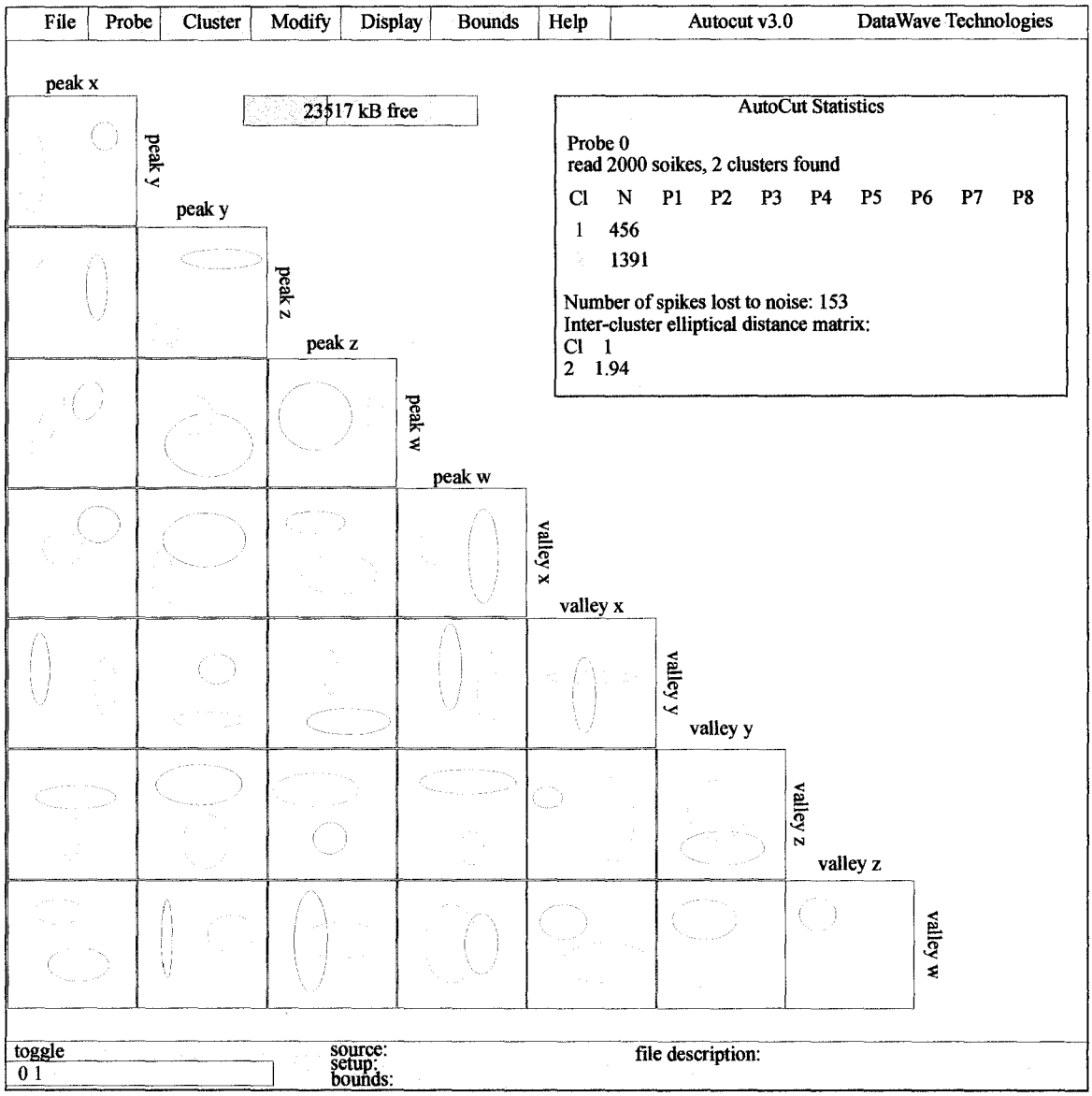

Appendix A.3 Layout of the main display of AutoCut spike separation software, version 3.0. 28 2 dimensional plots are displayed. Each plot represents the comparison of two out of n parameters that the user has selected to be used in the spike separation. The clusters and the noise can be toggled on and off (displayed and not displayed) using the 0,1,and 2 keys on the keyboard. Clusters present in the current view are indicated at bottom left. The bar in the centre of the main window indicates the amount of memory available. The window at upper right displays the AutoCut statistics: how many spikes are present in the file being analysed, how many clusters were calculated, how many spikes were placed in each cluster (N), the z-statistics of each parameter for each cluster (P1, P2, ...), the amount of spikes lost to noise, and the inter-cluster elliptical distance matrix.

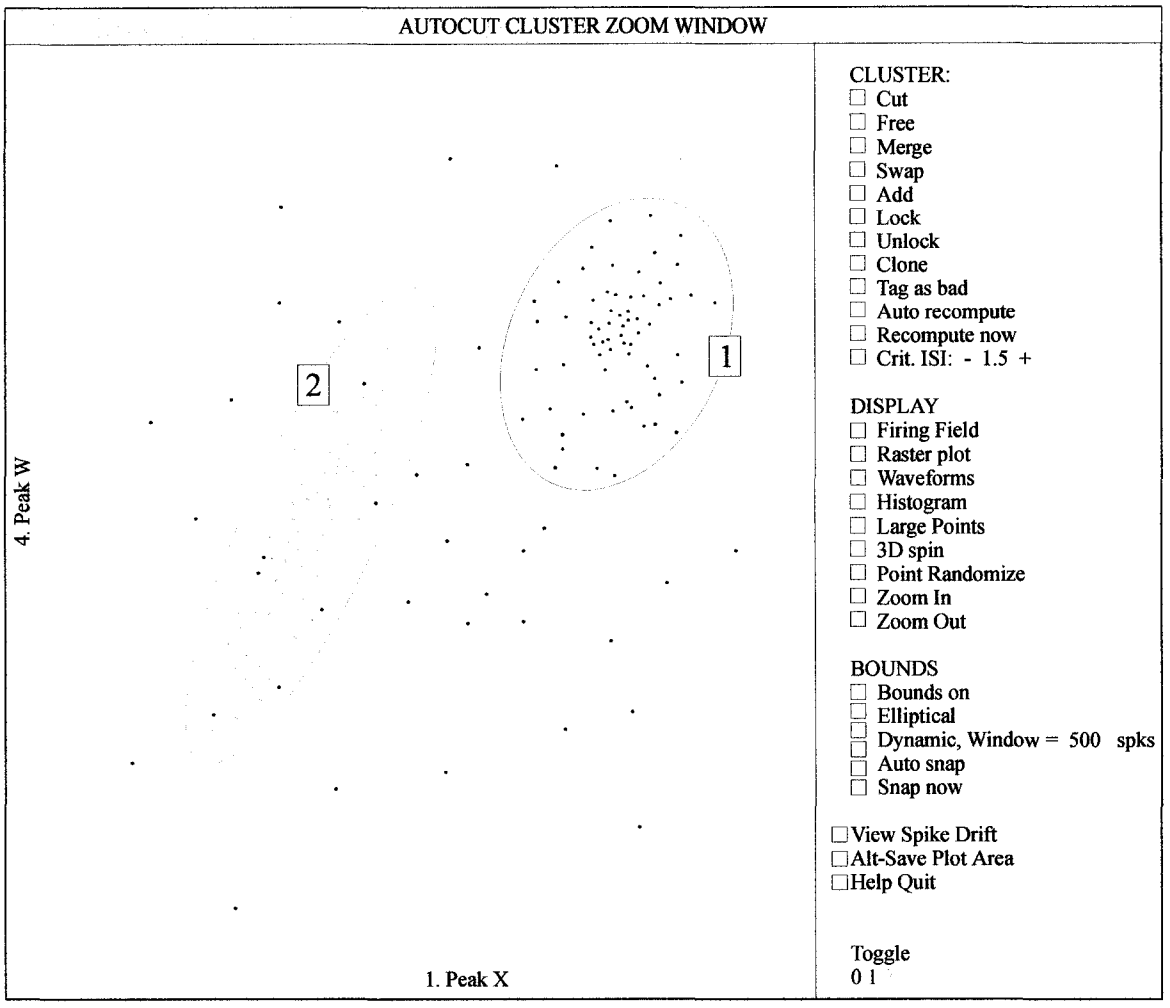

Appendix A.4 Layout of the Cluster Zoom Window in AutoCut. This 2D representation of the spike data plots Peak Amplitude values for channel 4 (W) versus channel 1 (X). Two clusters have been calculated (1 and 2) according to user selected parameters, indicating the presence of two cells in the data. The righthand column contains options for cluster formatting, display of other analysis windows, and cluster boundary options. The noise (0) and each cluster (1 and 2, including boundaries and spikes) can be toggled on and off (displayed and not displayed) using the 0, 1,and 2 keys on the keyboard. Clusters present in the current view are indicated at bottom right.

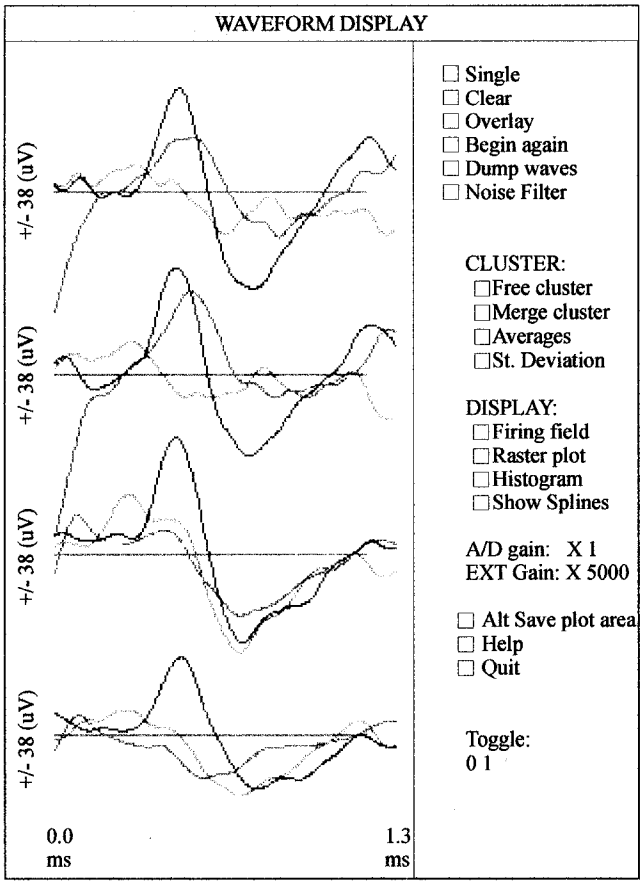

Appendix A.5 Layout of the Waveform Display in AutoCut. The main window displays groups of waveforms or individual waveforms (not shown). Amplitude is given at left and time at bottom. The righthand column gives options for waveform display, cluster formatting, and display of other analysis windows. The waveforms for each cluster (1 and 2) and the noise (0) can be toggled on and off (displayed and not displayed) using the 0, 1,and 2 keys on the keyboard. Waveforms for clusters present in the current view are indicated at bottom right.

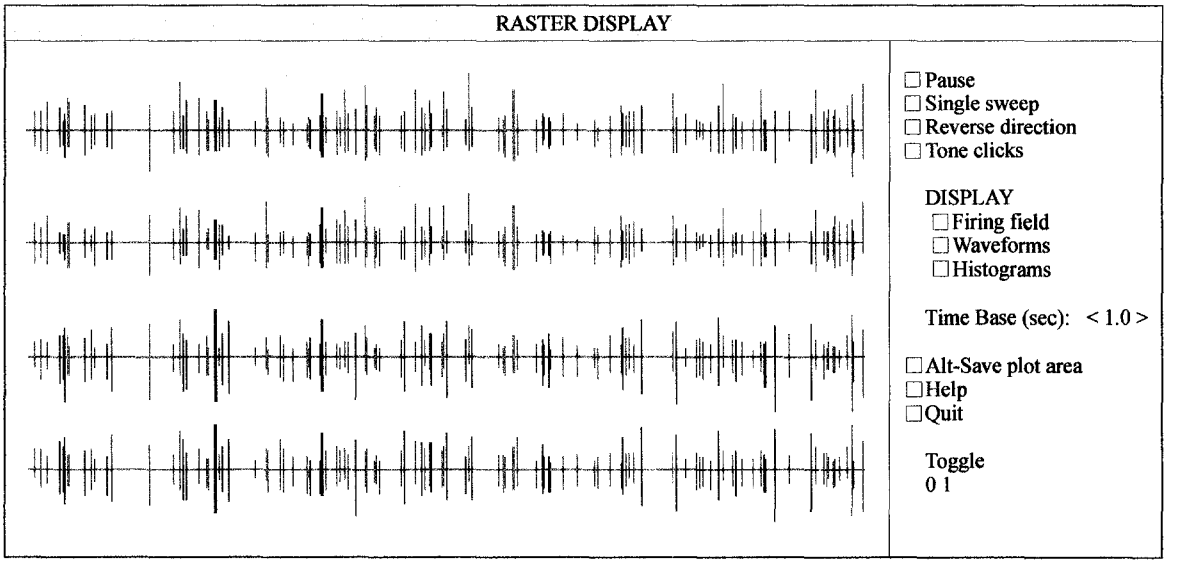

Appendix A.6 Layout of the Raster Display in AutoCut. The main window displays sweeps of the sequential occurrence of each spike in the data file, or up to 16 383 spikes maximum if the file contains more spikes than 16 383 spikes. The duration of the sweep can be changed by varying the Time Base setting in the righthand column. In the example given here, a sweep of 1 second duration is shown. The righthand column gives options for raster plot display and display of other analysis windows. The spikes for each cluster (1 and 2) and the noise (0) can be toggled on and off (displayed and not displayed) using the 0, 1,and 2 keys on the keyboard. Spikes for clusters present in the current view are indicated at bottom right.

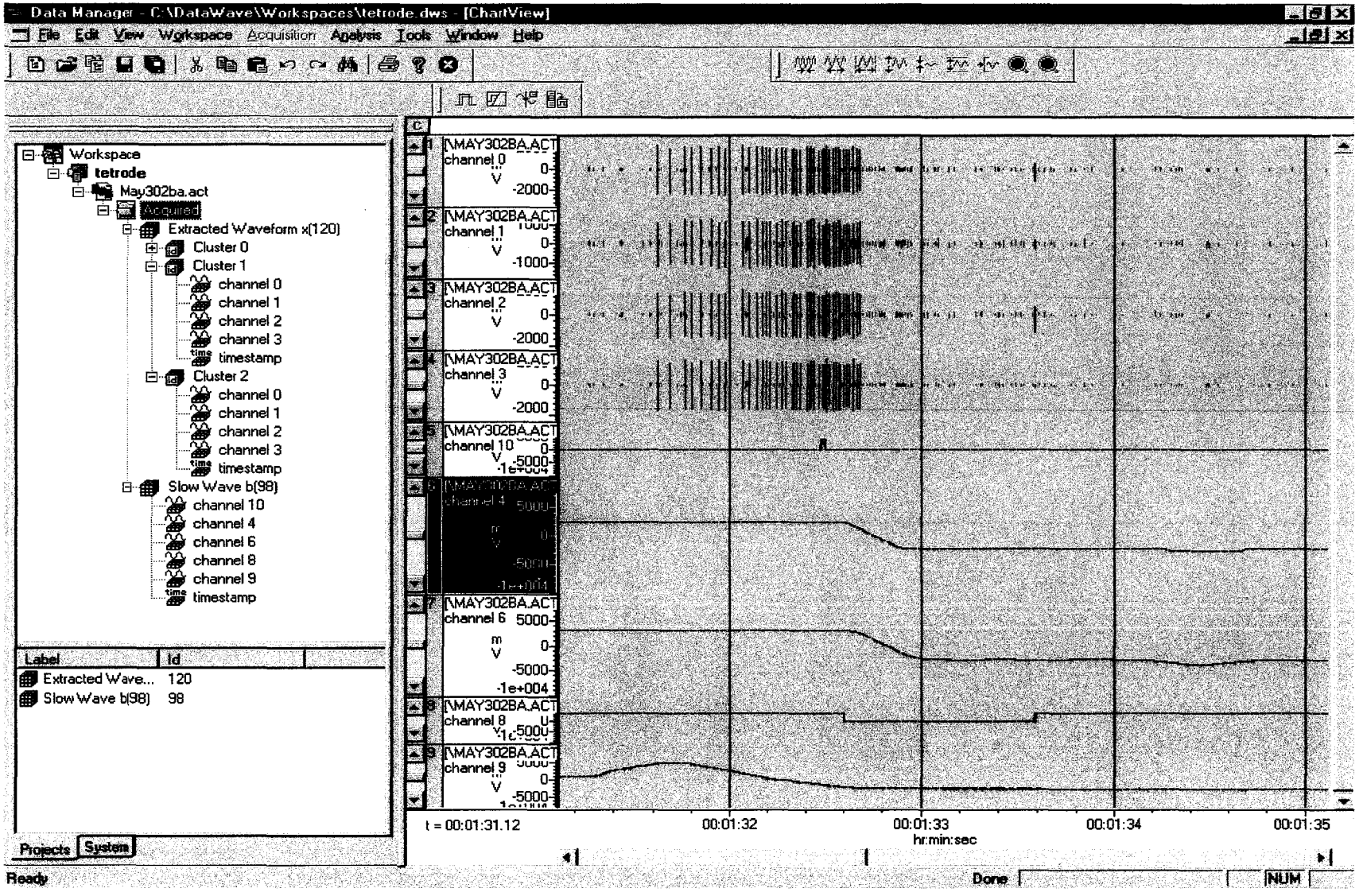

Appendix A.7 Layout of the DataManager main window. The lefthand frame displays the files in use in the workspace. The righthand window displays, from top to bottom, the cell activity on the four tetrode wires, the target pulse indicator, head movement, eye movement, light status, and target spoon. The y-axis is measured in mV and the x-axis in seconds.

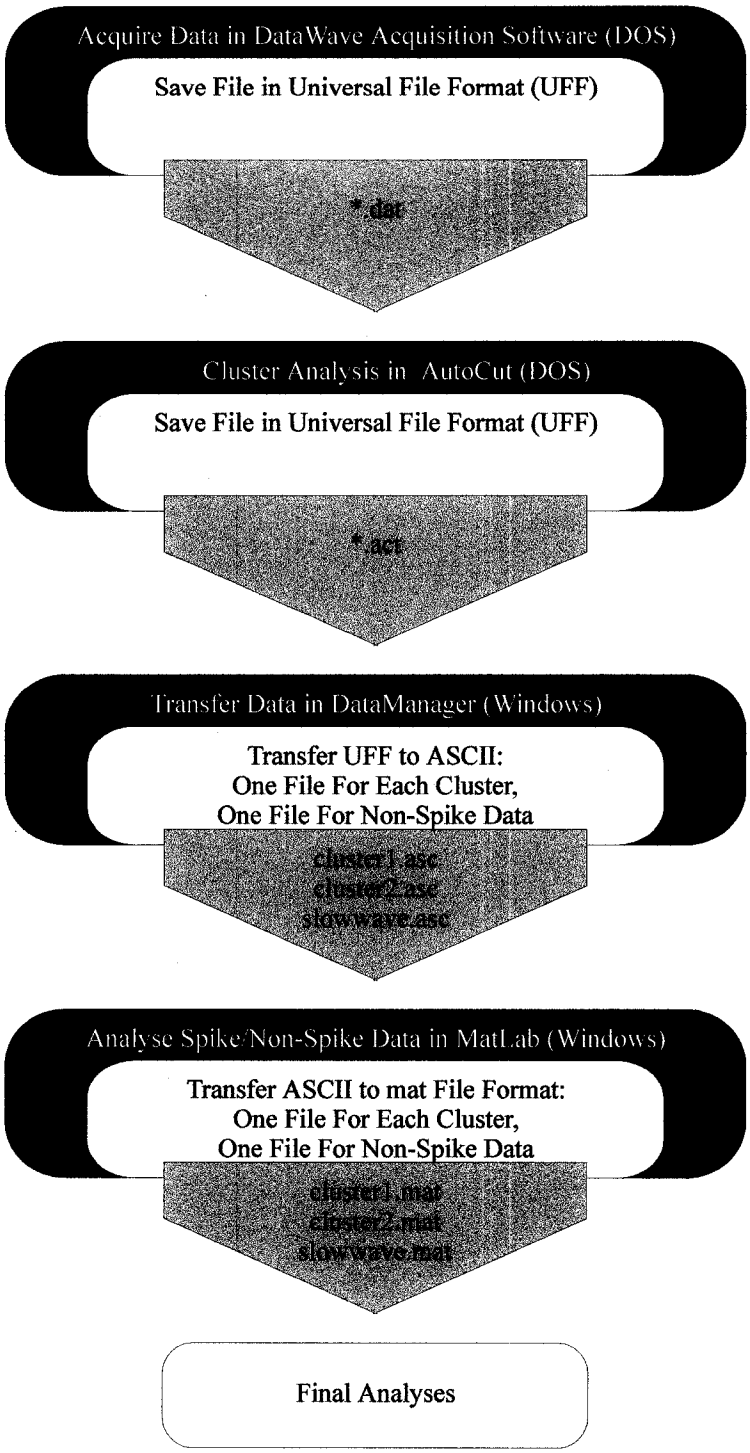

Appendix A.8 Flow chart of data progression in tetrode recording and analysis. Software programs used to record and analyse tetrode data are represented by the outer boxes. The file formats in which the spike data is saved in each program are represented by the inner boxes. Output file names are represented by the arrows. * denotes a file name determined by the user.

Appendix A.9 Flow chart depicting spike and non-spike data manipulation by user-made programs in MatLab. Wham_bang.m uses 5 functions to produce spike, non-spike, and firing frequency data, all sorted by trial. Plots of single trials can then be made using 2 user-made plotting programs. Plots of multiple trials can be made by 3 user-made programs that can align the gaze traces of each trial on saccade start, saccade end, and target onset.

REFERENCES

Appell P.P., Behan M. Sources of subcortical GABAergic projections to the superior colliculus in the cat. *Journal of Comparative Neurology. 302(1):143-58, 1990.*

Anderson R.W., Keller E.L., Gandhi N.J., and Das S. Two-dimensional saccade-related population activity in superior colliculus in monkey. *Journal of Neurophysiology. 80(2):798-817, 1998.*

Antonetty C.M. and Webster K.E. The organization of the spinotectal projection. An experimental study in rat. *Journal of Comparative Neurology. 34: 898, 1975.*

Beckstead R.M. An autoradiographic examination of cortico-cortical and subcortical projections of the mediodorsal-projection (prefrontal) cortex in the rat. *Journal of Comparative Neurology. 184: 43, 1979.*

Behan M. and Kime N.M. Spatial distribution of tectotectal connections in the cat. *Progress in Brain Research. 112:131-42, 1996.*

Behan M. and Kime N.M. Intrinsic circuitry in the deep layers of the cat superior colliculus. *Visual Neuroscience. 13: 1031-1042, 1996.*

Caldwell R.B. and Mize R.R. Superior colliculus neurons which project to the cat lateral posterior nucleus have varying morphologies. *Journal of Comparative Neurology, 203:53, 1981.*

Casagrande V.A., Harting J.K., Hall W.C., Diamond I.T., and Martin G.F. Superior colliculus of the tree shrew *(Tupaia glis). Anat. Rec., 177:444, 1972.*

Chalupa L.M. Visual physiology of the mammalian superior colliculus. Comparative Neurology of the Optic Tectum, edited by H. Vanegas. New York: Plenum Press, 1984, p.775-818.

Csicsvari J., Hirase H., Czurko A., and Buzsaki G. Reliability and state dependence of pyramidal cell-interneuron synapses in the hippocampus: an ensemble approach in the behaving rat. *Neuron, 21(1): 179, 1998.*

Cynader H. and Berman N. Receptive field organization of monkey superior colliculus. *Journal of Neurophysiology. 35: 187, 1972.*

Drager U.C. and Hubel D.H. Topography of visual and somatosensory projections to mouse superior colliculus. *Journal of Neurophysiology. 39:91, 1976.*

Edwards S.B. The commissural projection of the superior colliculus in the cat. *Journal of Comparative Neurology. 154:117, 1977.*

Edwards S.B., Rosenquist A.C., and Palmer L. An autoradiographic study of the ventral lateral geniculate projections in the cat brain. *Brain Research. 72:282, 1974.*

Feldon, P. Kruger L. Topography of the retinal projection upon the superior colliculus of the cat. *Vision Research. 10(2):135-43, 1970.*

Ficalora A.S., Mize R.R. The neurons of the substantia nigra and zona incerta which project to the cat superior colliculus are GABA immunoreactive: a double-label study using GABA immunocytochemistry and lectin retrograde transport. *Neuroscience. 29(3):567-81, 1989.*

Flindt-Egebak P. An autoradiographical study of the projections from the feline sensorimotor cortex to the brainstem. *J. Hirnforsch. 20:375, 1979.*

Freedman E.G., Stanford T.R., and Sparks D.L. Combined eye-head gaze shifts produced by electrical stimulation of the superior colliculus in rhesus monkeys. *Journal of Neurophysiology 76:927-952, 1996.*

Fuchs A.F. and Robinson D.A. A method for measuring horizontal and vertical eye movement chronically in the monkey. *Journal of Applied Physiology. 21: 1068-70, 1966.*

Goldman P.S. and Nauta W.J.H. Autoradiographic demonstration of a projection from prefrontal association cortex to the superior colliculus in the rhesus monkey. *Brain Research. 116: 145, 1976.*

Grantyn A. and Berthoz A. Burst activity of identified tecto-reticulo-spinal neurons in the alert cat. *Experimental Brain Research 57:417-421, 1985.*

Grantyn A. and Grantyn R. Axonal patterns and sites of termination of cat superior colliculus neurons projecting in the tecto-bulbo-spinal tract. *Experimental Brain Research 46:243-256, 1982.*

Gray, C.M. Bursting cells in visual cortex exhibit properties of intrinsically bursting cells in sensorimotor cortex. *Soc. Neurosci. Abstr., 18:131.2, 1992.*

Gray C.M., Maldonado P.E. Wilson M. McNaughton B. Tetrodes markedly improve the reliability and yield of multiple single-unit isolation from multi-unit recordings in cat striate cortex. *Journal of Neuroscience Methods. 63(1-2):43-54, 1995.*

Graybiel A.M. Satellite system of the superior colliculus: The parabigeminal nucleus and its projections to the superficial collicular layers. *Brain Research. 145:365, 1978a.*

Graybiel A.M. organization of the nigrotectal connection: An experimental tracer study in the cat. *Brain Research. 143: 339, 1978b.*

Guitton D. & Munoz D.P. Control of orienting gaze shifts by the tecto-reticulo-spinal system in the heat-free cat. I. Identification, localization and effects of behavior on sensory responses. *Journal of Neurophysiology 66: 1605-1623, 1991.*

Guitton, D. (1991) Control of Saccadic Eye and Gaze Movements by the Superior Colliculus and Basal Ganglia. In *Eye Movements*.ed.Carpenter, R.H.S. pp. 244-276. London: The MacMillan Press Ltd.

Guitton D., Munoz D.P., Galiana H.L. Gaze control in the cat: studies and modeling of the coupling between orienting eye and head movements in different behavioral tasks. *Journal of Neurophysiology. 64(2):509-31, 1990.*

Guitton D., Douglas R.M., & Volle M. Coordinated eye head movements in the cat. *Journal of Neurophysiology. 52: 1030-1050, 1984.*

Hall W.C. and Lee P. Interlaminar connections of the Superior Colliculus in the tree shrew. I. the superficial gray layer. *The Journal of Comparative Neurology. 332: 213-223, 1993.*

Harris K.D., Henze D.A., Csicsvari J., Hirase H., Buzsaki G. Accuracy of the tetrode spike separation determined by simultaneous intracellular and extracellular measurements. *J. Neurophysiol. 84(1): 401, 2000.*

Harris L.R. The superior colliculus and movements of the head and eyes in cats. *Journal of Physiology 300:367-91:367-391, 1980.*

Harting J.K., Huerta M.F., Frankfurter A.J., Strominger N.L. and Royce, G.J. Ascending pathways from the monkey superior colliculus: an autoradiographic analysis. *Journal of Comparative Neurology. 192(4):853-82, 1980.*

Harting J.K., Huerta M.F., Weber J.T., and Royce G.L. A hypothalamo-tectal projection in the cat: Evidence of patch-like terminations within the superior colliculus. *Soc. Neurosci. Abstr. 5:787, 1979.*

Harting J.K., Hall W.C., Diamond I.T., and Martin G.F. Anterograde degeneration study of the superior colliculus in Tupaia glis: evidence for a subdivision between superficial and deep layers. *Journal of Comparative Neurology 148:361-386, 1973.*

Harting J.K., Glendenning K.K, Diamond I.T, Hall W.C. Evolution of the primate visual system: anterograde degeneration studies of the tecto-pulvinar system. *American Journal of Physical Anthropology. 38(2):383-92, 1973a.*

Harting J.K., Hall W.C. Diamond I.T., and Martin G.F. Anterograde degeneration study of the superior colliculus in Tupaia glis: evidence for a subdivision between superficial and deep layers. *Journal of Comparative Neurology. 148(3):361-86, 1973b.*

Harting J.K., Diamond I.T, and Hall W.C. Anterograde degeneration study of the cortical projections of the lateral geniculate and pulvinar nuclei in the tree shrew (Tupaia glis). *Journal of Comparative Neurology. 150(4):393-440, 1973c.*

Hashikawa T., Kawamura K. Identification of cells of origin of tectopontine fibers in the cat superior colliculus: an experimental study with the horseradish peroxidase method. *Brain Research. 130(1):65-79, 1977.*

Henze D.A., Borhegyi Z., Csicsvari J., Mamiya A., Harris K.D., Buzsaki G. Intracellular features predicted by extracellular recordings in the hippocampus in vivo. *J. Neurophysiol. 84(1):390, 2000.*

Hetherington P.A. and Swindale N.V. Receptive field and orientation scatter studied by tetrode recordings in cat area 17. *Visual Neuroscience. 16(4):637-52, 1999.*

Huerta M.F. and Harting J.K. The projection from the nucleus of the posterior commissure to the superior colliculus of the cat: patch-like endings within the intermediate and deep grey layers. *Brain Research. 238(2):426-32, 1982a.*

Huerta M.F. and Harting J.K. Tectal control of spinal cord activity: neuroanatomical demonstration of pathways connecting the superior colliculus with the cervical spinal cord grey. *Progress in Brain Research. 57:293-328, 1982b.*

Huerta, M.F., Franfurter, A., and Harting, J.K. Connections of the spinal trigeminal nucleus in the rat. *Anat. Rec. 199:121 A, 1981a.*

Huerta M.F., Frankfurter A.J., and Harting J.K. The trigeminocollicular projection in the cat: patch-like endings within the intermediate gray. *Brain Research. 211(1):1-13, 1981b.*

Illing R.B. The mosaic architecture of the superior colliculus. *Progress in Brain Research. 112:17-34, 1996.*

Illing R.B. Association of efferent neurons to the compartmental architecture of the superior colliculus. Proceedings of the National Academy of Sciences of the United States of America. 89(22):10900-4, 1992.

Isa T., Endo T., and Saito Y. The visuo-motor pathway in the local circuit of the rat superior colliculus. *Journal of Neuroscience. 18(20):8496-504, 1998.*

Kanaseki T. and Sprague J.M. Anatomical organization of pretectal nuclei and tectal laminae in the cat. *Journal of Comparative Neurology 158:319-337, 1974.*

Kandal E.R., Schwartz J.H., and Jessell T.M. Principles of Neuroscience. Elsevier Science Publishing Co., Inc.: New York, NewYork, 1991.

Kawamura S. and Kobayashi E. Identification of laminar origin of some tecto-thalamic fibres in the cat. *Brain Research. 91:281, 1975.*

Kawamura S., Fukushima N., Hattori S., and Kudo M. Laminar segregation of cells of origin of ascending projections from the superficial layers of the superior colliculus. *Brain Research. 184:486, 1980.*

Kawamura S., Hattori S., Higo S., and Matsuyama T. The cerebellar projections to the superior colliculus and pretectum in the cat: An autoradiographic and horseradish peroxidase study. *Neuroscience. 7:1673, 1982.*

Kilpatrick I.C., Collingridge G.L., and Starr M.S. Evidence for the participation of nigrotectal γ-aminobutyrate-containing neurons in striatal and nigral-derived circling in the rat. *Neuroscience. 7:207, 1982.*

Kunzle H., Akert K., and Wurtz R.H. Projection of area 8 (frontal eye field) to superior colliculus in the monkey. An autoradiographic study. *Brain Research. 117:487, 1976.*

Langer T.P., Lund R.D. The upper layers of the superior colliculus of the rat: a Golgi study. *Journal of Comparative Neurology. 158(4):418-35, 1974.*

Lee P.H., Helms M.C., Augustine G.J., and Hall W.C. Role of intrinsic synaptic circuitry in collicular sensorimotor integration. Proceedings of the National Academy of Sciences of the United States of America. 94(24):13299-304, 1997 Nov 25.

Leichnetz G.R., Spencer R.F., Hardy S.G.P., and Astruc J. The prefrontal corticotectal projection in the monkey: An anterograde and retrograde horseradish peroxidase study. *Neuroscience. 6:1023, 1981.*

Maldonado P.E., Godecke I., Gray C.M., and Bonhoeffer T. Orientation selectivity in pinwheel centers in cat striate cortex. *Science. 276(5318):1551-5, 1997 Jun 6.*

Maldonado P.E., Gray C.M. Heterogeneity in local distributions of orientation-selective neurons in the cat primary visual cortex. *Visual Neuroscience. 13(3):509-16, 1996.*

McNaughton B.L., O'Keefe J., Barnes C.A. The stereotrode: a new technique for simultaneous isolation of several single units in the central nervous system from multiple unit records. *Journal of Neuroscience Methods. 8(4):391-7, 1983.*

Mize R.R. Neurochemical microcircuitry underlying visual and oculomotor function in the cat superior colliculus. *Progress in Brain Research. 112:35-55, 1996.*

Mize R.R. The organization of GABAergic neurons in the mammalian superior colliculus. [Review] *Progress in Brain Research. 90:219-48, 1992.*

Mize, R.R. Patterns of convergence and divergence of retinal and cortical synaptic terminals in the cat superior colliculus. *Exp. Brain Res. 269:211, 1983.*

Moschovakis A.K., Karabelas A.B., and Highstein S.M. Structure-function relationships in the primate superior colliculus. I. Morphological classification of efferent neurons. *Journal of Neurophysiology 60: 232-262, 1988a.*

Moschovakis A.K., Karabelas A.B., & Highstein S.M. Structure-function relationships in the primate superior colliculus. II. Morphological identity of presaccadic neurons. *Journal of Neurophysiology 60: 263-302, 1988b.*

Moschovakis A.K. and Karabelas A.B. Observations on the somatodendritic morphology and axonal trajectory of intracellularly HRP-labeled efferent neurons located in the deeper layers of the superior colliculus of the cat. *Journal of Comparative Neurology 239:276-308, 1985.*

Munoz D.P. and Istvan P.J. Lateral inhibitory interactions in the intermediate layers of the monkey superior colliculus. *Journal of Neurophysiology. 79(3):1193-209, 1998.*

Munoz D.P. and Wurtz, R.H. Activity in Monkey Superior Colliculus II. Spread of Activity During Saccades. *Journal of Neurophysiology. 73(6):2334-48, 1995.*

Munoz D.P. and Wurtz R.H. Fixation cells in monkey superior colliculus. II. Reversible activation and deactivation. *Journal of Neurophysiology. 70(2):576-89, 1993a.*

Munoz D.P. and Wurtz R.H. Fixation cells in monkey superior colliculus. I. Characteristics of cell discharge. *Journal of Neurophysiology. 70(2):559-75, 1993b.*

Munoz D.P. and Guitton D. Control of orienting gaze shifts by the tectoreticulospinal system in the head-free cat. II. Sustained discharges during motor preparation and fixation. *Journal of Neurophysiology. 66:1624-1641, 1991.*

Munoz D.P., Guitton D., and Pelisson D. Control of orienting gaze shifts by the tectoreticulospinal system in the head-free cat. III. Spatiotemporal characteristics of phasic motor discharges. *Journal of Neurophysiology 66:1642-1666, 1991a.*

Munoz D.P., Pelisson D., and Guitton D. Movement of neural activity on the superior colliculus motor map during gaze shifts. *Science 251:1358-1360, 1991b.*

Norita M. Neurons and synaptic patterns in the deep layers of the superior colliculus of the cat. A Golgi and electron microscopic study. *Journal of Comparative Neurology. 190(1):29-48, 1980.*

Okada Y. The distribution and function of gamma-aminobutyric acid (GABA) in the superior colliculus. [Review] *Progress in Brain Research. 90:249-62, 1992.*

O'Keefe J. Recce ML. Phase relationship between hippocampal place units and the EEG theta rhythm. *Hippocampus. 3(3):317-30, 1993.*

Paré M., Crommelinck M., and Guitton, D. Gaze shifts evoked by stimulation of the superior colliculus in the head-free cat conform to the motor map but also depend on stimulus strength and fixation activity. *Experimental Brain Research. 101:123-39, 1994b.*

Pettit D.L., Helms M.C., Lee P., and Augustine GJ. Hall WC. Local excitatory circuits in the intermediate gray layer of the superior colliculus. *Journal of Neurophysiology. 81(3):1424-7, 1999.*

Rhoades R.W., Mooney R.D., Rohrer W.H., Nikoletseas M.M., and Fish S.E. Organization of the projection from the superficial to the deep layers of the hamster's superior colliculus as demonstrated by the anterograde transport of Phaseolus vulgaris leucoagglutinin. *Journal of Comparative Neurology. 283(1):54-70, 1989.*

Robinson D.A. Eye movements evoked by collicular stimulation in the alert monkey. *Vision Research 12:1795-1808, 1972.*

Rodrigo-Angulo M.L. and Reinoso-Suarez F. Topographical organization of the brainstem afferents to the lateral posterior-pulvinar thalamic complex in the cat. *Neuroscience. 7:1495, 1982.*

Roucoux A., Guitton D., and Crommelinck M. Stimulation of the superior colliculus in the alert cat. II. Eye and head movements evoked when the head is unrestrained. *Experimental Brain Research. 39:75-85, 1980.*

Schiller P.H. and Stryker M. Single-unit recording and stimulation in superior colliculus of the alert rhesus monkey. *Journal of Neurophysiology 35:915-924, 1972.*

Schiller P.H. and Koerner F. Discharge characteristics of single units in superior colliculus of the alert rhesus monkey. *Journal of Neurophysiology 34:920-936, 1971.*

Segraves M.A. and Goldberg M.E. Properties of eye and head movement evoked by electrical stimulation in the monkey superior colliculus. In: The head-neck sensory motor system, edited by A. Berthoz, W. Graf and P.P. Vidal. New York: Oxford University Press, p. 292-295, 1992.

Sparks D.L. Translation of sensory signals into commands for control of saccadic eye movements: role of primate superior colliculus. *Physiological Reviews. 66(1):118-71, 1986.*

Sparks D.L. Response properties of eye movement-related neurons in the monkey superior colliculus. Brain Research, *90:147-152, 1975.*

Spreafico R., Kirk C., Franceschetti S., and Avanzini G. brainstem projections to the pulvinar-lateralis posterior complex of the cat. *Exp. Brain Res. 40:209, 1980.*

Stein B.E., Magalhaes-Castro B., and Kruger L. Relationship between visual and tactile representations in the cat superior colliculus. *Journal of Neurophysiology, 39:401, 1983.*

Stein B.E., Spencer R.F., and Edwards S.B. Corticotectal and corticothalamic efferent projections of SIV somatosensory cortex in cat. *Journal of Neurophysiology. 50(4):896-909, 1983.*

Stein B.E. Organization of the rodent superior colliculus: Some comparisons with other mammals. *Behav. Brain Res. 3:175, 1981.*

Sugimoto T., Mizuno N., and Uchida K. Distribution of cerebellar fiber terminals in the midbrain visuomotor areas: an autoradiographic study in the cat. *Brain Research. 238(2):353-70, 1982.*

Tashiro T., Kudo M., and Kawamura S. Discontinuous spatial distribution of the tectal afferents from the trigeminal nucleus in the cat. *Neuroscience Letters. 20(3):249-52, 1980.*

Tigges J. and Tigges M. Distribution of retinofugal and corticofugal axon terminals in the superior colliculus of squirrel monkey. *Investigative Ophthalmology & Visual Science. 20(2):149-58, 1981.*

Uchida K., Mizuno N., Sugimoto T., Itoh K., and Kudo M. Direct projections from the cerebellar nuclei to the superior colliculus in the rabbit: an HRP study. *Journal of Comparative Neurology. 216(3):319-26, 1983.*

Updyke B.V. Topographic organization of the projections from cortical areas 17, 18 and 19 onto the thalamus, pretectum and superior colliculus in the cat. *Journal of Comparative Neurology. 173(1):81-122, 1977.*

Vanegas, Horacio. Comparative Neurology of the Optic Tectum. Plenum Press, New York and London: 1984, 687-773.

Weber J.T., Partlow G.D., and Harting JK. The projection of the superior colliculus upon the inferior olivary complex of the cat: an autoradiographic and horseradish peroxidase study. *Brain Research. 144(2):369-77, 1978.*

Wise S.P. and Jones E.G. Somatotopic and columnar organization in the corticotectal projection of the rat somatic sensory cortex. *Brain Research. 133(2):223-35, 1977.*

Wurtz R.H. and Goldberg M.E. Activity of superior colliculus in behaving monkey. III. Cells discharging before eye movements. *Journal of Neurophysiology 35:575-586, 1972.*